Development Of Design Criteria For Mechanical Roof Bolting In Underground Coal Mines

David Hsin-Ying Tang

8417577

Tang, David Hsin-Ying

DEVELOPMENT OF DESIGN CRITERIA FOR MECHANICAL ROOF BOLTING
IN UNDERGROUND COAL MINES

West Virginia University PH.D. 1984

University
Microfilms
International 300 N. Zeeb Road, Ann Arbor, MI 48106

PLEASE NOTE:

In all cases this material has been filmed in the best possible way from the available copy. Problems encountered with this document have been identified here with a check mark √.

1. Glossy photographs or pages _____
2. Colored illustrations, paper or print _____
3. Photographs with dark background _____
4. Illustrations are poor copy √
5. Pages with black marks, not original copy _____
6. Print shows through as there is text on both sides of page _____
7. Indistinct, broken or small print on several pages √
8. Print exceeds margin requirements _____
9. Tightly bound copy with print lost in spine _____
10. Computer printout pages with indistinct print √
11. Page(s) _____ lacking when material received, and not available from school or author.
12. Page(s) _____ seem to be missing in numbering only as text follows.
13. Two pages numbered _____. Text follows.
14. Curling and wrinkled pages _____
15. Other _____

University Microfilms International

DEVELOPMENT OF DESIGN CRITERIA FOR MECHANICAL ROOF BOLTING IN UNDERGROUND COAL MINES

by

David Hsin-Ying Tang, M.S. Engineering

A Dissertation

Submitted to the Faculty of

Department of Mining Engineering

College of Mineral and Energy Resources

West Virginia University

In Partial Fulfillment of the Requirements

for the Degree of

Doctor of Philosophy

in

Mining Engineering

Morgantown, West Virginia

March 1984

ABSTRACT

In spite of the widespread usage of mechanical roof bolts as a support system in the underground coal mines, the mechanisms by which roof bolts reinforce the mine roof are still not fully understood. The general practices of roof bolting system are largely based on some empirical rules, which tend to either underdesign or overdesign.

In order to design the roof bolting system safely and economically, it is essential to understand the flexural behavior of the immediate roof. Based on the strata sequence, the strata in the immediate roof are divided into three types. The flexural behavior of the three strata types are investigated in terms of the following effects: roof span, horizontal stress, thickness and Young's modulus of the lowest stratum.

The reinforcement mechanism of suspension effect is analyzed based on beam-column theory. The equations of the maximum bending stress, deflection and transferred bolt load for the bolted strata are derived. In the analysis, the bolt load is assumed to be point load and the horizontal stress is uniformly applied to each stratum. The reinforcement mechanism of friction effect is also investigated. The major function of roof bolting in this case is to create the frictional resistance between the strata by the tensioning of roof bolts, thereby the individual layers are combined into one single thick layer.

Based on the results of this research, the bolts should be equally spaced when the immediate roof is reinforced by the suspension effect. However the bolts should be spaced based on equal shear force concept when the immediate roof is reinforced by friction effect.

An efficient computer program and nomographs are developed for the determination of proper bolting pattern and bolt tension. It is hoped that this development can lead to maximum safety with minimum cost for the design of roof bolting system in underground coal mines.

ACKNOWLEDGMENTS

The author wishes to express his sincere gratitude to his advisor, Dr. Syd S. Peng for his instruction, encouragement and support during the course of this research.

Sincere thanks are due to the other members of the Ph.D. advisory committee, Dr. A. W. Khair, Dr. L. K. Moulton, Dr. N. T. Sivaneri and Dr. Y. J. Wang for their guidance and suggestions.

The author is thankful to Alice Kerns, for her efficient and accurate typing of the manuscript.

Finally, the author is grateful to his wife, Mei, and his sons, Paul and John, for their love, help, patience and understanding throughout the course of this research.

TABLE OF CONTENTS

Page

LIST OF FIGURES

Page

LIST OF TABLES

LIST OF SYMBOLS

α, β	factors used in suspension effect, depending on bolt number and bolt spacing
α_{21}, α_{31}, α_{3c} ... α_{63}	α factors for different number of bolts at different locations; the first subscript refers to number of bolts per row and the second subscript refers to the location of the bolt. Subscript c refers to the center of the roof span and subscripts 1, 2, 3 refer to the first, second and third bolt from the ribs, respectively.
A1, A2, A3	constants used in Appendix I
B, b	length of the opening; row spacing
B1, B2, B3	constants used in Appendix I
C1, C2, C3	constants used in Appendix I
C5D, C6D	constants used in Appendix I
C	Constant used in torque-tension relationship
C_B	factor used in friction effect, related to segment of equal shear force
C_p	compressive strength of rock
C_T	tensile strength of rock
C_x	coefficient used in friction effect
E	Young's modulus
$\Delta\varepsilon_f$	decrease in bending strain due to friction effect
ε_{nfs}	bending strain of unbolted strata
F	factor due to horizontal stress, equal to X(u) u/tan u
F_1	F factor for the lowest layer in the combined stratum

F_{SA}	average shear force at the interface for each segment of equal shear force
γ	factor used in friction effect related to the segment of equal shear force.
h	bolt length or total thickness of bolted strata
H_S	horizontal stress
I, I_z	moment of inertia
I_A	statical moment of area
K	equal to $1 + \beta R$
K1, K2, K3	constants used in Appendix I
L	roof span
$\lambda(u)$	equal to $2(1 - \cos u)/(u^2 \cos u)$
M	mean size of rock fragment
M_o	maximum bending moment due to self weight of the stratum
M_B	maximum bending moment due to roof bolting
$M_{B1}, M_{B2}, \ldots, M_{B6}$	M_B for one, two ... six bolts, respectively.
m_1, m_2, m_2	ratio of distance of bolt from the rib to the roof span for the first, second and third bolts, respectively.
N, N_1	number of bolts per row
N_2	number of rows along the opening
n	number of strata in the bolted roof
P	(1) bolt load; (2) axial load
P_A	allowable anchorage capacity
P_B	bolt tension
P_{cr}	critical load for a beam, above which the beam will buckle

Q	shear flow
Q_{ave}	average shear flow
$Q_{N/2}$	shear flow at $X_{E(\frac{N}{2})}$
$Q_{N/2 - 1}$	shear flow at $X_{E(\frac{N}{2} - 1)}$
q	uniformly distributed load per unit length
Δq	change in q
q_1'	adjusted q for the lowest layer in the combined stratum
R_i	equal to $\left(\sum_{x=1}^{n} \frac{q_K}{\frac{E_K I_K}{S_K}}\right) / \left(q_i / \frac{E_i I_i}{S_i}\right) - 1$
RF	reinforcement factor
S	(1) spacing between bearing plates; (2) equal to 5 $\eta(u)$ - 4 u $X(u)\lambda(u)/\tan u$
σ_B	maximum bending stress in the bolted stratum
σ_H	horizontal stress
σ_{TL}	total lower-fiber stress
σ_{TU}	total upper-fiber stress
σ_x	bending stress
σ_{max}	maximum bending stress
σ_{1max}	maximum bending stress in the lowest layer of combined stratum
$\Delta\sigma$	change in bending stress
T	applied torque
T_i	transferred bolt load for i-th layer

$T_{1c}, T_{21}, \ldots, T_{63}$	transferred bolt load for various number of bolts at different locations. The definition of subscripts is same as that in $\alpha_{21}, \alpha_{31} \cdots \alpha_{63}$
t	thickness of stratum
t_{ave}	average thickness of bolted strata
t_1	thickness of the lowest layer in the combined stratum
τ_{xy}	shear stress
$(\tau_{xy})_{max}$	maximum shear stress
u	equal to $L/2(P/EI)^{\frac{1}{2}}$
μ	coefficient of friction at interface
V	shear force
V_{max}	maximum shear force
v_x	deflection of stratum
v_{max}	maximum deflection of stratum
v_B	deflection of bolted stratum
Δv	change in deflection
W	total transverse load
w	unit weight of rock
w_{1a}	adjusted unit weight of rock for the lowest layer in the combined stratum
w_{ave}	average unit weight of rock
$\overline{w}$	equivalent unit weight of bolted strata
$X(u)$	equal to $3(\tan u - u)/u^3$
$\eta(u)$	equal to $12(2 \sec u - 2 - u^2)/(5\ u^4)$

CHAPTER 1

INTRODUCTION

1.1 General

Today, roof bolting is the primary support system in underground coal mines, because more than 95% of the underground coal mined in the United States are mined under roof-bolted roofs (1). The use of roof bolts has resulted in a great reduction in the number of fatal and nonfatal roof-fall accidents in coal mines (2). Furthermore, since the bolted mine roof can provide an unobstructed opening with minimum maintenance, the productivity has increased, the cost decreased, and the ventilation improved.

In general, based on the types of anchor, roof bolts can be divided into two groups. One is the point-anchored bolt (or mechanical bolt) and the other is the full-length-anchored bolt (or resin bolt). While resin bolting has met with increasing growth in the past decade, mechanical bolting (mainly the expansion-shell bolt) still reinforces the roof strata, safely and economically, in the vast majority of underground coal mines in the United States (3).

In spite of the widespread usage of roof bolts as a support system in the underground mining, the mechanisms by which roof bolts reinforce the mine roof are still relatively unknown. In particular, there is no consensus regarding the design criteria for the bolting pattern (i.e., bolt length and bolt spacing both along and across the opening) and bolt tension at which it should be installed to reinforce the mine roof with safety and economy. The common practices of roof bolting systems are largely based on some empirical rules, which tend to either overdesign or underdesign.

Although it is generally believed that the reinforcement mechanisms for mechanical bolting in horizontally bedded strata are due to the suspension effect and/or the friction effect (or beam-building effect), a complete and detailed theory is not as clear as it should be, and is still not fully developed (2). This is mainly due to the fact that different geological and geometrical conditions exist for different mines. For example, one bolting plan which is suitable for one mine may not be adequate for the other mines. The commonly used 4 x 4 ft. (1.22 x 1.22 m) pattern is merely based on the rule-of-thumb, which is obviously not good for every situation.

Since the reinforcement mechanism and the design of bolting systems are closely related to the strata behavior, it is necessary to systematically analyze the flexural behavior of the immediate roofs that are likely to be encountered in coal mines.

Generally, based on the strata sequence, the immediate roofs in the underground coal mines can be divided into three types. They are: (a) each stratum deflects independently, (b) some stratum (or strata) deflects more than that of the underlying strata, and (c) each stratum deflects more than that of the underlying stratum (Fig. 1.1)(5). Among them strata type A is

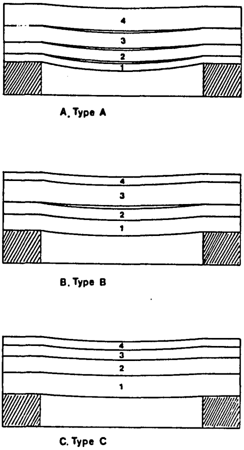

Fig. 1.1. Three strata types of immediate roof (5).

usually the most critical to the stability of the immediate roof. Therefore, an adequately designed roof bolting system is necessary. For strata type C, if the strength of the thick stratum is strong enough, there is no need to install any roof bolt. For type B immediate roof, a suitable roof bolting system is needed, depending on the strength of the roof strata and the location of the thick (or strong) stratum (5). However, in real situation, the strata sequence of the immediate roof is arbitrary, thus the analysis of the flexural behavior of the immediate roof may become very complicated. In order to overcome this difficulty, it is essential to develop a computer program which can deal with the analysis of the flexural behavior of any immediate roof that is likely to be encountered.

In underground coal mines, since high in-situ horizontal stress always coexists with vertical stress because of lateral constraint or tectonic activities (6, 7), the effect of axial loading due to the horizontal force should be considered in the design of roof bolting system. The effect of horizontal stress will not only increase the bending stress, but also influence the total stress (i.e., the sum of horizontal stress and bending stress) on the outer fiber of the roof stratum. When the horizontal stress is very high, the buckling action may cause the roof strata to fail suddenly. It should also be noted that due to the existence of the horizontal stress, total stress instead of bending stress should be used in the design of bolting system for more accurate results (6-8).

1.2 Objectives

The primary objective of this research is to analyze the reinforcement mechanisms of the mechanical roof bolting for a generalized immediate roof, which is made up of multiple strata with variable thicknesses, different material properties and arbitrary strata sequence. In addition, based on the results of this analysis, a computer program and nomographs are developed, from which a set of design criteria for proper bolting pattern and bolt tension is established.

1.3 Scope

The scope of this research is confined to the following conditions:

(1) A rectangular opening with a generalized immediate roof in the horizontally bedded rock.

(2) The ratio of the length to the span (width) of the opening is two or more.

(3) The mechanical bolts are of equal lengths and vertically installed into the immediate roof.

CHAPTER 2

LITERATURE REVIEW

2.1 Characteristics of Mechanical Roof Bolts

Although there are various types of mechanical bolts, all of them consist of the following common elements (Fig. 2.1)(9):

(a) a solid steel bar or shank,

(b) an anchoring device at the top end of the bar, and

(c) a tensioning device at the lower end of the bar.

2.1.1 Solid Steel Bar

Most roof bolts in coal mines have a solid steel bar, although wood rods have also been used for some particular situations. The steel bar, generally 5/8 in. (1.59 cm) in diameter, has either a smooth surface or a deformed appearance such as rebar or screwed thread. At the anchoring end, the bar either has a formed slot to accept a steel wedge for the slot-and-wedge anchorage, or is threaded to accept the expansion-shell anchorage. At the tensioning end, the bar may either be threaded to accept a torque nut or have an integral forged head (10).

The yield strength of the steel bar is a fundamental parameter in the determination of bolt tension, which in turn is very important for the effectiveness of the mechanical bolt. Generally, the yield strength of the steel bar ranges from 30,000 to 75,000 psi (206.85 to 517.125 MPa)(11), depending on the carbon content, with higher carbon for higher yield strength (12). Although a roof bolt of high strength is desirable, the use of very high strength bolt should be avoided because if the bolt fails it will shoot out of the hole with a high velocity creating a safety hazard. It is therefore recommended that the installed bolt tension should not exceed 60% of: (a) the yield load of the bolt, i.e. 12,000 to 14,000 lb. (5,433 to 6,350 Kg) for 5/8 in. (1.59 cm) extra-strength bolts; 18,000 to 20,000 lb. (8,165 to 9,072 Kg) for 3/4 in. (1.91 cm) extra-strength bolts or (b) the anchorage capacity, whichever is lower (1).

2.1.2 Anchor Types

There are three major types of anchor, i.e., slot-and wedge, expansion shell, and grouted anchorage (Fig. 2.1)(9). In addition to these three types of anchor, there are another two types of anchor, i.e., explosive-set anchor (13) and combination anchor (14), which have also been successfully introduced. Table 2.1 summarizes the various types of mechanical roof bolts.

(1) Slot-and-Wedge

This type of anchor was most common in the early period of roof bolt development. The usual practice is to install a 1 in. (2.54 cm) bolt in a 1 1/4 in. (3.18 cm) hole drilled with an air powered stopper or jackleg drill (1). The anchorage is obtained by inserting a steel wedge into a center slot formed at the top end of the bolt and expanding the slot by driving the wedge against the bottom of the hole. To achieve a good anchorage, the length of the hole has to be carefully controlled (15). At present, the use of this type of roof bolt has become obsolete in the U. S. and has been superseded

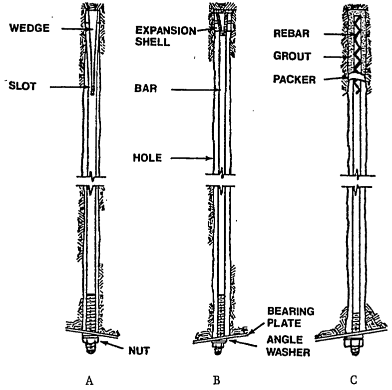

Fig. 2.1. Three types of mechanical roof bolts. (A) Slot and wedge type; (B) Expansion shell type; (C) Grouted anchorage type (9).

Table 2.1. Various Types of Mechanical Roof Bolts

Type of Anchor	Suitable Strata Type	Comments	Ref.
Slot-and-Wedge	hard rock	used in early stages	15
Expansion Shell:		most commin in U. S.	15
a. Standard anchor	medium-strength rock		
b. Bail anchor	soft rock		
Grouted anchor:	most strata, especially good for weak rock	increased usage recently	3
a. Pure point anchor		grouted length < 24 in. (61 cm)	16
b. Combination system		grouted length > 24 in. (61 cm)	16
Explosive-Set	lower-strength rock	limited usage	13
Combination Anchor (Expansion shell and no mix resin)	most strata	good anchorage with "No Mix Resin"	14

by the expansion-shell bolt due to the general unavailability of compressed air and the introduction of hydraulic rotary drilling in the underground coal mines (15).

(2) Expansion Shell

This is the most commonly used type of anchor in the underground coal mines. The general practice is to install a 5/8 in. (1.59 cm) bolt in a 1 3/8 in. (3.49 cm) hole. The anchorage is obtained by applying torque to the bolt head, which in turn pulls the wedge-shaped plug down into the shell and expands the serrated leaves against the sides of the hole. In this type of anchor, the depth of the hole need not be accurately controlled (15). But the diameter of the hole is important, since an oversized hole can result in poor anchorage (12). The fact that hydraulic-rotary-percussion drill can anchor and tighten the bolt simultaneously contributes to the popularity of expansion-shell anchors in modern coal mines (15).

A large number of expansion-shell designs are available with major variations in shell length, type of serration, angle of plug and number of leaves forming the shell. In general, they can be divided into two types of anchor: standard type and bail type. The standard expansion shell resembles a short tubing split lengthwise into two or four pieces, with a solid unsplit portion left at the lower end. In the bail type, the shell body is commonly split into halves for its full length, but kept together with a yoke-shaped steel band. X-ray radiographs by Mitchell and Debevec (17) and Foster, et al (18) have shown that standard and bail expansion shells produce different shell-borehole interface contacts. The contact area for the standard shells is restricted to the length of the plug because of the rigid shell-leaf attachment at the base. The bail type on the other hand, is able to make full contact of the whole length of the shell. Therefore, the bail anchors can provide a better anchorage in soft rock due to smaller stress concentration, whereas the standard anchors can penetrate into hard rock and provide a better grip due to higher stress concentration.

The shape and type of serrations on the expansion shell are very important factors for good anchorage. Stefanko and de la Cruz (19) analyzed the anchorage performance between the commercial shell and the modified shell (Fig. 2.2). They stated that the serration on the commercial shell contributed to the failure of the rock which resulted in excessive bleed-off, because the force transmitted by the wedge was in the direction of the tip of the serration, thus resulting in excessive stress concentration. While for the modified shell, due to the reversal of the serration (i.e., with the flat edge upward), the force transmitted by the wedge was permitted to act nearly normal to the face of the serration. Thus the anchorage was improved since excessive stress concentration can be avoided. This resulted in much lower rates of bleed-off.

(3) Grouted Anchor

In this type of anchor some portions of the bolt near the top end are grouted. The anchorage is achieved by the bonding between the grout, bolt and hole wall. The grouted length depends on the type of rock and the grouting material. Many grouting media have

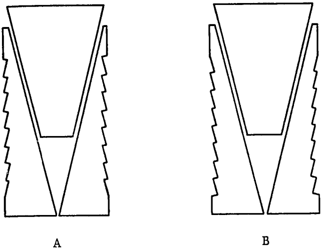

Fig. 2.2. Arrangement of serrations on an expansion shell. (A) Commercial serrations; (B) Modified serrations (19).

been used, such as Portland cement, mortar, gypsum, chemical grout, polyester resin and epoxy resin. Among them the resin type anchorage is most popular due to its high strength and quick setting time. Generally, this type of anchorage can be categorized into two groups (16): (a) the pure point-anchored system having 24 in. (61 cm) or less of grouted length, and (b) the combination bolting system having grouted length more than 24 in. (61 cm). For the pure point-anchored system it functions as a mechanical bolt, while for the combination bolting system, the grouted portion reinforces the upper strata as a fully grouted bolt with the ungrouted part held by a clamping force as in the mechanical bolt (16).

(4) Explosive-Set Anchor

In this type of anchor, explosives are inserted in an anchor tube at the end of the bolt. By expanding the anchor tube with explosives, a corrugated effect is produced to secure a firm bond between the bolt and the sides of the hole (13). Although this type of anchorage is successful for the weak rock, it has a limited use due to its complexity and higher cost.

(5) Combination Anchor (Expansion Shell and "No Mix Resin")

In this type of anchor, the effective anchorage is achieved by adding the advantage of resin bonding to the mechanical expansion shell. In addition, due to the fact that no spin mixing of resin cartridge is used, the speed of installation is much faster (14).

The increased anchor performance resulting from the "No Mix Resin" is as follows (14)(Fig. 2.3):

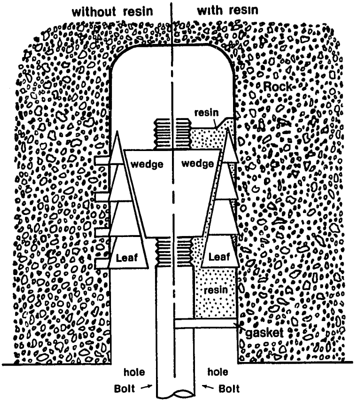

Fig. 2.3. Increased anchor performance resulting from "No Mix Resins" (14).

(1) Increase the leaf bearing area by filling the voids between the serrations on each metal leaf.

(2) Form a 360° bearing area by resin filling the space between the leaf, wedge and hole wall.

(3) Creates a longer plug that maintains contact with the total available leaf area.

(4) Generates additional resistance to anchor movement by accumulating resin below the shell but above the gasket.

2.1.3 Bearing Plate and Washer

Bearing plates used between the bolt head and the roofline are generally flat or bell- or doughnut-shaped and range from 6 to 8 in. square (15.24 to 20.32 cm square) in size. The major function of the bearing plate is to distribute the load from the bolt to the rock surface. The bearing stress exerted by the bearing plate should not exceed the bearing capacity of the rock surface so that failure will not occur, thus maintaining the proper bolt tension.

In practice, the roof surface and hence the bearing plate is not always perpendicular to the bolt. The angle washers or spherical washers are used to create a uniform bearing surface for the nut or bolt head, which is normal to the bolt axis. A hardened flat washer is normally used between bearing plate and the nut or bolt head. The use of a hardened washer not only increases the torque-tension ratio, but also decreases the random variations of bolt tension induced in the installation (20).

2.1.4 Torque-Tension Relationship

The relationship between the applied torque and the induced tension in the bolt is generally expressed as

$$P = CT \tag{2.1}$$

where P and T are bolt tension in lb. and applied torque in ft-lb, respectively, and C is a constant. C is different for different bolt diameters and installation techniques. The rule of thumb is C = 50 for 5/8 in. (1.59 cm) bolts, 40 for 3/4 in. (1.91 cm) bolts, 30 for self-centering headed bolts, and 60 for bolts with hardened steel washers (13). For the roof bolt with integral head, which is tensioned by the applied torque, the steel shank is subjected to a combination of torsional shear stress and tensile stress. The combined stress has the effect of reducing the yield strength of the bolt (9, 21).

2.1.5 Anchorage Capacity

The maximum load a bolt can withstand without its anchorage slipping at a certain horizon in the roof can be determined by underground in-situ pull tests of roof bolts (1). From these tests, the characteristics of the anchorage can be represented by a graph of bolt displacement versus bolt load. The load at which a slight increase in load causes excessive anchorage displacement is defined as the anchorage capacity of the bolt for that horizon (1). Since the rock property is different from mine to mine it is advisable to carry out the pull tests to determine the anchorage capacity, which is essential in the design of roof bolting system.

2.2 Theories of Roof Bolting

It has been estimated that over 100 million roof bolts are used in the United States each year. Despite its widespread usage, the complete theory of roof bolting remains underdeveloped (2). Although numerous theories (22-26,27-35) have been proposed and a great amount of research has been carried out elsewhere, the real mechanism or mechanisms by which the roof bolts reinforce the immediate roof of underground coal mines are not fully understood.

In general, the existing theories regarding the mechanisms by which the roof bolts reinforce the mine roof are: (a) suspension effect, (b) friction effect (or beam-building effect), (c) arching effect, and (d) keying effect.

2.2.1 Suspension Effect

Basically, there are two types of reinforcement due to suspension effect. One is the simple suspension and the other is the beam suspension.

(1) Simple Suspension

The simple suspension effect is that the weight of a weak (or loose) rock layer is suspended from the upper competent rock stratum through the use of roof bolts. This type of support was probably the earliest mode of reinforcement and is still used for this purpose in the underground coal mines today.

The load carried by a bolt, P, is given by the following equation (22):

$$P = \frac{wtBL}{(N_1 + 1)(N_2 + 2)} \tag{2.2}$$

where w = unit weight of roof rock

t = thickness of the roof layer

L = roof span (or width of the opening)

B = length of the opening

N_1 = number of bolts per row across the opening

N_2 = number of rows along the opening

It should be noted that this equation is valid only if the weight of the weak rock layers is completely suspended at the upper competent rock stratum by the roof bolts. However, in real underground situations, a portion of the weight of the roof layers is generally supported at the abutments on both sides of the opening. Therefore this equation mostly represents the upper limit of the suspension load for each bolt, which tends to overdesign the bolting system.

(2) Beam Suspension

In horizontally bedded strata, to which most immediate roofs in coal mines belong, the strata are either unbonded or the bonding strengths between them are small compared to the tensile strength of the roof strata. After an opening is excavated, the immediate roof will become detached from the overlying strata either immediately or after a short time (22). Generally the immediate roof over an underground opening is assumed to behave like a series of beams with the ends of the beams fixed or restrained at the pillars on each side of the opening (8,22,23). The suspension effect under this condition is mainly due to the transfer of parts of the weight of the weaker strata to the competent stratum (or strata) through roof bolting.

Panek (24-26) analyzed the suspension effect by both experimental method and theoretical study. The experiment method used a centrifugal testing to simulate the gravitational forces exerted on the roof rock of underground opening. The theoretical analyses were based on the fixed-end beam theory with the following assumptions:

(a) All beams are bolted such that equal deflections occur at the bolt locations and at the support ends.

(b) The beams have frictionless surfaces of contact.

(c) The total load to be supported by each beam consists of two parts. One part is the transferred load due to bolting, which is assumed to be a point load. The other part is the uniformly distributed load due to its own weight.

The results of his studies showed that the suspension effect by roof bolting in a horizontally bedded mine roof depended principally on the number of bolted roof layers and their relative flexural rigidities. In order to prevent strata separations at the bolt locations, a sufficient bolt tension was necessary. The results also indicated that for the bolted roof the maximum bending stresses in the thick beds were usually greater than that in the thinner beds. Thus, in a bolted roof, the thickest bed is usually the critical one, and the failure of this member may cause the failure of the whole bolted unit.

Although Panek's work contributed a lot to the design of roof bolting systems, several important effects were not taken into consideration in his studies. These included, in particular, the analysis of the flexural behavior of a generalized immediate roof and the effect of axial loading due to high horizontal force. Moreover, the maximum bending stress instead of the total stress was used in the design of roof bolting system, which is valid only when the horizontal stress is zero or very small (8). However, in most cases, the in-situ horizontal stress is very high (6,27).

In order to design, safely and economically, the roof bolting system for underground openings, it is essential to understand the flexural behavior of the generalized immediate roof. As stated in Chapter 1, the immediate roofs can generally be divided into three types based on the strata sequence. Basically, Panek only considered strata type A for the study of suspension effect. Strata type B was not analyzed due to complexity. It is worth noting that although the bolt load calculated based on strata type A can develop the maximum possible suspension effect for all possible strata sequence, it will overdesign the bolt load for the immediate roof of strata type B.

2.2.2 Friction Effect

The reinforcement of a laminated roof by the friction effect results from the clamping force of the tensioned bolts, which creates frictional resistance to slip on the interfaces between laminae, thus decreasing the flexure and strengthening the roof.

Panek (28-30) analyzed the friction effect of bolting in a horizontally bedded roof by centrifugal testing of mine roof models. The following restrictions were imposed: (a) The immediate roof consisted of beds of equal thicknesses, all beds being of the same material, with no bond between the beds. (b) The bolts were installed vertically in straight lines across the opening and were not anchored in a thick bed, the case of suspension effect therefore being excluded (30). By means of regression analysis of the data from model studies, he found that the relationship between the decrease in maximum bending strain, $\Delta\varepsilon_f$, due to friction effect and the maximum bending strain of the unbolted strata, ε_{nfs}, can be expressed by the following equation (31):

$$\frac{\Delta\varepsilon_f}{\varepsilon_{nfs}} = -\ 0.375\ \mu(bL)^{-0.5}[NP(h/t_{ave}-1)/w_{ave}]^{0.33} \qquad (2.3)$$

where μ = coefficient of friction between the bedding planes

b = spacing of rows of bolts

L = roof span

N = number of bolts per row

P = bolt tension

h = bolt length, or total thickness of the bolted roof beds

t_{ave} = average thickness of the bolted roof beds

w_{ave} = average unit weight of the bolted roof beds

The reinforcement factor, RF, due to friction effect, is then defined as

$$RF = \frac{1}{1 + \frac{\Delta\varepsilon_f}{\varepsilon_{nfs}}} \tag{2.4}$$

which is used to evaluate the effectiveness of the friction effect of roof bolting. Based on these two equations, a nomograph was derived, from which the reinforcement factor of a bolted roof can be quickly determined. It should be mentioned that this nomograph is based on $\mu = 0.7$ and $w_{ave} = 0.09$ lb/in^3 (2.49 g/cm^3). Besides, the material property (e.g., Young's modulus) of each roof layer is the same. Therefore, in order to apply these equations and nomograph with confidence to the design of roof bolting system in the real underground situations, the above mentioned assumptions should be understood and satisfied in the prototype, otherwise either over-design or underdesign will result.

Janek investigated the behavior of the bolted mine roof by the finite element method (32). In an analysis of beam-building effect, he used one model to determine whether or not two separate slender beams which were bolted with seven bolts could behave as one single beam. He concluded that a bolt load of 15,000 lbs. (6,804 kg) was not sufficiently high to "build" one thick beam from two thin ones. Based on the results of the model tests, Panek also stated that the bolted unit could be made to act like a solid beam for wider spans if several times as many bolts were used (30).

Van Ham and Tsur-Lavie performed experiments with photoelastic materials subjected to uniformly distributed loading (33). They concluded that: (a) the highest stresses occur in the lowest roof layer of a multilayer roof, (b) a bolted multilayer roof does not behave as one single thick beam, and (c) in a perpendicularly bolted roof, the center roof bolt has a negligible influence on the roof reinforcement.

2.2.3 Arching Effect

The reinforcement of the immediate roof by the arching effect through roof bolting was observed in the underground mining (34). Generally this type of reinforcement occurred in a circular or an arch-shaped opening. It also occurred in the rectangular opening with blocky ground in the roof, possessing little or no tensile strength.

Through the systematic use of the roof bolts, a ring (or zone) of compressed reinforced rock may be formed around an opening. The reinforced layer acts as a structural membrane or unit capable of not only providing its own support, but also supporting the rock above.

With this type of reinforcement, the in-situ horizontal stress plays an important role. Gerdeen, et al. (34) analyzed the stability of the bolted mine roof under different horizontal stresses. They pointed out that under low lateral stress, roof bolts of adequate length are required to maintain the arch. But under high lateral stress, the bolts may not be required to maintain the arch. This was also confirmed by the finite element analysis (34).

2.2.4 Keying Effect

In underground coal mines, the stratified immediate roof may be intersected by the planes of weakness. Roof bolting across these planes of weakness will prevent or reduce movements of roof strata along these planes. The reinforcement effect is mainly due to the frictional resistance and interlocking phenomena from the tensioning of the bolts. Lang (35) made a series of model experiments using fine (i.e., < 3/16 in. or 4.76 mm), crushed rock, plastic rods or marbles to simulate the fractured roof. From the test results, he concluded that in order to make the roof behave stable, the following equation must be satisfied:

$$S/M \leq 3.0 \tag{2.5}$$

where S is the spacing between the bearing plates of the bolts and M is the mean size of the rock fragments.

2.3 Bolting Pattern--Length and Spacing of Bolts

One of the most important aspects in the success of any roof bolting endeavor is the pattern in which the bolts are placed in the roof strata. In most instances it has been found that a systematic pattern of roof bolting produces the most consistent results (36). An adequate design of bolting pattern will not only increase the safety of the mine roof, but also reduce the labor and cost of materials for roof bolting system.

2.3.1 Bolt Length

An adequate bolt length must be chosen with regard to the mechanical characteristics of the rock and the dimension of the opening. Dejean and Raffoux (37) stated that:

(a) for strong and homogeneous ground, the sufficient length of the bolt is in the order of 1 m,

(b) for weak and homogeneous ground, the bolt length is usually equal to one-half or one-third of the width of the opening,

(c) for strong stratified ground, the bolt length usually will not be less than 1.5 m, and

(d) for weak stratified ground, the roof bolting will not be the only support and the length of the bolt should be greater than one-third of the width of the opening.

Tincelin (38) suggested that the bolt length to be used is equal to or greater than one-third of the width of the opening. Alexander and Hosking (39) pointed out that the bolt length should be at least three times the width of the joint blocks. Generally, it is believed that the length of the bolt should be such that it can be anchored in the most competent layer.

2.3.2 Bolt Spacing

Although the bolt spacing and, hence the bolting pattern are the key parameters in determining the overall effects of reinforcing the mine roof, the current practice are mostly dependent on empirical rules.

In the United States, roof bolts are commonly installed vertically into the roof in a 4 x 4-ft. (1.22 x 1.22-m) or 5 x 5-ft. (1.53 x 1.53-m), or combination pattern (1,29,40), although it had been pointed out that such pattern is not suitable for every situation (4). In France, bolting density generally ranges from 0.5 to 1 bolt per square meter of the roof to be supported, with higher number for weaker rocks (38). It has also been pointed out that in fractured rock the ratio of bolt length to bolt spacing should not be less than two (10,36). With regard to the installation of the inclined bolts above the ribs, some investigation has been made (41). It was found that only a slight benefit is gained over the vertical bolts. But the inherent cost involved with the installation of the inclined bolts and the longer installation time result in the recommendation that no inclined roof bolts are used in normal mining operations.

2.4 Bolt Tension

Tensioning of the mechanical bolt is a very important factor for successful reinforcement of the immediate roof. The proper tension with which the roof bolts should be used depends on many parameters. These include the geometry of the opening, geological properties of the immediate roof, strata sequence, bolting pattern, strength of the bolt, and the method of installation.

Although numerous tests on the anchorage capacity and the yield strength have been done, very few studies have been made on the adequate tension which should be used for a specific bolt pattern.

In general practice, it is recommended that the bolt should be installed with bolt tension equal to smaller of (a) 60% of the anchorage capacity, or (b) 60% of the yield load of the bolt in pure tension (15). It was also stated that with the expansion-shell bolt, a bolt load of 5 to 6 tons should be installed (38). The required bolt tension for a specific bolt pattern can be determined from the nomograph developed by Panek (29). But the limitation of that nomograph should be understood and satisfied.

CHAPTER 3

FLEXURAL BEHAVIOR OF IMMEDIATE ROOF

3.1 General

In order to analyze the reinforcement mechanisms and to design the roof bolting system, it is essential to first understand the flexural behavior of the immediate roof. Since in some cases, the strength of the immediate roof is sufficiently strong, there is no need to install any support. On the other hand, suitable roof bolting systems should be installed in other cases to maintain the roof stability; otherwise, failure of roof strata will occur.

Before analyzing the flexural behavior of the immediate roof, the definition of immediate roof should be made clear. In the horizontally bedded strata composed of a succession of parallel layers, the layers are either unbonded or the bond strength between them is small compared to the tensile strength of the rock. Generally, after an opening is excavated, the roof strata will become detached from the overlying rock either immediately or after a short time. The detached layer (or layers) is called the immediate roof and the overlying rock is called the main roof (22).

Generally, based on the strata sequence, the immediate roofs can be divided into three types. They are: (A) the deflection of each stratum is larger than or equal to that of its overlying stratum, therefore, each stratum deflects independently, (B) some stratum (or strata) deflects more than that of the underlying stratum, and (C) each stratum deflects more than that of the underlying stratum, therefore, all strata will become one equivalent stratum (see Fig. 1.1).

For type A roof strata, the flexural behavior can be determined by applying the beam-column theory directly. For type C roof strata, as long as the equivalent stratum is formed, the flexural behavior can be determined by using the beam-column theory without much difficulty. For type B roof strata, its flexural behavior cannot be determined immediately because some strata need to be combined into one equivalent stratum. Furthermore, in some cases, the strata sequence may be such that the process of combining strata need to be repeated once or several times, which makes the problem not only complicated but also time-consuming in the analysis. In order to overcome this difficulty, a computer program based on the beam-column theory is developed for the strata combination process and the calculation of the maximum bending stress and deflection for a generalized immediate roof.

3.2 Theoretical Analysis

In investigating the flexural behavior of the immediate roof, the following assumptions are made:

(1) The rock within each stratum is homogeneous, elastic and isotropic.

(2) There is no bonding between the strata.

(3) The coefficient of friction between the strata is constant.

(4) Each stratum is subjected to a uniform transverse load (due to its own weight) and an axial load (due to the horizontal stress).

(5) If upper stratum loads on the lower stratum, the deflection of the two strata are equal at each point along the roof span.

(6) All strata are of same length and width.

(7) The horizontal stress is uniformly applied to each stratum.

3.2.1 Individual Stratum

For an individual (single) stratum subjected to transverse loading and axial loading simultaneously (Fig. 3.1), the following equations are derived based on the beam-column theory (42).

$$v_x = \frac{q\,L^4}{384\,EI} S_x \tag{3.1}$$

$$v_{max} = \frac{q\,L^4}{384\,EI} S = \frac{w\,L^4}{32\,Et^2} S \quad \text{at } x = L/2 \tag{3.2}$$

$$\sigma_x = \frac{q}{12}(6LX - L^2 - 6x^2)F_x \tag{3.3}$$

$$\sigma_{max} = \frac{w\,L^2}{2t} F \qquad \text{at } x = 0 \text{ and } x = L \tag{3.4}$$

where

v_x = deflection along the span of each stratum

v_{max} = maximum deflection at the center of the span

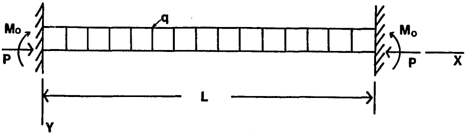

Fig. 3.1. Diagram for a fixed-end beam subjected to transverse and axial loadings (42).

σ_x = bending stress along the span of each stratum

σ_{max} = maximum bending stress at the ends of the beam

q = uniformly distributed load per unit length of each stratum

E = Young's modulus of each rock stratum

I = moment of inertia of each stratum

L = roof span

w = unit weight of rock

t = thickness of each stratum

S_x, F_x = factor due to the horizontal stress

S = $5\eta(u) - 4uX(u)\lambda(u)/\tan u$

F = $X(u)u/\tan u$

u = $\frac{L}{2}(P/EI)^{\frac{1}{2}}$

$X(u)$ = $3(\tan u - u)/u^3$

$\eta(u)$ = $12(2 \sec u - 2 - u^2)/(5u^4)$

$\lambda(u)$ = $2(1 - \cos u)/(u^2 \cos u)$

P = axial load

3.2.2 Combined Statum (Upper Stratum Loads on Lower Stratum)

For an immediate roof consisting of more than two layers, and the thinner layer overlies the thicker layer, the lower layer is loaded by the upper one. To simplify the discussion initially, the number of layers will be restricted to two. Consider two beams of equal length with their ends clamped together as shown in Fig. 3.2.

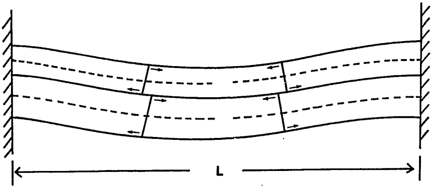

A

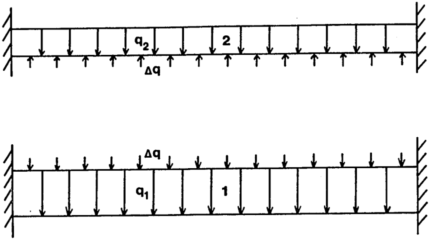

B

Fig. 3.2. (A) Multiple strata diagrams (22).
(B) Transverse loading on upper and lower stratum, respectively.

For these two beams under the conditions assumed above, the deflection for either the lower or the upper beam is (22,42):

$$v'_{1x} = v'_{2x} = \frac{(q_1 + \Delta q)x^2}{24\, E_1\, I_1} (L - x)^2 S_1$$

$$= \frac{(q_2 - \Delta q)x^2}{24\, E_2\, I_2} (L - x)^2 S_2 \qquad (3.5)$$

where the subscripts 1 and 2 refer to the lower beam and the upper beam respectively, the superscript "'" denotes the combined beam, and Δq is the added load or support which has been added to and substracted from the lower and upper beam, respectively. Since Equation 3.5 must hold for all values of x, therefore

$$\frac{q_1 + \Delta q}{E_1\, I_1} S_1 = \frac{q_2 - \Delta q}{E_2\, I_2} S_2 \qquad (3.6)$$

Solving Equation 3.6 for the adjusted load, Δq,

$$\Delta q = \frac{q_2 \frac{E_1\, I_1}{S_1} - q_1 \frac{E_2\, I_2}{S_2}}{\frac{E_1\, I_1}{S_1} + \frac{E_2\, I_2}{S_2}} \qquad (3.7)$$

Substituting Equation 3.7 into Equation 3.6 and rearranges:

$$q'_1 = q_1 + \Delta q = \frac{\frac{E_1\, I_1}{S_1} (q_1 + q_2)}{\frac{E_1\, I_1}{S_1} + \frac{E_2\, I_2}{S_2}} \qquad (3.8)$$

$$q_2' = q_2 - \Delta q = \frac{\frac{E_2 I_2}{S_2}(q_1 + q_2)}{\frac{E_1 I_1}{S_1} + \frac{E_2 I_2}{S_2}} \qquad (3.9)$$

By substituting Equations 3.8 and 3.9 into Equation 3.5, the deflection for either the lower or the upper beam is obtained:

$$v_{1x}' = v_{2x}' = \frac{(q_1 + q_2)x^2}{24(\frac{E_1 I_1}{S_1} + \frac{E_2 I_2}{S_2})}(L - x)^2 \qquad (3.10)$$

This procedure can be extended to any number of beams. The basic requirement is that each beam rests upon and loads on the underlying beam. For the immediate roof consisting of multiple layers, the following equations are obtained:

$$v_x' = \frac{(q_1 + q_2 + \dots + q_n)x^2 (L - x)^2}{24(\frac{E_1 I_1}{S_1} + \frac{E_2 I_2}{S_2} + \dots + \frac{E_n I_n}{S_n})} \qquad (3.11)$$

$$q_1' = \frac{\frac{E_1 I_1}{S_1}(q_1 + q_2 + \dots + q_n)}{\frac{E_1 I_1}{S_1} + \frac{E_2 I_2}{S_2} + \dots + \frac{E_n I_n}{S_n}} \qquad (3.12)$$

$$v_{max}' = \frac{(q_1 + q_2 + \dots + q_n)\, L^4}{384(\frac{E_1 I_1}{S_1} + \frac{E_2 I_2}{S_2} + \dots + \frac{E_n I_n}{S_n})} \qquad (3.13)$$

$$\sigma'_{1max} = \frac{w_{1a}\ L^2}{2\ t_1} F_1 \tag{3.14}$$

where

v'_x = deflection of each combined stratum

q'_1 = adjusted uniformly distributed load per unit length of the lowest layer in the combined stratum

v'_{max} = maximum deflection at the center of the span for the combined stratum

σ'_{1max} = maximum bending stress in the lowest layer in the combined stratum

w_{1a} = adjusted unit weight of the lowest layer in the combined stratum. It is equal to $q'_1/(bt_1)$

b = width of the cross section of each layer or row spacing

t_1 = thickness of the lowest layer in the combined stratum

F_1 = F factor for the lowest layer in the combined stratum

n = number of strata in the bolted roof

It should be noted that even though the deflection is the same for all layers in the combined stratum, the maximum bending stress is different for each layer. In this research, only the maximum bending stress in the lowest layer is considered. The reason for this is that the lowest layer, being supporting the upper ones, subjects to the largest bending stress. Therefore, when the lowest layer fails, the upper ones will also fail due to loss of support.

3.3 Procedure for Combining Strata

Whenever one stratum loads on its underlying stratum, the combination of two strata into one equivalent stratum is needed. The basic criterion is that the deflection of the upper stratum is larger than that of the lower stratum. However, for some sequences, in which $v_2 < v_1$, $v_3 > v_2$ (the numbering sequence in the subscript is increased from the lower stratum to the upper ones), it is possible that $v_2' > v_1$ (v_2' is the deflection of the equivalent stratum combined from stratum 2 and stratum 3). The same condition may occur for other strata. Besides, after the first combination for all the strata, a second combination of the equivalent strata from the first combination may still be needed. Figure 3.3 shows such an example. It should also be noted that after each combination process, the numbering of the stratum is changed, which can also be seen in Fig. 3.3.

Figure 3.4 is a simplified flow chart for the combination of strata and the related calculation of the maximum bending stress and deflection. The computer program which is written in FORTRAN IV is given in Appendix II under the title of "Flexural Behavior of Immediate Roof."

3.4 Parametric Study

In this study, the flexural behavior of the immediate roof with three types of strata sequence are investigated as a function of the following factors: roof span, horizontal stress, thickness and Young's modulus of the lowest stratum. Three models which

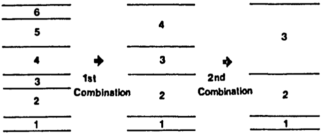

Fig. 3.3. Example of strata combination procedure.

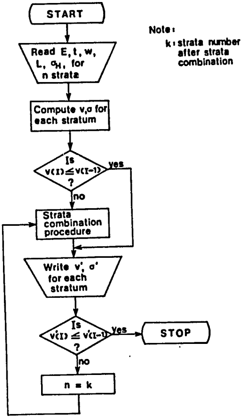

Fig. 3.4. Flow chart of strata combination procedure.

represent three types of strata sequence are used. The strata sequence, Young's modulus, thickness and unit weight of each model are shown in Table 3.1. A horizontal stress of 300 psi (2.07 MPa) is applied to each stratum except in the case of studying the effect of horizontal stress. Besides, for most cases, only the maximum bending stress and deflection of the lowest stratum are investigated, because it is usually the most critical stratum in the design of the roof spans.

3.4.1 Effect of Roof Span

In the design of underground opening, the most important item is the roof span. For different strata sequence, the effects of roof span on the bending stress and deflection are shown in Fig. 3.5 and Fig. 3.6, respectively. It is shown from these figures that both the maximum bending stress and deflection increase with the roof span. Among the three models, model A shows the largest increase, especially when the roof span is larger than 25 ft. (7.62 m). Furthermore, when the roof span is larger than 30 ft. (9.14 m), both the maximum bending stress (> 1500 psi or > 10.34 MPa) and deflection (> 3 in. or > 76.2 mm) are too high for the roof to be stable.

3.4.2 Effect of Horizontal Stress

The effects of horizontal stresses on the maximum bending stress and the maximum deflection for the three models are shown in Fig. 3.7 and Fig. 3.8, respectively. It can be seen clearly from both figures that the three models exhibit different behaviors under

Table 3.1. Material Properties and Strata Sequence for the Three Models

Model	Stratum Number	Thickness in. (cm)	Young's Modulus x 10^6 psi (x 10^3 MPa)	Unit Weight lb/in^3 (g/cm^3)
A	6	36 (91.4)	2.15 (14.82)	0.0982 (2.72)
	5	12 (30.5)	2.15 (14.82)	0.0982 (2.72)
	4	12 (30.5)	0.90 (6.21)	0.0932 (2.58)
	3	12 (30.5)	0.72 (4.96)	0.0961 (2.66)
	2	6 (15.2)	0.90 (6.21)	0.0932 (2.58)
	1	6 (15.2)	0.72 (4.96)	0.0961 (2.66)
B	6	12 (30.5)	2.15 (14.82)	0.0982 (2.72)
	5	6 (15.2)	0.72 (4.96)	0.0961 (2.66)
	4	36 (91.4)	2.15 (14.82)	0.0982 (2.72)
	3	6 (15.2)	0.90 (6.21)	0.0932 (2.58)
	2	12 (30.5)	0.90 (6.21)	0.0932 (2.58)
	1	12 (30.5)	0.72 (4.96)	0.0961 (2.66)
C	6	6 (15.2)	0.72 (4.96)	0.0961 (2.66)
	5	6 (15.2)	0.90 (6.21)	0.0932 (2.58)
	4	12 (30.5)	0.72 (4.96)	0.0961 (2.66)
	3	12 (30.5)	0.90 (6.21)	0.0932 (2.58)
	2	12 (30.5)	2.15 (14.82)	0.0982 (2.72)
	1	36 (91.4)	2.15 (14.82)	0.0982 (2.72)

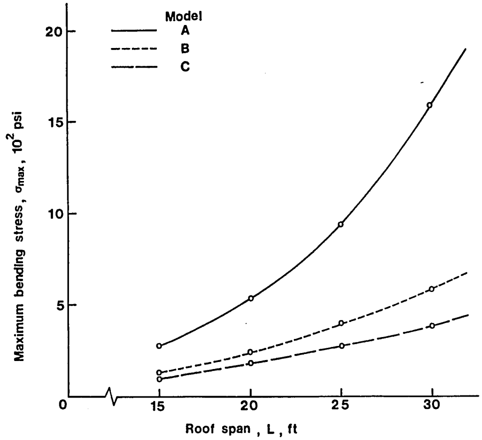

Fig. 3.5. Relationship between roof span and maximum bending stress.

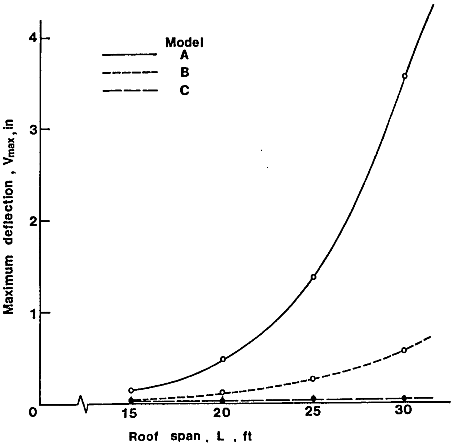

Fig. 3.6. Relationship between roof span and maximum deflection.

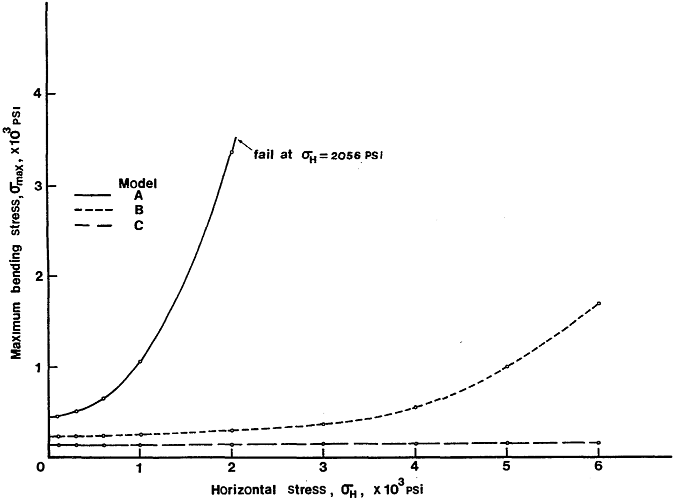

Fig. 3.7. Relationship between horizontal stress and maximum bending stress.

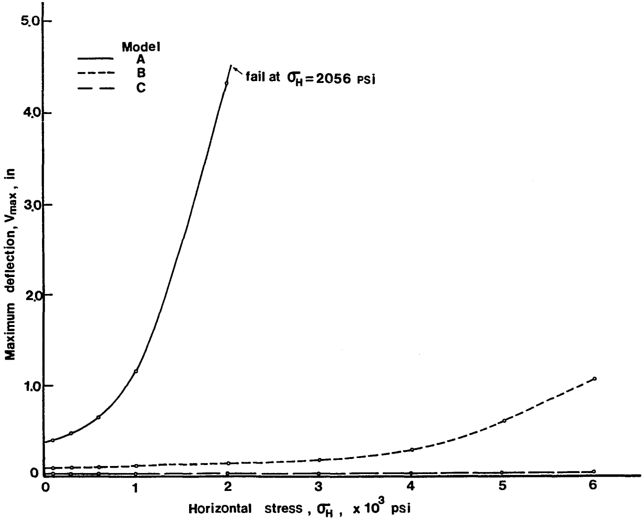

Fig. 3.8. Relationship between horizontal stress and maximum deflection.

various horizontal stresses. For model C, both maximum bending stress and deflection are almost independent of the horizontal stress. For model B, both maximum bending stress and deflection are independent of the horizontal stress when it is below 1000 psi (6.9 MPa) but increase with the horizontal stress when it is higher than 1000 psi (6.9 MPa). When the horizontal stress is very high, i.e., > 4000 psi (27.6 MPa), both the maximum horizontal stress and deflection increase sharply with the horizontal stress. For model A, of which the lowest layer is only 6 in. (15.24 cm) thick, both maximum bending stress and deflection increase sharply with the horizontal stress. When the horizontal stress is 2056 psi (14.18 MPa), the lowest layer fails due to buckling.

Table 3.2 and 3.3 show the results of maximum deflection and maximum bending stress, respectively, for each stratum in model A for various horizontal stresses. Figure 3.9 and 3.10 show the relationships of ratio of change in maximum deflection and maximum bending stress, respectively, for each stratum in model A for various horizontal stresses. It can be seen from both figures that the maximum deflection and maximum bending stress of the upper three thicker strata (No. 3 to No. 5) are not much influenced by the horizontal stress as those of the lower two thinner strata (No. 1 and No. 2). For the uppermost stratum (No. 6) which is the thickest and most stiff, neither maximum deflection nor maximum bending stress is affected by the horizontal stress. In addition, when the horizontal stress is larger than 1250 psi (8.62 MPa), for the lower two thinner strata, the increases of both maximum deflection and

Table 3.2. Maximum Deflection of Each Stratum for Various Horizontal Stresses, Model A

	σ_H = 1 psi	σ_H = 300 psi			σ_H = 1000 psi			σ_H = 2000 psi			σ_H = 3000 psi		
Stratum Number	v_{1max} in.	v_{2max} in.	Δ in.	Δ/v_{1max}	v_{3max} in.	Δ in.	Δ/v_{1max}	v_{4max} in.	Δ in.	Δ/v_{1max}	v_{5max} in.	Δ in.	Δ/v_{1max}
1	0.385	0.481	0.096	0.25	1.173	0.078	2.05	4.306	3.925	10.19	-*	-	-
2	0.298	0.355	0.057	0.19	0.644	0.346	1.16	3.341	3.042	10.21	-*	-	-
3	0.096	0.101	0.005	0.05	0.115	0.109	0.20	0.144	0.048	0.50	0.193	0.097	1.01
4	0.075	0.078	0.003	0.04	0.086	0.011	0.15	0.102	0.027	0.36	0.125	0.050	0.67
5	0.033	0.033	0	0	0.035	0.002	0.06	0.037	0.004	0.12	0.040	0.007	0.21
6	0.004	0.004	0	0	0.004	0	0	0.004	0	0	0.004	0	0

*stratum fail due to buckling

Table 3.3. Maximum Bending Stress of Each Stratum for Various Horizontal Stresses, Model A

	σ_H = 1 psi	σ_H = 300 psi			σ_H = 1000 psi			σ_H = 2000 psi			σ_H = 3000 psi		
Stratum Number	σ_{1max} psi	σ_{2max} psi	Δ psi	Δ/σ_{1max}	σ_{3max} psi	Δ psi	Δ/σ_{1max}	σ_{4max} psi	Δ psi	Δ/σ_{1max}	σ_{5max} psi	Δ psi	Δ/σ_{1max}
1	461	537	76	0.17	1063	602	1.31	3390	2929	6.35	-*	-	-
2	448	504	56	0.13	781	333	0.74	3287	2839	6.34	-*	-	-
3	231	239	8	0.04	261	30	0.13	306	75	0.33	381	150	0.65
4	224	230	6	0.03	246	22	0.10	277	53	0.24	321	97	0.43
5	236	238	2	0.01	245	9	0.04	255	19	0.08	267	31	0.13
6	79	79	0	0	79	0	0	79	0	0	80	1	0.01

*stratum fail due to buckling

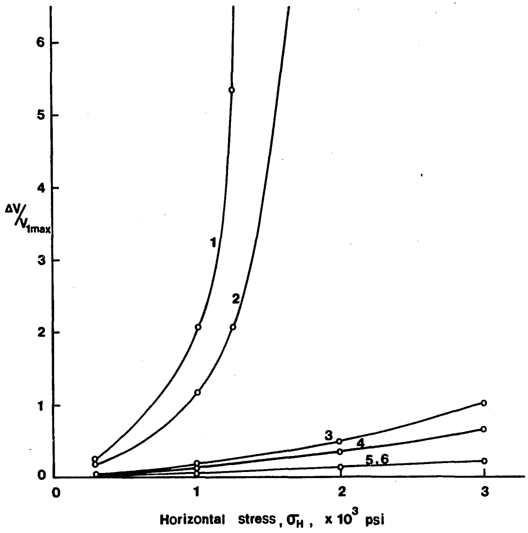

Fig. 3.9. Relationship between horizontal stress and ratio of change in maximum deflection.

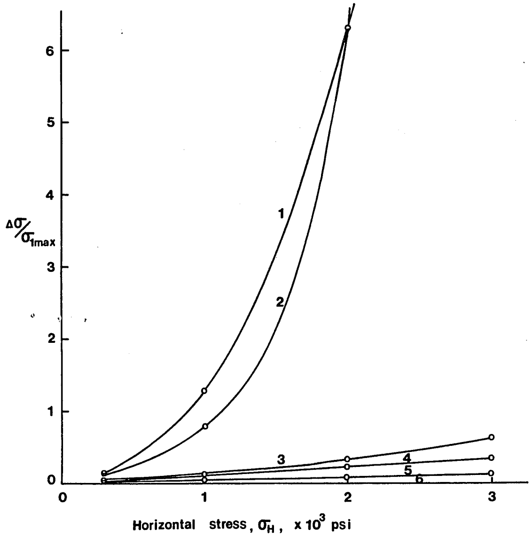

Fig. 3.10. Relationship between horizontal stress and ratio of change in maximum bending stress.

maximum bending stress are very large, i.e., more than two times of its original values, which usually may cause the problem of roof stability.

Figure 3.11 shows the relationship between the horizontal stress and total outer-fiber stress for the three models. It can be seen from this figure that almost all total outer-fiber stresses decrease with the horizontal stress except the total upper-fiber stress for model A, which increases sharply with the horizontal stress. Also, most total outer-fiber stresses are negative, i.e., compressive stresses. This phenomenon implies that in terms of total stress, the horizontal stress is a major factor for strata stability especially when it is very high (43). For instance, when the horizontal stress is greater than 5000 psi (34.48 MPa), all the total outer-fiber stresses are subjected to high compressive stress, i.e., > 4000 psi (27.58 MPa), which may initiate the shear failure in the roof strata. On the other hand, when the horizontal stress is low, i.e., < 200 psi (1.38 MPa), the total upper-fiber stresses for all three models are in tension, which may cause the tensile failure of the roof rock due to its low tensile strength.

3.4.3 Effect of Thickness of the Lowest Stratum

For a single stratum, other things being equal, the thinner is the stratum, the bigger is the deflection. However for the immediate roof made up of multiple strata, the deflection of individual stratum is affected by other strata depending on the flexural rigidity of the strata. Since the lowest stratum is the

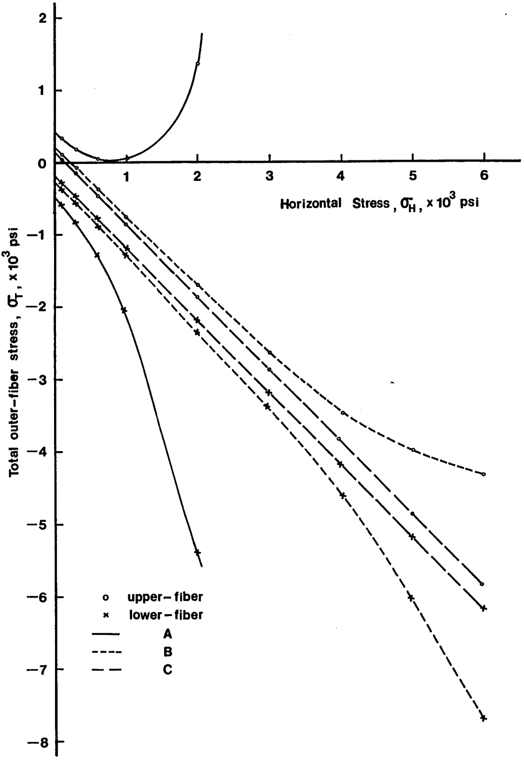

Fig. 3.11. Relationship between horizontal stress and total outer-fiber stress.

one that is visible and is always subjected to the largest bending stress and deflection, the effects of varying its thickness on the flexural behavior of the stratum is investigated.

Figure 3.12 shows the maximum deflection and the maximum bending stress for various thicknesses of the lowest stratum for model B. It is seen that as the thickness increases, both the bending stress and deflection decrease. But when the thickness decrease to one half of its original value, i.e., 6 in. (15.24 cm), both the bending stress and deflection increase sharply. The reason for this is that when the stratum is very thin, it will deflect considerably and separate from the upper strata. Also, it can be seen that if the thickness is doubled, i.e. 24 in. (61 cm), the deflection, 0.039 in. (0.99 mm), is larger than one fourth of the original value, 0.103 in. (2.62 mm), and the bending stress, 186 psi (1.28 MPa) is less than one half of the original value, 244 psi (1.68 MPa). This is mainly due to the added loading from the upper strata, which make the lowest layer deflect more and subject to larger bending stress.

3.4.4 Effect of Young's Modulus of the Lowest Stratum

For a single stratum, other things being equal, the stiffer is the stratum, the smaller is the deflection. But for the immediate roof which consists of multiple strata, the flexural behavior is different. Figure 3.13 shows the maximum deflection and the maximum bending stress for different Young's moduli. When the Young's modulus is doubled, i.e., 1.44×10^6 psi (9,929 MPa),

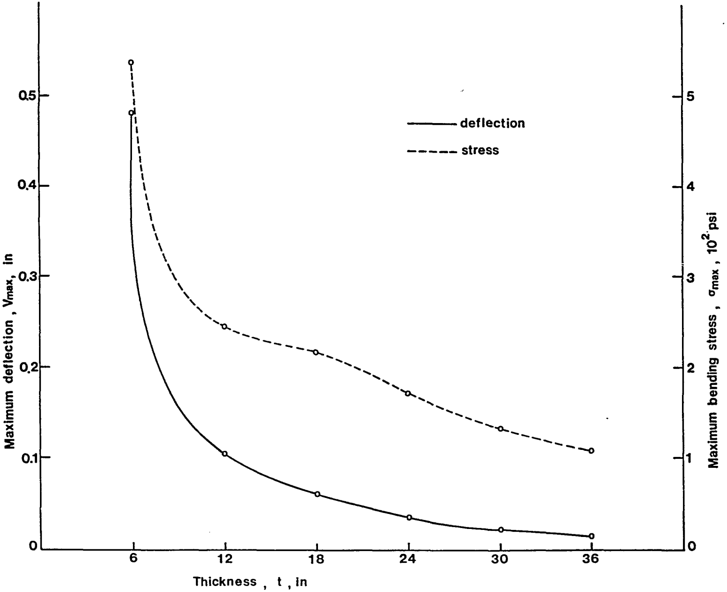

Fig. 3.12. Relationship between maximum deflection, maximum bending stress and thickness of the stratum.

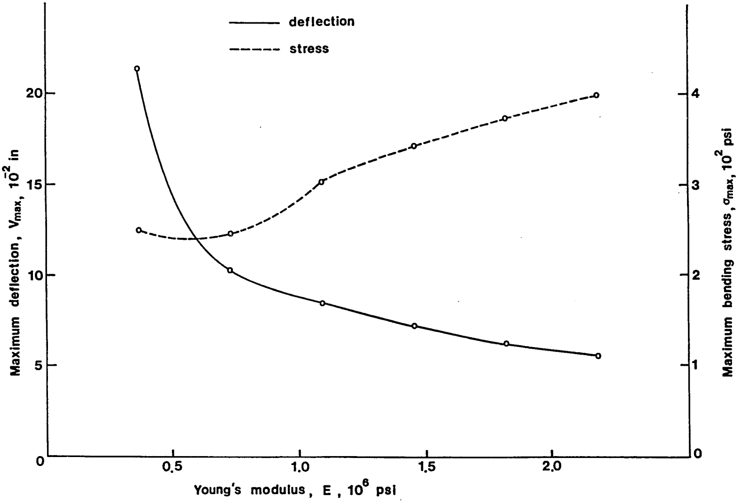

Fig. 3.13. Relationship between maximum deflection, maximum bending stress and Young's modulus of the stratum.

the deflection, 0.072 in. (1.83 mm) is larger than one half of its original value, 0.103 in. (2.62 mm). This is caused by the added loading from the upper strata. Also, the maximum bending stress increase with Young's modulus. This is due to the fact that under a specified amount of deflection, a higher bending stress will be induced in a beam with the higher Young's modulus. Furthermore, when the Young's modulus becomes very small, i.e., 0.32 x 10^6 psi (2,206 MPa), the stratum will deflect more and separate from the upper strata.

3.5 Buckling of Roof Strata

In underground opening, where the in-situ horizontal stress is high, the thinly laminated strata in the lower part of the immediate roof may fail due to buckling (44-46).

Structural analysis can be used to predict the roof stability of coal mine entry. For a beam-column fixed at both ends (see Fig. 3.1), the critical load (due to the horizontal force), P_{cr}, is (42,47)

$$P_{cr} = \frac{4 \pi^2 E I}{L^2} \tag{3.15}$$

where

E = Young's modulus of roof stratum

I = moment of inertia of cross sectional area of the stratum

L = roof span

Then, by comparing Equation 3.15 with the following equation

$$P = \frac{4\ u^2\ E\ I}{L^2} \tag{3.16}$$

which is rearranged from the definition $u = \frac{L}{2}\ (P/EI)^{\frac{1}{2}}$ (see Section 3.2.1). A simple criterion for the buckling of roof stratum, or the limit for the stratum to be stable is obtained, i.e.,

$$u < \pi \tag{3.17}$$

where

$$u = \frac{L}{2}\ (P/EI)^{\frac{1}{2}} \tag{3.18}$$

or

$$u = L(3p/Et^2)^{\frac{1}{2}} \tag{3.19}$$

p = horizontal stress. It is equal to $P/(\beta t)$.

Based on Equations (3.17) and (3.19), a nomograph (Fig. 3.14) is derived, which can be used to find u for any roof stratum under various horizontal stresses. As an example of using this nomograph, u = 1.55 results from the following conditions (follow dotted line abcde):

a = Horizontal stress	σ_H	2000 psi (13.79 MPa)
b = Roof span	L	240 in. (6.096 m)
c = Young's modulus	E	1.0×10^6 psi (6,895 MPa)
d = Stratum thickness	t	12 in. (30.4 cm)
e = u factor	u	1.55

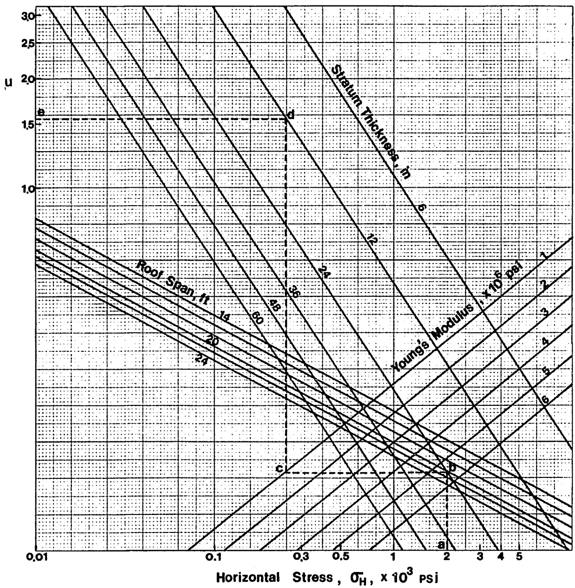

Fig. 3.14. Nomograph for the determination of u.

A further analysis of Fig. 3.14 shows that u increases with increasing roof span (L) and horizontal stress (p), and decreasing Young's modulus (E) and stratum thickness (t). In some underground situations. where the stratum thickness is very small, say, less than 6 in. (15.2 cm) and the in-situ horizontal stress is high, say, larger than 3000 psi (20.69 MPa), u is larger than π (= 3.14). Then, based on Equation 3.17, the roof stratum will fail due to buckling. It should also be noted that for any stratum whose corresponding u value is larger than 3.0, both the bending stress and deflection are greatly increased, i.e., twenty times larger than those whose corresponding u is zero. Therefore, for practical application, whenever u is larger than or equal to 3.0, it will be changed to 3.0 in the analysis of the flexural behavior of the immediate roof.

3.6 Failure Criteria for the Unbolted Roof Strata

For uniformly loaded beam (roof stratum) with fixed-ends, the maximum bending moment is acting at the two ends, where the maximum bending stress and shear stress occur. Since in underground situation, the width of the opening (roof span) is long compared to the thickness of the roof layer (usually with the span-to-thickness ratio greater than 5), the tensile stress is more than three times the shear stress (22,48). Since for the sedimentary rock the tensile strength is usually less than the shear strength, the shear stress can be neglected with little error in the design of roof spans (22,42,48). It should also be noted that because of the existence of horizontal stress, the total stress (i.e., the sum of the bending stress and the horizontal stress) instead of the bending stress should be taken into consideration (8). Furthermore, since the tensile strength is not equal to the compressive strength for most sedimentary rock, the failure conditions for tension and compression must be considered separately (22,49).

Based on the foregoing discussion, the following failure criteria are used in this research (6-8,49)

(i) $\sigma_{TU} \leq C_T$ in tension (3.20)

(ii) $|\sigma_{TL}| \leq C_p$ in compression (3.21)

where σ_{TU} = total upper-fiber stress

$= \sigma_H + \sigma_{max}$ (3.22)

σ_{TL} = total lower-fiber stress

$= \sigma_H - \sigma_{max}$ (3.23)

C_T = tensile strength of rock

C_p = compressive strength of rock

σ_H = horizontal stress (compressive)

σ_{max} = bending stress, expressed in tensile stress

Substituting Equations 3.4 and 3.14 into Equations 3.20 and 3.21 respectively, the failure criteria for the unbolted roof are obtained.

(a) Individual Stratum

(i) $\sigma_H + \frac{wL^2}{2t} F \leq C_T$ in tension (3.24)

(ii) $|\sigma_H - \frac{wL^2}{2t} F| \leq C_p$ in compression (3.25)

(b) Combined Stratum

(i) $\sigma_H + \frac{w_{1a} L^2}{2t_1} F \leq C_T$ in tension (3.26)

(ii) $|\sigma_H - \frac{w_{1a} L^2}{2t_1} F_1| \leq C_p$ in compression (3.27)

Where F is a function of u (see p. 32), it can be determined immediately from Fig. 3.15. Moreover, it should be noted that for combined stratum only the lowest layer is considered because it is the most critical one.

According to Equation 3.24 through 3.27, Fig. 3.16 and Fig. 3.17 are derived based on L = 20 ft. (6.09 m), w = 160 lb/ft^3 (2.56 g/cm^3) and E = 1.0 x 10^6 psi (6,893 MPa) which are representative values. Figure 3.16 shows the relationship between the total upper-fiber stress and the thickness of the stratum for various horizontal stresses. It can be seen from this figure that in order to prevent failure in the upper fiber, either the tensile strength of the rock should be larger than the induced tensile stress when the horizontal stress is low or the compressive strength of the rock should be larger than the induced compressive stress when the

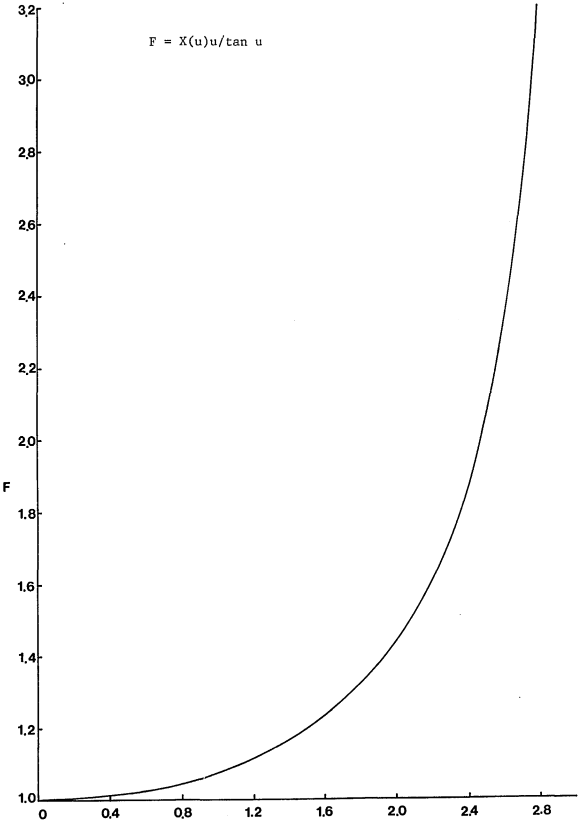

Fig. 3.15. Relationship between u and F.

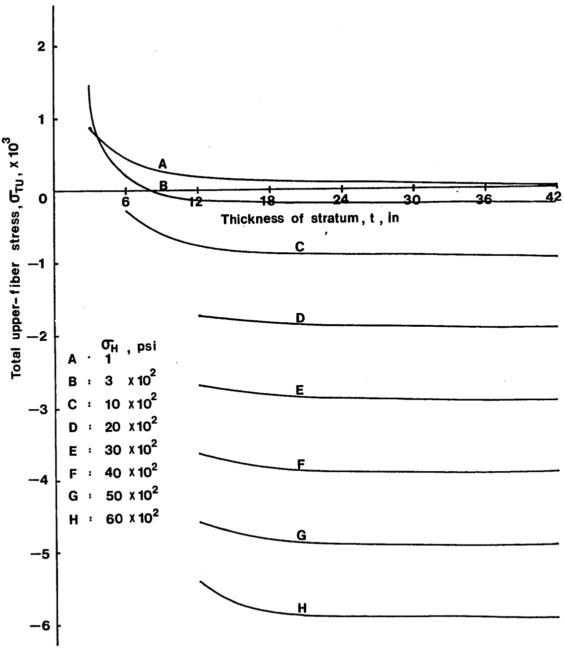

Fig. 3.16. Relationship between thickness of stratum and total upper-fiber stress for various horizontal stresses. $L = 20$ ft, $w = 160$ lb/ft^3, $E = 1 \times 10^6$ psi

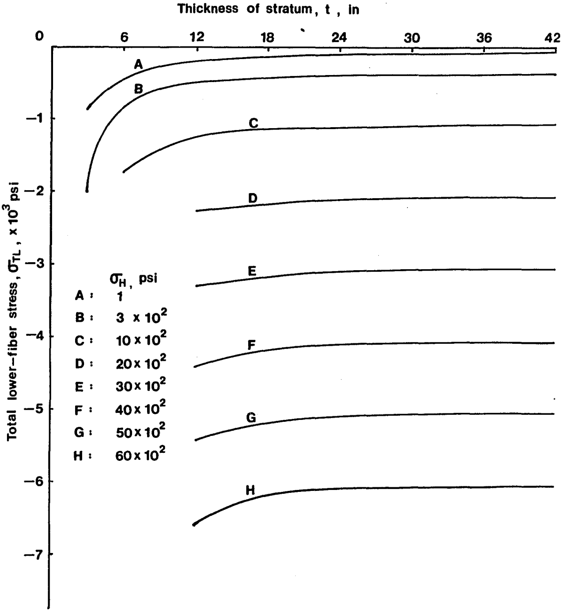

Fig. 3.17. Relationship between thickness of stratum and total lower-fiber stress for various horizontal stresses. L = 20 ft, w = 160 lb/ft^3, E = 1 x 10^6 psi

horizontal stress is high. It can also be found that when the horizontal stress is larger than 2000 psi (13.79 MPa), the thinner stratum (i.e., < 12 in. or < 30.5 cm) will fail due to buckling. Figure 3.17 shows the relationship between the total lower-fiber stress and the thickness of the stratum for various horizontal stresses. It can be seen from this figure that in order to prevent failure, the required compressive strength of the rock to overcome the induced compressive stress varies with the horizontal stress, with the higher compressive strength for higher horizontal stress. Also, when the horizontal stress is high, i.e., > 2000 psi (13.79 MPa), the thinner stratum (i.e., < 12 in. or < 3.05 cm) will fail due to buckling. It should also be noted for the horizontal stress which is not shown in the graph, the relationship between the total outer-fiber stress and the thickness of the stratum still can be found by interpolation in both figures.

Based on Equations 3.24 through 3.27, a computer program is written for the evaluation of stability for a generalized immediate roof (the computer program is listed in Appendix II). From this computer program, once the information about any immediate roof such as material properties, strata sequence, opening geometry and in-situ horizontal stresses is used as the input, the stability condition of the immediate roof (i.e., whether it fails or not) will be determined and printed out in the output.

CHAPTER 4

THEORETICAL ANALYSIS OF REINFORCEMENT MECHANISMS FOR MECHANICAL BOLTING

4.1 Suspension Effect

4.1.1 Reinforcement Mechanism

Generally, the suspension effect through roof bolting in the underground openings is to transfer a portion of the weight of the lower weaker strata to the upper competent strata. The reinforcement mechanism of the beam suspension effect which is valid for this condition (see definition in page 18) is investigated in this research. But the effect of simple suspension is excluded.

Throughout the analysis of reinforcement mechanisms of suspension effect, the following conditions are assumed (Fig. 4.1):

(1) Each stratum is homogeneous, isotropic, and elastic.

(2) All strata in the immediate roof are constrained to have equal deflections at bolt locations due to adequate tension of roof bolts.

(3) There is no friction (or interaction) at the contact points between the roof strata.

(4) Each stratum is subjected to both transverse loading (due to the self weight of each stratum and the load transferred through bolting) and axial loading (due to in-situ horizontal stress).

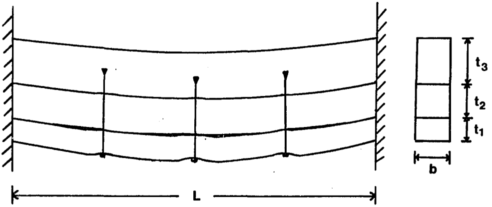

Fig. 4.1. Schematic illustration of suspension effect.

(5) The transferred load through roof bolting acts as a point (or concentrated) load.

(6) The horizontal stress is uniformly applied to each stratum.

For this type of reinforcement mechanism to be applicable, the strata sequence of the immediate roof should be such that the deflection of each stratum is larger than that of its upper stratum. However, this kind of strata sequence is not limited to the original strata sequence such as strate type A (see Fig. 1.1). It can also be applied to strata type B (see Fig. 1.1) as long as the final strata sequence (after strata combination) is of such an order. Figure 4.1 shows the general sequence of the fixed-end rectangular beams, having common span L and width B. For simplicity, only three layers and three bolts are shown in the figure. However, for general application, the number of roof layers and roof bolts can be arbitrary. The numbering sequence for the roof layers is increasing from the lower to the upper layers.

Since in this type of the immediate roof each stratum will deflect independently without roof bolting. Thus separation will occur between strata. Moreover, the lower strata may subject to very high bending stress at the support ends (i.e., ribs), which will either cause tensile failure or initiate shear failure (see Section 3.4.2). The function (or mechanism) of roof bolting in this type of immediate roof is: (a) to decrease the deflection and (b) to decrease the bending stress of the weaker strata.

However it should be noted that, in the meantime, the deflection and bending stress of the competent stratum (or strata) are increased. Therefore, the load transferred by roof bolting is not without a limit. Rather it is dependent on the flexural rigidities and strengths of both the weaker and competent strata. Furthermore, for the optimum design of the bolting pattern and bolt tension, it should also consider the anchorage capacity of the anchoring horizon (or stratum), which will be discussed in Chapter 5.

Figure 4.2 shows a general procedure for determining the suspension effect in terms of the deflection, bending stress, transferred bolt load, and bolt tension in this section. The step-by-step analysis is discussed as follows:

For the i-th layer in the bolted roof, its deflection at the bolt locations, v_{Bi}, is composed of two parts, v_i and Δv_i,

$$v_{Bi} = v_i + \Delta v_i \tag{4.1}$$

where v_i is the deflection before bolting and Δv_i is the additional deflection due to the transferred bolt load. It should be noted that in the calculation of v_i and Δv_i, the horizontal stress is applied simultaneously.

Equation 4.1 can be expressed in another form, i.e.,

$$v_{Bi} = v_i + R_i\, v_i \tag{4.2}$$

$$= (1 + R_i)v_i \tag{4.3}$$

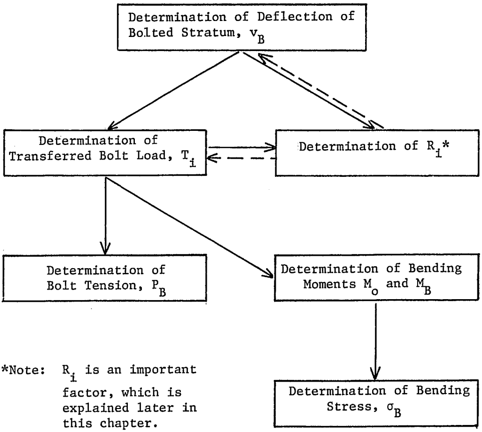

Fig. 4.2. Block diagram illustrating the procedure for determination of suspension effect.

where

$$R_i = \Delta v_i / v_i \tag{4.4}$$

Equation 4.2 implies that the additional deflection due to the transferred bolt load is a fraction of the deflection of the unbolted layer.

The deflection, v_i, due to the self weight of the i-th layer can be determined based on the beam-column theory (42)(the derivation of equation for v_i is given in Appendix I). The additional deflection, Δv_i, due to the transferred bolt load is obtained by assuming the load to be a concentrated one. For example, for one bolt installed at the center of the roof span, the deflection at this location is obtained as (see Equation A.1.21 in Appendix I)

$$\Delta v_i = \frac{T_i \; L^3}{192 \; E_i \; I_i} S_i \tag{4.5}$$

where T_i is the bolt load (concentrated load) in the i-th layer. By equating Equation 4.4 and Equation 4.5, the following equation is obtained:

$$\Delta v_i = \frac{T_i \; L^3}{192 \; E_i \; I_i} S_i = R_i \; v_i \tag{4.6}$$

Since the deflection of the center of the roof span is maximum, v_i is equal to v_{max} in Equation 3.2. Substituting Equation 3.2 into Equation 4.6 gives

$$\frac{T_i L^3}{192 E_i I_i} S_i = R_i \frac{q_i L^4}{384 E_i I_i} S_i \tag{4.7}$$

or

$$T_i = \frac{R_i q_i L}{2} \tag{4.8}$$

The transferred bolt load T_i for more than one roof bolt can be obtained in a similar way (the detailed derivation is given in Appendix I):

$$T_i = \alpha R_i q_i L \tag{4.9}$$

where α is a coefficient depending on the number and the locations of bolts with $\alpha = \frac{1}{2}$ when only one bolt is installed at the center. The equations for α for more than one bolt are given in the Appendix I.

It should also be noted that T_i is the transferred bolt load for the i-th layer. When only one bolt is used, T_i is equal to the transferred load for that bolt. But when more than one bolt is used, T_i is the sum of all transferred bolt loads in the i-th layer. Therefore, for N bolts in a row, T_i becomes:

$$T_i = \sum_{k=1}^{N} T_{ik} \tag{4.10}$$

where T_{ik} is the transferred load for each of the N bolts in a row.

The total transverse load to be supported by the i-th layer, W_i, is the sum of the weight of the layer and the transferred bolt load,

$$W_i = q_i L + T_i \tag{4.11}$$

The total transverse load on the whole bolted roof layers is equal to the sum of the weights of all roof layers,

$$\sum_{i=1}^{n} W_i = \sum_{i=1}^{n} q_i L \tag{4.12}$$

By summing both sides of Equation 4.11 and then equating it with Equation 4.12, the following equation is obtained:

$$\sum_{i=1}^{n} T_i = 0 \tag{4.13}$$

Equation 4.13 implies that the sum of the bolt loads transferred to the competent layers (positive value) is equal to the sum of the bolt loads transferred from the weak layers (negative value), i.e.,

$$\sum_{i=1}^{n-m} T_i\ (+) = - \sum_{i=n-m+1}^{n} T_i\ (-) \tag{4.14}$$

where m and n-m are the numbers of weak layers and competent layers, respectively.

Since the function of bolts in suspension effect is to transfer the bolt load from the weak strata, i.e., $\sum_{i=n-m+1}^{n} T_i\ (-)$, to the competent strata which provide the load, $\sum_{i=1}^{n-m} T_i\ (+)$, the following equation is therefore obtained:

$$\sum_{j=1}^{N} P_{Bj} = \sum_{i=1}^{n-m} T_i \, (+) = - \sum_{i=n-m+1}^{n} T_i \, (-) \tag{4.15}$$

where P_B is the bolt load (or bolt tension) for each bolt.

When the bolt load is the same for all bolts, Equation 4.15 becomes

$$N \, P_B = \sum_{i=1}^{n-m} T_i \, (+) = - \sum_{i=n-m+1}^{n} T_i \, (-) \tag{4.16}$$

For a fixed-end beam subjected to transverse loading and axial loading simultaneously, the maximum moment is at the supports (i.e. two fixed-ends)(42). At this cross-section, the maximum bending stress occurs at the farthest fiber from the neutral axis, with the tensile stress (positive value) at the uppermost fiber and the compressive stress (negative value) at the lowermost fiber (Fig. 4.3)(50). In this research, the equations related to the maximum bending stress are expressed in terms of the tensile stress.

The maximum bending stress of the i-th layer in the bolted roof, σ_{Bi}, can be expressed as follows:

$$\sigma_{Bi} = \sigma_{imax} + \Delta\sigma \tag{4.17}$$

where σ_{imax} is the maximum bending stress before bolting and $\Delta\sigma$ is the additional bending stress due to the transferred bolt load. To simplify notation, i is omitted from the subscripts in the equations related to the bending stress.

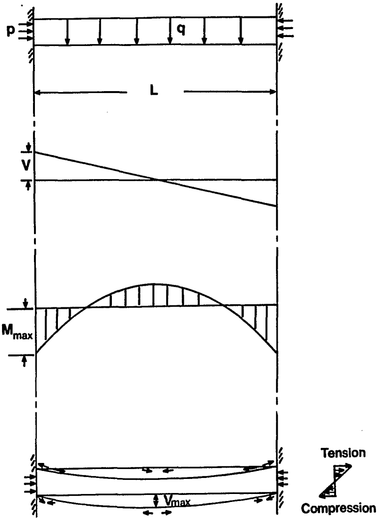

Fig. 4.3. Diagram for a fixed-end beam subject to uniform transverse and axial loadings (50).

Equation 4.17 can also be exppresed in another form, i.e.,

$$\sigma_B = \frac{6\ M_o}{b\ t^2} + \frac{6\ M_B}{b\ t^2} \tag{4.18}$$

$$= (1 + \frac{M_B}{M_o}) \frac{6\ M_o}{b\ t^2} \tag{4.19}$$

$$= K \frac{6\ M_o}{b\ t^2} \tag{4.20}$$

$$= (1 + \beta R) \frac{6\ M_o}{b\ t^2} \tag{4.21}$$

where M_o = bending moment due to the self weight of stratum

M_B = bending moment due to function of roof bolting

$\beta R = M_B/M_o$

$K = 1 + \beta R$

β = factor depending on number and location of roof bolts

It should also be noted that horizontal stress has been considered in the derivation of both bending moments.

The equations of bending moment due to the self weight and roof bolting are derived based on the beam-column theory. The detailed derivation is given in Appendix I. But the most important equations are listed as follows:

(a) the maximum bending moment due to self weight, M_o (Fig. 3.1)

$$M_o = -\frac{q\ L^2}{12} \frac{X(u)}{\tan u/u} \tag{4.22}$$

(b) the maximum bending moment due to roof bolting, M_B (Fig. 4.4)

(i) one bolt at the center of the span, M_{B1}

$$M_{B1} = - \frac{T_{1c}\, L}{8} \frac{\lambda(u)}{\tan u/u} \tag{4.23}$$

(ii) two bolts at symmetric locations, M_{B2}

$$M_{B2} = - \frac{T_{21}\, L}{2\, u \tan u}\left[\frac{\cos(u - 2uml) - \cos u}{\cos u}\right] \tag{4.24}$$

(iii) three bolts; one bolt at center, two bolts at symmetric locations, M_{B3}

$$M_{B3} = - \frac{L}{4\, u \sin u}[T_{3c}(1 - \cos u) - 2\, T_{31}(\cos u - \cos(u - 2uml))] \tag{4.25}$$

(iv) four bolts at symmetric locations, M_{B4}

$$M_{B4} = - \frac{L}{2\, u \tan u}\left[T_{41}\left(\frac{\cos(u - 2uml) - \cos u}{\cos u}\right) + T_{42}\left(\frac{\cos(u - 2um2) - \cos u}{\cos u}\right)\right] \tag{4.26}$$

(v) five bolts; one bolt at center, four bolts at symmetric locations, M_{B5}

$$M_{B5} = - \frac{L}{4\, u \sin u}[T_{5c}(1 - \cos u) - 2\, T_{51}(\cos u - \cos(u - 2uml)) - 2\, T_{52}(\cos u - \cos(u - 2um2))] \tag{4.27}$$

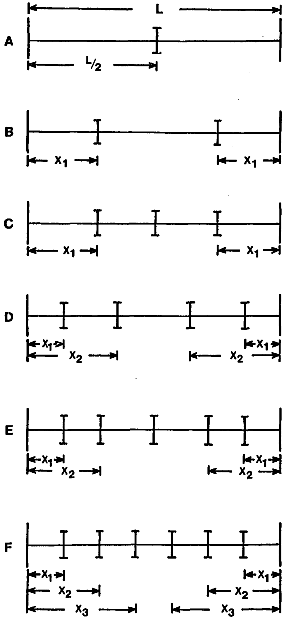

Fig. 4.4. Various locations for different number of roof bolts.

(vi) six bolts at symmetric locations, M_{B6}

$$M_{B6} = - \frac{L}{2\ u\ \tan u}[T_{61}(\frac{\cos(u - 2um1) - \cos u}{\cos u})$$

$$+ T_{62}(\frac{\cos(u - 2um2) - \cos u}{\cos u})$$

$$+ T_{63}(\frac{\cos(u - 2um3) - \cos u}{\cos u})] \tag{4.28}$$

where T_{1c}, T_{21}, T_{31}, ..., T_{63} are bolt loads at various locations for different number of roof bolts per row; the first subscript refers to the number of roof bolts per row while the second subscript refers to the location of each bolt. Subscript c refers to the center of the roof span and subscripts 1, 2 and 3 refer to the first, second and third bolt from the ribs, respectively.

m1, m2, m3 are ratios of distance of bolt from ribs to the roof span for the first, second, and third bolt. They are equal to X_1/L, X_2/L, and X_3/L, respectively.

From Equations 4.1 through 4.26, it can be found that in order to determine the deflection and the bending stress, R_i must be first determined. The determination of R_i is therefore a very important step. The procedure for determining R_i for each stratum in the bolted roof is illustrated in the following paragraphs.

Based on the assumption #2 made in p. 66 and Equation 4.3, the following equation is obtained for the deflections at the bolt locations for the bolted roof strata.

$$(1 + R_1) \frac{c\, S_1\, q_1\, L^4}{384\, E_1\, I_1} = (1 + R_2) \frac{c\, S_2\, q_2\, L^4}{384\, E_2\, I_2}$$

$$= \ldots = (1 + R_n) \frac{c\, S_n\, q_n\, L^4}{384\, E_n\, I_n} \qquad (4.29)$$

where c is a coefficient depending on the locations of the bolts, with c = 1 when one bolt is at the center of the roof span.

Equation 4.27 can be simplified as

$$(1 + R_1) \frac{S_1\, q_1}{E_1\, I_1} = (1 + R_2) \frac{S_2\, q_2}{E_2\, I_2} = \ldots$$

$$= (1 + R_n) \frac{S_n\, q_n}{E_n\, I_n} \qquad (4.30)$$

From Equation 4.28, the expression for each R_i can be determined in terms of one of the others, say R_1,

$$R_i\, q_i = \frac{(1 + R_1) q_1\, S_1\, E_i\, I_i}{E_1\, I_1\, S_i} - q_i \qquad (4.31)$$

Substituting T_i in Equation 4.9 into Equation 4.13, the following equation is obtained:

$$\alpha\, R_1\, q_1\, L + \alpha\, R_2\, q_2\, L + \ldots. + \alpha\, R_n\, q_n\, L = 0 \qquad (4.32)$$

or

$$R_1\, q_1 + R_2\, q_2 + \ldots. + R_n\, q_n = 0 \qquad (4.33)$$

Substituting Equation 4.31 into Equation 4.33 and rearranging, the expression for R_1 becomes:

$$R_1 = \frac{\dfrac{\sum_{k=1}^{n} q_k}{\sum_{k=1}^{n} \dfrac{E_k\, I_k}{S_k}}}{\dfrac{q_1}{\dfrac{E_1\, I_1}{S_1}}} - 1 \qquad (4.34)$$

Similarly, the expression for R_i is obtained as

$$R_i = \frac{\dfrac{\sum_{k=1}^{n} q_k}{\sum_{k=1}^{n} \dfrac{E_k\, I_k}{S_k}}}{\dfrac{q_i}{\dfrac{E_i\, I_i}{S_i}}} - 1 \qquad (4.35)$$

From Equation 4.35 the characteristics of R_i are:

(i) it is dependent on the flexural rigidity of the stratum itself and other strata in the bolted roof.

(ii) it is independent of the number of the bolts per row and hence the bolt spacing per row.

(iii) it is independent of the bolt load (tension).

(iv) it is affected by the horizontal stress on the stratum itself and on the other strata in the bolted roof.

(v) it can be positive or negative, with -1 as the limit of negative value. When R_i is positive, T_i

is also positive (see Equation 4.9), i.e., the transferred bolt load is added to the stratum, which will increase the maximum bending stress and deflection of that stratum. When R_i is negative, i.e., the transferred bolt load is substracted from the stratum, which will decrease the maximum bending stress and deflection of that stratum.

4.1.2 Failure Criteria for the Bolted Strata

In order to safely reinforce the immediate roof by suspension effect, the bolted strata must be in stable condition, i.e., no failure will occur in the bolted roof strata.

The failure criteria for the bolted roof strata are

$$\sigma_H + \sigma_B \leq C_T \quad \text{in tension} \tag{4.36}$$

or

$$|\sigma_H - \sigma_B| \leq C_p \quad \text{in compression} \tag{4.37}$$

where σ_B is expressed in Equation 4.18.

Equations 4.36 and 4.37 are basically the same as Equations 3.17 and 3.18, except that σ_B, instead of σ_{max}, is used in the former. It should also be noted that σ_B is different for different bolt number and bolt location in each row (see Equations 4.18 through 4.28). Furthermore, Equations 4.36 and 4.37 should be held for each stratum of the bolted strata to assure the integral stability.

4.2 Friction Effect

In some underground coal mines, there is no competent roof stratum within a reasonable distance above the roofline from which roof bolts can be anchored to suspend the lower weaker roof strata. Under this condition, the successful application of roof bolting to reinforce the immediate roof is by friction effect (or beam-building effect) (Fig. 4.5) (3).

4.2.1 Reinforcement Mechanism

The reinforcement of a horizontally bedded roof by the friction effect results from the clamping action of the tensioned roof bolts, which creates a frictional resistance to slip on the interface between the bedding planes and thus "building up" a single layer from several individual layers. Thereby the flexure of the roof strata is decreased and the stability of roof is increased. The function performed by roof bolts can be explained as follows:

Consider a single beam of thickness t and a multiple beam having four members each with thickness $t_1 = t/4$ (Fig. 4.6). Each member of the multiple beam is assumed to be made of the same material and having no interconnection among them. The beams considered have fixed ends and subject to uniformly transverse loading. The deflection of the thick beam will be only 1/16 of that of the four thin beams since the deflection of any beam is inversely proportional to the square of its thickness (see Equation 3.2). The maximum bending stress in the thick beam will be one-fourth of that in the four thin beams since the bending stress of any beam is inversely

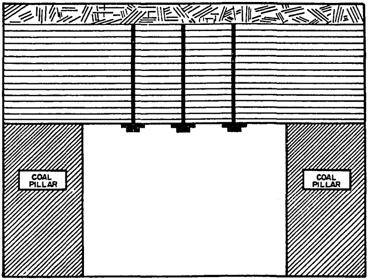

Fig. 4.5. Friction effect of roof bolting (3).

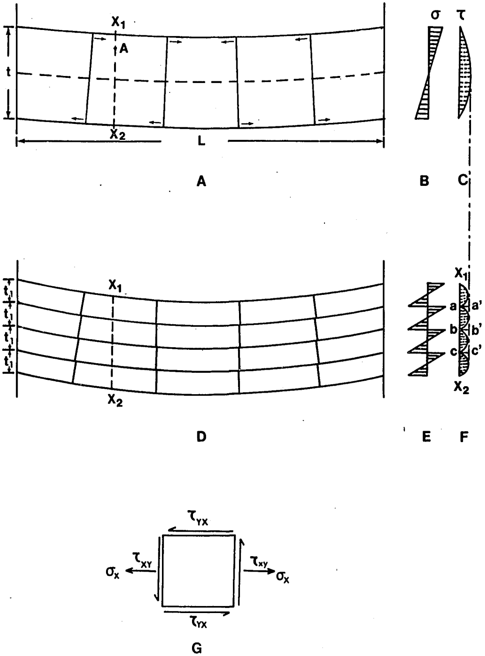

Fig. 4.6. Flexure of a fixed-end beam subject to transverse uniform loading: (A)(B)(C) - single thick layer; (D)(E)(F) - 4 thin layers; and (G) - stresses acting on an element at A.

proportional to its thickness (see Equation 3.4) (Fig. 4.6.B and Fig. 4.6.E). The difference between the two situations results in the slip along the individual layer interfaces. Figure 4.6.C shows that there is no discontinuity in shear stress distribution from top to bottom of the thick layer, while Fig. 4.6.F shows that the shear stress in each thin layer being maximum at the neutral axis drops to zero at the outer fiber, i.e., at the interface. Since the maximum shear stress, $(\tau_{xy})_{max}$, at any section is directly proportional to the span and is independent of the thickness, i.e.,

$$(\tau_{xy})_{max} = \frac{3\ w\ L}{4} \tag{4.38}$$

the maximum shear stress of each thin layer at the neutral axis is still equal to that of the thick layer even though the shear stress is nonexistent at the interface. It should also be noted that the shear stress acts horizontally as well as vertically, as shown in Fig. 4.6.G.

The foregoing discussion illustrates the major function of the roof bolting, that is, to increase the shear resistance along the interface, inhibiting slip and reducing the bending stress (4,30). If sufficient shear resistance is provided to prevent slip between the layers, then the four-member layer will behave as a single beam of the same total thickness. In order to achieve this, the required shear resistance should be of such magnitude that it can offer the shear stress of magnitude aa', bb' and cc' at three levels in cross section X_1X_2, which are necessary to cause the shear stress to be continuous (Fig. 4.6.F)(4). For mechanical roof bolting, this very shear resistance is caused by the clamping force due to the tensioning of roof bolts. Since all layers are clamped together under the bolt tension which is perpendicular to the bedding plane, the associated frictional (shear) force will create a shear resistance to slip along the interface. Therefore the individual layers being "built up" into a single thick layer will have less flexure and smaller bending stress than that of original ones; in other words, the stability of the roof strata is increased.

It is important to note that in the above discussion the assumption of the same material in each layer is merely made for illustration. For general application, there is no such limitation. As long as the deflection of each layer is smaller than or equal to that of the overlying layers, this reinforcing mechanism is applicable. From the discussion made in Chapter 3, the immediate roof of strata sequence C belongs to this category. Also, this type of reinforcement mechanism can be applied to strata type B if the strata sequence after strata combination is of such an order.

In this analysis, it is assumed that the frictional resistance is only caused by the clamping force due to tensioning of the roof bolts. The effect of the bolt itself is neglected. This is reasonable for mechanical bolting, because the bolt is only anchored at two ends with the remaining part of the bolt separated from the wall of the borehole. It is also assumed that the coefficient of friction along the interface between the bedding planes is constant. In addition, the small deflection theory is applicable and employed (51).

Based on the foregoing discussion, the theoreticl equations with regard to the friction effect are derived as follows:

For simplicity of illustration, a two-layer beam bolted by four bolts is considered (Fig. 4.7). First, the shear flow, Q, i.e., the shear force per unit length (47) in the interface of the two layers is determined:

$$Q = \frac{V\,I_A}{I_z} \tag{4.39}$$

where V = shear force at any section

I_A = statical moment of area of lower (or upper) layer around the neutral axis of the whole section, i.e. $\int_{\text{area fghj}} y\, dA$

I_z = moment of inertia around the neutral axis of the whole section, i.e., $\int y^2\, dA$

Since for a fixed-end beam subject to uniformly transverse loading, the shear force varies from maximum at two ends to zero at the center of the span (Fig. 4.3 and Fig. 4.7), the proper location or spacing of the roof bolts should be such that more bolts need to be installed toward the ends of the beam while no bolt is necessary at the center of the span (30,33,52,53). Furthermore, in order to have each bolt subject to equal shear force which is required for

A

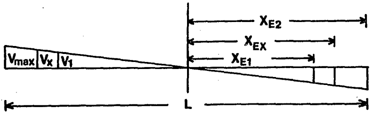

B

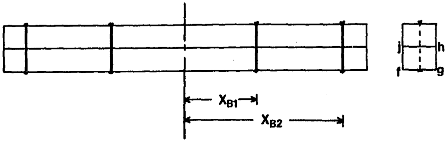

Fig. 4.7. (A) Equal shear force diagram.
(B) Bolt spacing based on "equal shear force" concept.

maintaining the equilibrium of the force system on both sides of each bolt, the "equal shear force" concept should be considered in the determination of proper bolt spacing.

Based on the foregoing discussion and the principle of geometric similarity, the equations related to the segment of equal shear force and bolt spacing can be derived as follows:

(1) one bolt in half of the span (i.e., two bolts in a row)

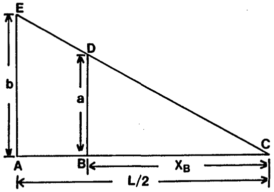

Fig. 4.8. Equal shear force diagram, one bolt.

Since each bolt is subjected to equal shear force on both sides, i.e., Area ABDE = Area BCD, or Area BCD = ½ Area ACE, which can be expressed as

$$\frac{a\ X_B}{2} = \frac{b}{2}\left(\frac{L}{2}\right) \qquad (4.40)$$

or

$$a = \frac{b}{X_B}\left(\frac{L}{2}\right) \tag{4.41}$$

Triangle BCD is similar to triangle ACE. From the similarity of geometry,

$$\frac{a}{b} = \frac{X_B}{L/2} \tag{4.42}$$

Substituting Equation 4.42 into Equation 4.41 and rearranging, we get

$$2\,X_B^2 = \left(\frac{L}{2}\right)^2 \tag{4.43}$$

or

$$X_B = \left(\frac{1}{2}\right)^{\frac{1}{2}}\left(\frac{L}{2}\right) = 0.707\left(\frac{L}{2}\right) \tag{4.44}$$

In this case, there is only one segment of equal shear force. The distance between the center of the span and the left end of this segment is L/2, i.e. $X_E = L/2$

(2) Two bolts in half of the span (i.e., four bolts in a row)

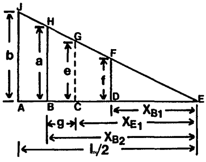

Fig. 4.9. Equal shear force diagram, two bolts.

In this case, there are two segments of equal shear force in half of the span, i.e., Area CEG = Area ACGJ. From the previous discussion, we get $X_{E1} = (\frac{1}{2})^{\frac{1}{2}} (\frac{L}{2})$. Similarly, since Area DEF = Area CDFG, we get $X_{B1} = (\frac{1}{2})^{\frac{1}{2}} (X_{E1}) = \frac{1}{2} (\frac{L}{2})$.

In area ACGJ, since Area BCGH = Area ABHJ, then

$$\frac{a + e}{2} g = \frac{1}{2} \frac{b + e}{2}(\frac{L}{2} - X_{E1}) = \frac{1}{2}(b + e)(0.293)\frac{L}{2} \qquad (4.45)$$

or

$$(a + e)g = \frac{1}{2}(b + e)(0.293)L \qquad (4.46)$$

Since $\frac{e}{b} = \frac{X_{E1}}{L/2}$ we get $e = 0.707b(\frac{L}{2})$

Also, from $\frac{a}{b} = \frac{0.707(\frac{L}{2}) + g}{\frac{L}{2}}$, we get $a = (0.707b + bg)$

Substituting e and a into Equation 4.46, we get

$$1.414\ bg + bg^2 = 0.25\ b$$

Solving for this equation, we get

$$g = 0.159\ (\frac{L}{2})$$

Furthermore

$$X_{B2} = X_{E1} + g = 0.707\ (\frac{L}{2}) + 0.159\ (\frac{L}{2}) = 0.866\ (\frac{L}{2})$$

$$= (\frac{3}{4})^{\frac{1}{2}} (\frac{L}{2}) \qquad (4.47)$$

The derivation of X_E and X_B for more than two bolts (in half of the roof span) can be obtained in a similar way.

Therefore, for N bolts in a row, the following equations are obtained:

(i) Segment of equal shear force

$$X_{Ei} = \left(\frac{2i}{N} \right)^{\frac{1}{2}} \frac{L}{2}, \qquad i = 1, 2, \ldots, N/2 \qquad (4.48)$$

where X_{Ei} is the distance between the center of the span and the rib end of the i-th segment.

(ii) Bolt spacing in each row

$$X_{Bi} = \left(\frac{2i - 1}{N} \right)^{\frac{1}{2}} \frac{L}{2}, \quad i = 1, 2, \ldots, N/2 \qquad (4.49)$$

It should be noted that the number of segment of each shear force is equal to that of the bolts in each row.

For the case shown in Fig. 4.7, the corresponding X_{Ei} and X_{Bi} are obtained from Equations 4.48 and 4.49, respectively; they are

$$X_{E1} = 0.354L; \; X_{E2} = 0.5L \text{ and } X_{B1} = 0.25L, \; X_{B2} = 0.433L$$

Based on the principle of geometric similarity, the shear force, V_x at any section can be determined by

$$V_x = V_{max} \frac{X_{Ex}}{(L/2)} \qquad (4.50)$$

where V_{max} = maximum shear force at two ends

X_{Ex} = distance between the center of the span and the concerned interval of equal shear force

In the case shown in Fig. 4.7, $V_x = V_{max} \frac{0.354L}{(L/2)} = 0.708\ V_{max}$. The average shear flow, Q_{ave}, for the farthest segment is

$$Q_{ave} = \frac{Q_{N/2-1} + Q_{N/2}}{2} \tag{4.51}$$

where $Q_{N/2-1}$ = shear flow at $X_{E(N/2-1)}$; it is equal to

$$\frac{V_{(N/2-1)}\ I_A}{I_z}$$

$Q_{N/2}$ = shear flow at $X_{E(N/2)}$; it is equal to

$$\frac{V_{N/2}\ I_A}{I_z}$$

By multiplying Q_{ave} by the length in that segment, the average shear force, F_{SA}, in that segment is obtained

$$F_{SA} = Q_{ave}[\frac{L}{2} - X_{E(N/2-1)}] \tag{4.52}$$

Since each bolt is subjected to equal force, F_{SA} in Equation 4.52 is actually valid for any other interval.

The required bolt tension, P_B, is, therefore, obtained by dividing F_{SA} by the coefficient of friction along the interface, μ,

$$P_B = F_{SA}/\mu \tag{4.53}$$

For the case shown in Fig. 4.7, $P_B = 0.146\ Q_{ave}\ L/\mu$.

It should be noted that the procedure for determining the bolt spacing and bolt tension described above can also be applied to the roof strata made up of multiple layers with different material properties and thicknesses. However, under this condition, several points must be carefully considered in order to achieve proper results. First, for roof strata made of different material properties, the equivalent unit weight of all bolted layers is used in Equation 4.38. The equivalent unit weight of n layers of different material properties and thicknesses, $\bar{w}$, is defined as (22)

$$\bar{w} = \frac{w_1 t_1 + w_2 t_2 + \ldots + w_n t_n}{t_1 + t_2 + \ldots + t_n} \tag{4.54}$$

$$= \frac{\sum_{k=1}^{n} w_k \, t_k}{\sum_{k=1}^{n} t_k} \tag{4.55}$$

Second, the equivalent (or transformed) cross-sectional areas instead of the original ones should be used in the analysis (see Fig. 4.10) (44,47,54). After a beam of several materials is reduced to an equivalent beam of one material, the previous formulae (i.e., Equations 4.38 through 4.53) and the equations for calculating the deflection and bending stress for beam of one material still apply. The transformation of a section is accomplished by changing the dimensions perpendicular to the axis of symmetry of the various materials in the ratio of their elastic moduli (47). For example, if an equivalent section in terms of material 1 is required, the

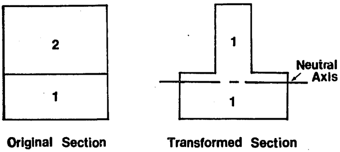

Fig. 4.10. Transformed cross-section for two materials.

dimensions corresponding to material 1 do not change. The horizontal dimensions for material 2 are modified by a ratio C, where C = E_2/E_1, Fig. 4.10. On the other hand, if the transformed section is to be in terms of material 2, the horizontal dimension of material 1 is changed by a ratio C1 = E_1/E_2, where C1 = 1/C. In this research, the transformed section is usually in terms of material 1, i.e., the material in the lowest stratum. Because in order to apply friction effect, the stiffness of the lowest stratum is generally larger than or equal to that of its upper strata. Moreover, for a beam of transformed section, the static moment of area, I_A, and moment of inertia, I_z, about the neutral axis of the new cross section can be determined by utilizing the theorem of parallex axis (47,54).

4.2.2 Failure Criteria for Bolted Strata

The failure criteria for roof strata reinforced by friction effect through roof bolting is basically the same as that of the bolted roof by suspension effect. Therefore, Equations 4.36 and 4.37 are also utilized for evaluating the stability of roof strata. However, it should be noted that only the uppermost layer and the lowermost layer in the equivalent beam is considered in this evaluation. The reason for this is that since all layers are bolted such that they behave as a single layer, then, only the outerfiber of the beam, which is most critical to the flexural stability will be taken into consideration.

In this case, the maximum bending stress, σ_B, in Equations 4.36 and 4.37 is obtained from

$$\sigma_B = \frac{6 M_B}{b t^2} \tag{4.56}$$

where M_B is the maximum bending moment at the ends, resulting from the total weight of all the bolted layers. The effect of horizontal stress is included in the determination of M_B. Furthermore, for a beam of various materials, the bending stress in each layer of the actual beam can be determined by multiplying those obtained for the transformed section by E_i/E_t, where E_i is the Young's modulus of the i-th layer and E_t is the Young's modulus for the very layer on which the transformation of section is based. In this research, E_t is the Young's modulus of the lowest layer in the equivalent beam.

CHAPTER 5

ANALYSIS OF BOLTING PATTERN AND BOLT TENSION

5.1 General

Adequate design of bolting pattern and bolt tension are the most important aspects in the success of mechanical roof bolting. Yet, in spite of the widespread use of roof bolts as a primary support system in the underground mining, there is still no consensus regarding the design criteria for the bolting pattern and bolt tension at which roof bolts should be installed to reinforce the mine roof safely and economically. The common practices are largely based on empirical rules, which obviously tend to either overdesign or underdesign.

Since the function of roof bolting is so closely related to the strata behavior, it is advisable to carry out the analysis of bolting pattern and bolt tension under different strata types. For example, in an immediate roof which contains a competent layer within the length of the bolt, the reinforcement mechanism through roof bolting is mainly due to the suspension effect. In this case, roof bolts must be long enough to be anchored at the competent layer so that the suspension effect can be achieved. The bolt spacing in this case should be determined in conjunction with the result of suspension effect. On the other hand, if there is no competent layer in the immediate roof, the bolt spacing should be determined based on the friction effect. In this case, for example, there is no need to install any roof bolt in the center of the roof span. With regard to bolt tension, which is an extremely important factor for mechanical bolting to be effective, it should also be determined based on the function of roof bolting in that specific strata. Furthermore, the proper bolt tension should be the smaller of (a) 60% of anchorage capacity, or (b) 60% of the yield load of the bolt in pure tension (15). In practice, since the yield strength of the bolt is generally larger than the anchorage capacity, the anchorage capacity is usually an important factor for the determination of bolt tension.

5.2 Bolt Spacing and Bolt Tension in Suspension Effect

In the analysis of bolting pattern for the immediate roofs to which the suspension effect applies, the bolt length is a fixed constant equal to the minimum distance required to reach the anchoring horizon (or stratum). According to the Federal Law (CFR30) (55), the bolt length should be such that at least 12 inches (30.5 cm) anchored in the stronger strata to suspend the immediate roof. In order to be effective, therefore, in this research, it is required that the bolt should be of such a length that it can be anchored at least 12 inches (30.5 cm) in that anchoring horizon of the bolted strata.

The determination of row spacing is mainly controlled by the anchorage capacity. It will be discussed in Section 5.4. In the following section, analysis of bolt spacing along the span will first be discussed.

In Chapter 4, the reinforcement mechanism of suspension effect has been investigated. The equations for determining the deflection, transferred bolt load, maximum bending moment, and maximum bending stress have been derived (see Equations 4.1 through 4.28, 4.36, 4.37 and those listed in Appendix I). Among them, the equations related to the transferred bolt load, maximum bending moment and maximum bending stress (Equations 4.9, 4.15 through 4.28, 4.36, 4.37 and those in Appendix I) are of importance in the determination of bolt spacing and bolt tension because they are directly related to the stability of the bolted roof strata.

In all of those equations the locations of the bolts are expressed in terms of X, i.e., the locations of the bolts are variable. In order to find out what is the optimum (or adequate) bolt spacing and bolt tension, comparisons between various bolt locations (or bolt spacings) should be made for various number of bolts. To achieve this goal, a hypothetical coal mine is used for illustration. The strata sequence, material properties, and in-situ horizontal stress of the immediate roof in this mine is shown in Table 5.1. The roof span is 20 ft. (6.1 m). In the following comparisons, only the first and the third layers are considered because the former is the lowest and thinnest while the latter is the anchoring layer. These two layers are considered to be most critical to the stability of the bolted strata.

5.2.1 Comparisons Between Various Bolt Spacings

The investigations into the adequate bolt spacings are made for various number of bolts, ranging from one to six bolts. When

Table 5.1. Strata Properties for An Example Mine

Stratum Number	Thickness in. (cm)	Horizontal Stress psi (MPa)	Young's Modulus $\times 10^6$ psi	($\times 10^3$ MPa)	Unit Weight lb/in^3 (g/cm^3)
3	48 (121.6)	300 (2.1)	2.19	(15.10)	0.0982 (2.72)
2	24 (60.8)	300 (2.1)	0.90	(6.21)	0.0932 (2.58)
1	18 (45.6)	300 (2.1)	0.72	(4.96)	0.0652 (1.80)

only one bolt is installed, the location of the bolt is a fixed value, i.e., at the center of the roof span. For two and three bolts, the bolt locations are shown in Fig. 5.1 and Fig. 5.2, respectively. For four bolts, 8 series of bolt locations are considered (Fig. 5.3 through Fig. 5.10). In each series, the location of one bolt is fixed while that of the other one varies (only half of the span is considered since the bolt location is symmetric with respect to mid-span). Therefore in total, there are 36 cases of bolt locations.

For five bolts, the bolt locations are almost the same as those for four bolts except that there is one more bolt installed at the center of the roof span. In addition, there is one more case in which the spacings between the bolts are equal, Fig. 5.11. In a similar way, the analysis of bolt spacing for six bolts is made. However, in each series, the locations of two bolts are kept constant while the third one is changed. In total, 84 cases of bolt locations are investigated. But only 5 major arrangements of bolt locations, which are representative of the other patterns, are shown in Fig. 5.12.

The results of comparisons in bending stress and bolt load for different number of bolts with various bolt spacings are shown in Table 5.2 through Table 5.22. In these tables, σ_{max} represents the maximum bending stress of the unbolted roof stratum, σ_{B1} and σ_{B3} refer to the maximum bending stress for the roof stratum after bolting, T indicates the transferred bolt load for that layer, and

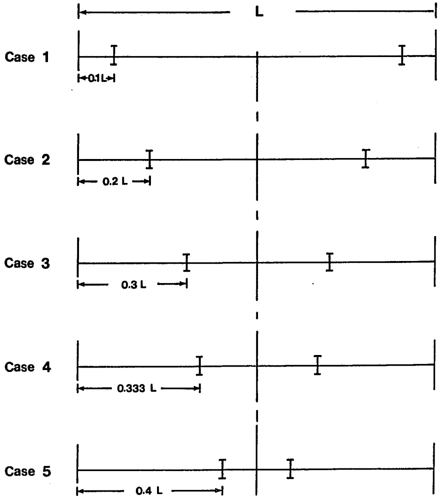

Fig. 5.1. Various locations of two bolts.

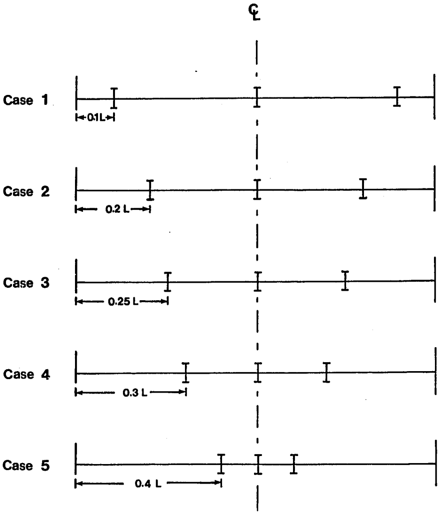

Fig. 5.2. Various locations of three bolts.

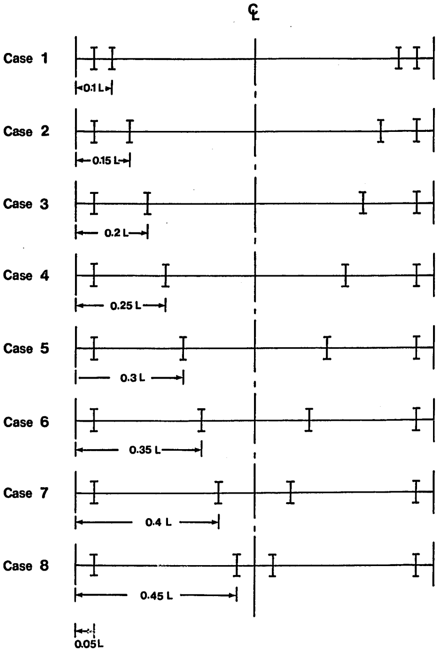

Fig. 5.3. Various locations of four bolts, Series 1.

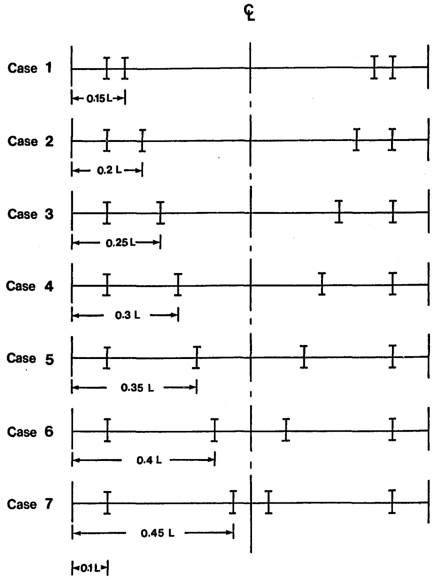

Fig. 5.4. Various locations of four bolts, Series 2.

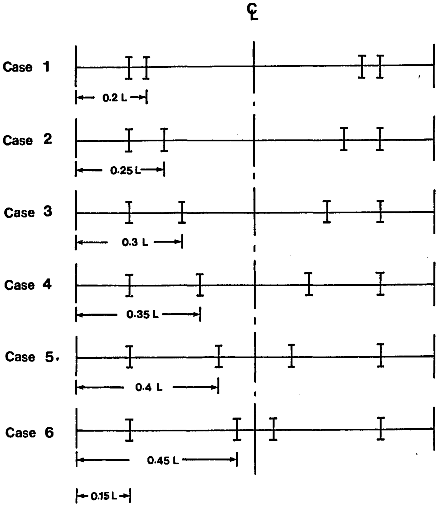

Fig. 5.5. Various locations of four bolts, Series 3.

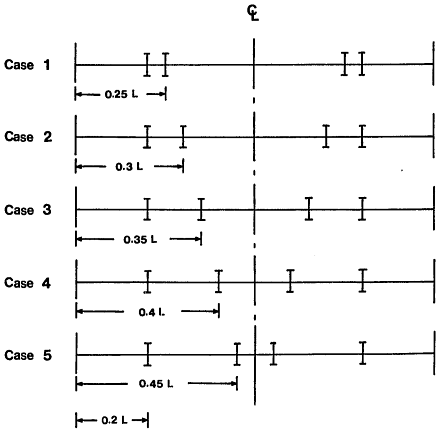

Fig. 5.6. Various locations of four bolts, Series 4.

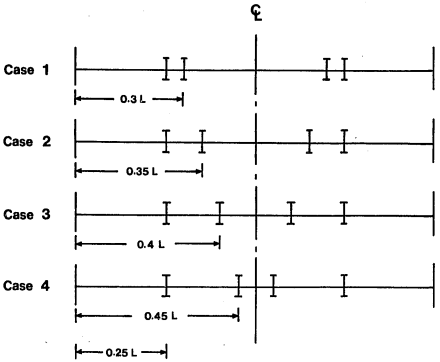

Fig. 5.7. Various locations of four bolts, Series 5.

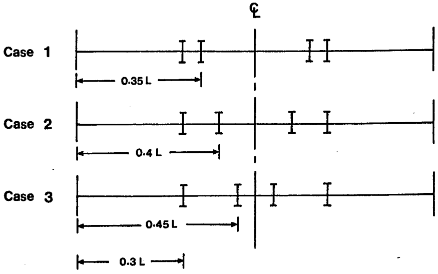

Fig. 5.8. Various locations of four bolts, Series 6.

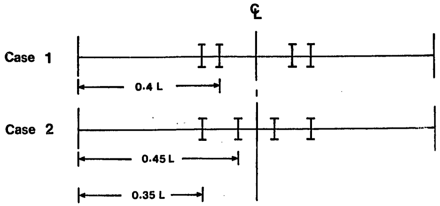

Fig. 5.9. Various locations of four bolts, Series 7.

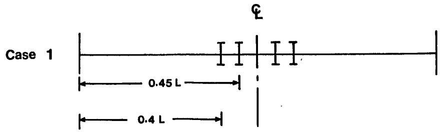

Fig. 5.10. Location of four bolts, Series 8.

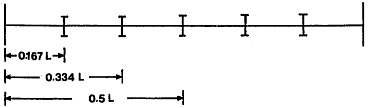

Fig. 5.11. Location of five bolts, equal spacing.

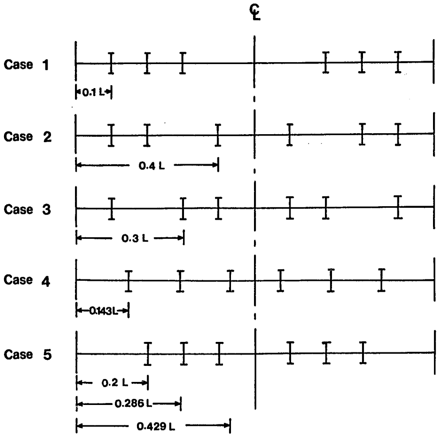

Fig. 5.12. Major arrangements of various locations of six bolts.

Table 5.2. Bending Stress and Bolt Load for One Bolt

Stratum Number	σ_{max} psi	σ_B psi	T_{1c} lbs
3	59.0	86.1	16670
1	105.9	35.0	-

Table 5.3. Comparisons Between Bending Stress and Bolt Load--Two Bolts

Case	1	2	3	4	5
X_1^*/L	0.1	0.2	0.3	0.333	0.4
σ_{B1} (psi)	-15.3	2.5	17.6	22.0	29.4
σ_{B3} (psi)	105.5	98.7	92.8	91.1	88.3
T (lbs)	79450	38110	24750	22230	18750
T_{21} (lbs)	39725	19055	12375	11115	9375

*X_1 is the distance of the first bolt (counting from the rib end) to the rib. L is the roof span.

Table 5.4. Comparisons Between Bending Stress and Bolt Load--
Three Bolts

Case	1	2	3	4	5
X_1^*/L	0.1	0.2	0.25	0.3	0.4
σ_{B1} (psi)	7.0	14.0	17.5	21.0	27.9
σ_{B3} (psi)	97.0	94.3	92.9	91.5	88.8
T (lbs)	40010	27920	25000	22780	19380
T_{31} (lbs)	13020	8682	8335	8682	13020
T_{3c} (lbs)	13960	10560	8335	5417	-6669

*X_1 is the distance of the first bolt (counting from the rib end) to the rib. L is the roof span.

Table 5.5. Comparisons Between Bending Stress and Bolt Load--Four Bolts, Series 1

Case	1	2	3	4	5	6	7	8
σ_{B1} (psi)	20.1	19.2	16.7	13.9	11.0	8.3	6.0	4.3
σ_{B3} (psi)	91.9	92.2	93.2	94.3	95.4	96.5	97.4	98.0
T (lbs)	2341	5570	14450	24710	34950	44480	52740	58970
T_{41} (lbs)	-56990	-27490	-13080	-2835	5360	12120	17570	21490
T_{42} (lbs)	58160	30270	20310	15190	12110	10120	8802	7991

Table 5.6. Comparisons Between Bending Stress and Bolt Load--Four Bolts, Series 2

Case	1	2	3	4	5	6	7
σ_{B1} (psi)	17.1	16.9	15.2	13.2	11.1	9.2	7.7
σ_{B3} (psi)	93.1	93.2	93.8	94.6	95.4	96.1	96.7
T (lbs)	21960	22390	25270	28930	32690	36120	38800
T_{41} (lbs)	-32450	-11890	-3103	2544	6713	9879	12090
T_{42} (lbs)	43430	23090	15740	11920	9631	8180	7308

Table 5.7. Comparisons Between Bending Stress and Bolt Load--Four Bolts, Series 3

Case	1	2	3	4	5	6
σ_{B1} (psi)	16.5	16.4	15.3	13.8	12.3	11.1
σ_{B3} (psi)	93.29	93.33	93.8	94.3	94.9	95.4
T (lbs)	25090	25210	26540	28290	30070	31540
T_{41} (lbs)	-19310	-4572	1405	5039	7548	9226
T_{42} (lbs)	31850	17180	11870	9109	7486	6543

Table 5.8. Comparisons Between Bending Stress and Bolt Load--Four Bolts, Series 4

Case	1	2	3	4	5
σ_{B1} (psi)	17.2	17.1	16.4	15.4	14.4
σ_{B3} (psi)	93.02	93.03	93.32	93.7	94.1
T (lbs)	25070	25090	25770	26670	27500
T_{41} (lbs)	-9579	407	4364	6668	8099
T_{42} (lbs)	22110	12140	8523	6668	5652

Table 5.9. Comparisons Between Bending Stress and Bolt Load--Four Bolts, Series 5

Case	1	2	3	4
σ_{B1} (psi)	18.75	18.82	18.4	17.8
σ_{B3} (psi)	92.40	92.37	92.5	92.8
T (lbs)	24080	24030	24350	24770
T_{41} (lbs)	-1684	4231	6565	7834
T_{42} (lbs)	13720	7783	5610	4548

Table 5.10. Comparisons Between Bending Stress and Bolt Load--Four Bolts, Series 6

Case	1	2	3
σ_{B1} (psi)	21.08	21.3	21.11
σ_{B3} (psi)	91.5	91.4	91.5
T (lbs)	22700	22590	22680
T_{41} (lbs)	4918	7322	8307
T_{42} (lbs)	6434	3971	3034

Table 5.11. Comparisons Between Bending Stress and Bolt Load--Four Bolts, Series 7

Case	1	2
σ_{B1} (psi)	24.0	24.4
σ_{B3} (psi)	90.3	90.2
T (lbs)	21170	20990
T_{41} (lbs)	10510	9953
T_{42} (lbs)	71	541

Table 5.12. Comparisons Between Stress and Bolt Load--Four Bolts, Series 8

Case	1
σ_{B1} (psi)	27.6
σ_{B3} (psi)	89.0
T (lbs)	19550
T_{41} (lbs)	15450
T_{42} (lbs)	-5678

Table 5.13. Comparisons Between Bending Stress and Bolt Load--Five Bolts, Series 1

Case	1	2	3	4	5	6	7	8
σ_{B1} (psi)	13.7	13.1	12.0	10.7	9.3	7.9	6.4	5.0
σ_{B3} (psi)	94.4	94.6	95.0	95.5	96.1	96.6	97.2	97.8
T (lbs)	25110	27360	31350	35960	40870	45950	51140	56390
T_{51} (lbs)	-11460	-2972	1932	5953	9625	13120	16520	19860
T_{52} (lbs)	17140	10500	8425	7716	7802	8737	11300	19860
T_{5c} (lbs)	13750	12300	10630	8621	6019	2236	-4501	-23050

Table 5.14. Comparisons Between Bending Stress and Bolt Load--Five Bolts, Series 2

Case	1	2	3	4	5	6	7
σ_{B1} (psi)	13.7	13.4	12.6	11.6	10.5	9.4	8.2
σ_{B3} (psi)	94.4	94.5	94.8	95.2	95.6	96.0	96.5
T (lbs)	28050	28630	30010	31740	33680	35720	37840
T_{51} (lbs)	-5032	575	3473	5708	7681	9526	11300
T_{52} (lbs)	13010	8431	7112	6885	7504	9526	16520
T_{5c} (lbs)	12100	10610	8835	6559	3306	-2382	-17800

Table 5.15. Comparisons Between Bending Stress and Bolt Load--Five Bolts, Series 3

Case	1	2	3	4	5	6
σ_{B1} (psi)	14.5	14.4	13.9	13.2	12.3	11.4
σ_{B3} (psi)	94.0	94.1	94.3	94.6	94.9	95.3
T (lbs)	27390	27560	28190	29050	30030	31100
T_{51} (lbs)	-946	2778	4702	6188	7504	8737
T_{52} (lbs)	9414	6535	5890	6188	7681	13120
T_{5c} (lbs)	10450	8935	7004	4294	-337	-12610

Table 5.16. Comparisons Between Bending Stress and Bolt Load--
Five Bolts, Series 4

Case	1	2	3	4	5
σ_{B1} (psi)	16.1	16.1	15.7	15.2	14.6
σ_{B3} (psi)	93.4	93.4	93.6	93.8	94.0
T (lbs)	26050	26050	26330	26780	27320
T_{51} (lbs)	2604	4688	5890	6885	7802
T_{52} (lbs)	6001	4688	4702	5708	9625
T_{5c} (lbs)	8835	7293	5150	1594	-7533

Table 5.17. Comparisons Between Bending Stress and Bolt Load--
Five Bolts, Series 5

Case	1	2	3	4
σ_{B1} (psi)	18.2	18.3	18.2	17.9
σ_{B3} (psi)	92.6	92.6	92.6	92.7
T (lbs)	24500	24400	24500	24720
T_{51} (lbs)	6001	6535	7112	7716
T_{52} (lbs)	2604	2778	3473	5953
T_{5c} (lbs)	7293	5779	3334	-2620

Table 5.18. Comparisons Between Bending Stress and Bolt Load--Five Bolts, Series 6

Case	1	2	3
σ_{B1} (psi)	20.8	21.0	21.1
σ_{B3} (psi)	91.6	91.5	91.5
T (lbs)	22890	22720	22710
T_{51} (lbs)	9414	8431	8425
T_{52} (lbs)	-946	575	1932
T_{5c} (lbs)	5953	4714	1994

Table 5.19. Comparisons Between Bending Stress and Bolt Load--Five Bolts, Series 7

Case	1	2
σ_{B1} (psi)	23.9	24.3
σ_{B3} (psi)	90.4	90.3
T (lbs)	21240	21040
T_{51} (lbs)	13010	10500
T_{52} (lbs)	-5032	-2972
T_{5c} (lbs)	5286	5975

Table 5.20. Comparisons Between Bending Stress and Bolt Load--Five Bolts, Series 8

Case	1
σ_{B1} (psi)	27.5
σ_{B3} (psi)	89.0
T (lbs)	19590
T_{51} (lbs)	17140
T_{52} (lbs)	-11460
T_{5c} (lbs)	8232

Table 5.21. Comparisons Between Bending Stress and Bolt Load--Five Equally Spaced Bolts

Case	1
σ_{B1} (psi)	14.2
σ_{B3} (psi)	94.2
T (lbs)	27780
T_{51} (lbs)	5557
T_{52} (lbs)	5557
T_{5c} (lbs)	5557

Table 5.22. Comparisons Between Bending Stress and Bolt Load--Six Bolts

Case	1	2	3	4	5
σ_{B1} (psi)	12.0	12.5	13.0	13.5	15.7
σ_{B3} (psi)	95.0	94.9	94.7	94.4	93.6
T (lbs)	31090	30220	29310	28580	26370
T_{61} (lbs)	5512	3763	2967	4763	6125
T_{62} (lbs)	-14220	2459	12470	4763	-4076
T_{63} (lbs)	24250	8887	-779	4763	11130

T_{1c}, T_{21}, ..., T_{63} represent the transferred bolt loads for the first through the sixth bolts (see their definitions in Chapter 4). It should be pointed out that only the transferred bolt load for the third layer (i.e., anchoring layer) is shown because it is actually the bolt tension of the bolt at that location.

(1) Two Bolts

From Fig. 5.1 and Table 5.3 it can be seen that when bolts are installed closer to the ribs, the maximum bending stresses are reduced while the bolt loads are increased. Although the smaller is the bending stress, the better is the stability of the roof strata, the bolt load shouldn't be too large. Otherwise anchorage failure will occur. Furthermore, since the bending stresses in case 3 and case 4 are pretty small as compared to that of the unbolted layer (see Table 5.2), and their corresponding bolt loads are much smaller than those of the bolts close to the ribs, they are better than other cases. Comparisons between them show that case 4 not only provides the best overall coverage of the exposed roof, thus minimizing the risk of roof falls between the bolts. It also has the smaller bending stress. Therefore, with two bolts in a row, case 4, i.e., bolts with equal spacing is most adequate for the design of roof bolting pattern.

Figure 5.13 shows the bending stress in the first and the third layers in various cases. It is seen that the extent of decrease in the bending stress for the third layer is not as much as the extent of increase in the bending stress for the first layer when bolt spacing varies from case 1 to case 5.

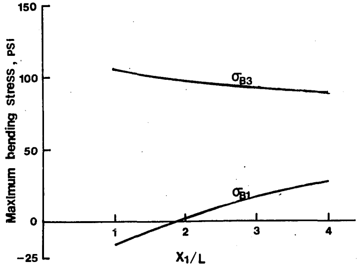

Fig. 5.13. Bending stress for various bolt locations for two bolts. X_1 is the distance of the bolt from the rib.

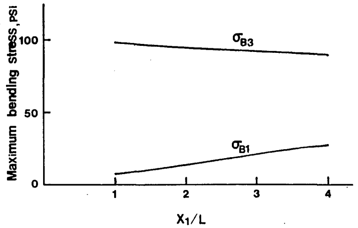

Fig. 5.14. Bending stress for various bolt locations for three bolts. X_1 is the distance of the first bolt from the rib.

(2) Three Bolts

From Fig. 5.2 and Table 5.4 it can be seen that when the bolts are installed closer to the ribs, the bending stresses are decreased while the bolt loads are increased. For case 3 and case 4, although the degree of decrease in bending stress is not as much as that of case 1 and case 2, the bending stresses in those two cases have been decreased to pretty small values. Moreover, their bolt loads are much smaller than those of case 1 and case 2. Comparison between case 3 and case 4 shows that case 3 has the smaller bending stress and the bolt load is equal for each bolt. Considering each bolt and its surrounding rock as a reinforcement unit, each unit is subjected to an equal vertical force on both sides of the bolt. But for other cases, unequal vertical forces act on both sides of the bolts, which are not desirable from the viewpoint of equilibrium of force system. In addition, equal bolt loads with equal spacing is also good for the installation and inspection. Therefore, it is concluded that case 3 (i.e., equal spacing of the bolts) is the best for the design of roof bolting system.

Figure 5.14 shows the bending stress in the first and the third layers for various cases. It can be seen from the figure that the difference in the bending stresses of the third layer is quite small among various cases. For the bending stress in the first layer, although it has the same trend as that in Fig. 5.13, the extent of the increase is less than that of the two bolts.

(3) Four Bolts

For four bolts in a row, there are 8 series of various bolt locations (Fig. 5.3 through Fig. 5.10). The results of comparisons in the bending stress and bolt load among various series are shown in Table 5.5 through 5.12.

Although there are 36 sets of results corresponding to 36 cases of bolt spacing, their trends in the bending stress and bolt load are similar. This trend can be represented by Fig. 5.15 and Fig. 5.16. In Fig. 5.15, the relationship between the bending stress and X_1/L ratio for the first layer is shown. It can be seen that the bending stress of the last case increases with the X_1/L ratio. But the bending stress of the first case first decreases when X_1/L is less than 0.15 then increases with the X_1/L ratio. This may be explained as follows: since in the first case of each series, the distance between the two bolts (only half of the span is considered) is constant (i.e., 0.05 L) but the distance between them and the ribs are variable. When the distance between those two bolts and the ribs is less than 0.2 L, the bending stress of the first layer is larger when the bolts are closer to the ribs. However, when the distance between these two bolts and the ribs is larger than 0.2 L, the closer are the bolts to the mid-span, the larger is the bending stress of the first layer. Figure 5.16 shows the relationship between transferred bolt load, T, and X_2/L ratio. It can be seen that the transferred bolt load is independent of X_2/L ratio when X_2/L is less than 0.3, but increases with X_2/L

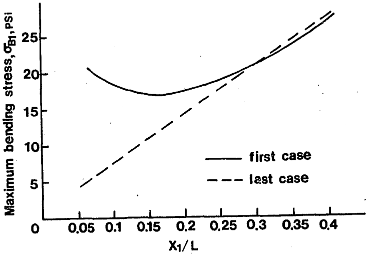

Fig. 5.15. Bending stress for various bolt locations for four bolts. X_1 is the distance of the first bolt from the rib. In the first case the distance between two bolts is 0.05 L. In the last case the location of the second bolt is kept at X_2 = 0.45 L.

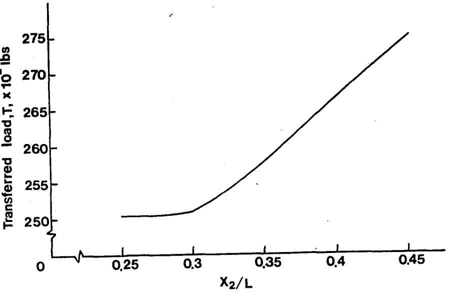

Fig. 5.16. Transferred load, T, for various bolt locations for four bolts, Series 4. X_2 is the distance of the second bolt from the rib. The location of the first bolt is kept at X_1 = 0.2 L.

ratio when X_2/L is greater than 0.3. This implies that when one bolt is fixed and the other one is moving closer to the mid-span, a larger bolt load is needed for the stratum.

After careful comparisons between all the cases, case 4 in series 4 (i.e., equal spacing between the bolts) is considered as the best one for the design of bolt spacing. The major reason is that it is the only one case in which not only the bolt load is equal for each bolt but also the bolts are equally spaced. Although in a few cases, the bolt loads are equal for each bolt but the bolts are not equally spaced (see Fig. 5.17). All other cases have different bolt loads for bolts in different locations. In addition, the bending stress of the first layer in this case is pretty small, which is good for the stability of the bolted roof strata. Furthermore, the bolt tension is only 6668 lbs. (3027 Kg) for each bolt, which is also desirable from the viewpoint of anchorage capacity.

(4) Five Bolts

With five bolts in a row, there are 37 cases of bolt locations. Among them, 36 cases are of the same bolt location as those of four bolts except that an additional bolt is used at the center of the roof span. The results of the comparisons between bending stresses and bolt loads for different cases are shown in Tables 5.13 through 5.20. There is one more case in which the spacing between the bolts is equal. The result of this case is shown in Table 5.21.

From Tables 5.13 through 5.20 it can be found that the trend in the bending stress and bolt load is similar for all the cases. This trend is plotted in Fig. 5.18 and Fig. 5.19. In Fig. 5.18 the

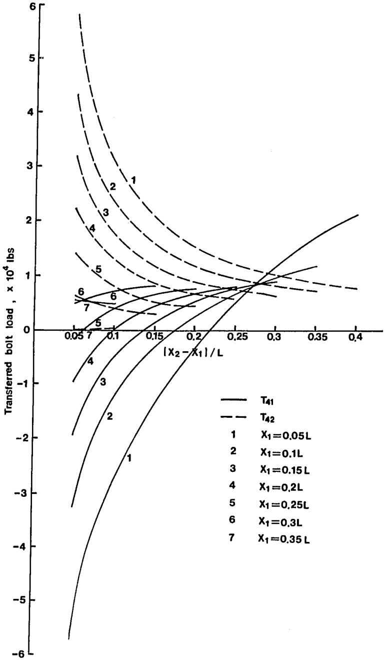

Fig. 5.17. Transferred bolt loads for various bolt locations for four bolts.

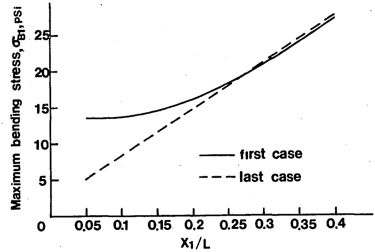

Fig. 5.18. Bending stress for various bolt locations for five bolts. X_1 is the distance of the first bolt from the rib. In the first case, the distance between two bolts is 0.05 L. In the last case, the location of the second bolt is kept at X_2 = 0.45 L.

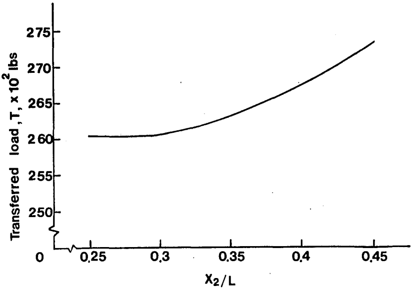

Fig. 5.19. Transferred load, T, for various bolt locations for five bolts, Series 4. X_2 is the distance of the second bolt from the rib. The location of the first bolt is kept at X_1 = 0.2 L.

relationship between bending stress and X_1/L ratio for the first layer is shown. Comparing this figure with Fig. 5.15, it can be seen that the general trend is the same between four and five bolts. The only difference is that in Fig. 5.18 when X_1/L is less than 0.15 the bending stresses are approximately equal, but in Fig. 5.15 the bending stress decreases. Figure 5.19 shows the relationship between the transferred bolt load, T, and X_2/L ratio. The trend is similar to that in Fig. 5.16. But the transferred bolt loads in Fig. 5.19 are larger than that in Fig. 5.16 when X_2/L is less than 0.3.

Table 5.21 shows the result of five equally spaced bolts. Comparing Table 5.21 with Tables 5.13 through 5.20, again, it is found that only in this case the bolt load is equal for each bolt and the bolts are equally spaced. Moreover, since in this case, the bending stress is pretty small and the load for each bolt is only 5557 lbs. (2523 Kg), it is determined that equal spacing in five bolts will provide the best design.

(5) Six Bolts

With six bolts in a row, a total of 84 cases of bolt locations are investigated. After a prudent inspection, only the result of five major cases are shown in Table 5.22.

After careful comparisons among the results of those five cases, case 4 (i.e., equal spacing) is chosen as the most adequate bolt spacing based on the following reasons: First, the load for each bolt is equal while for other spacings the difference in bolt load is quite large. Second, both the bending stress and the magnitude of the bolt load (i.e., 4763 lbs. or 2162 Kg) are pretty small, which are good for the stability of the roof strata and anchorage capacity.

After an extensive study about the bolt spacing for various bolt locations for different number of bolts, it is concluded that the bolt spacing with equal distance will yield the best results from both theoretical and practical (i.e., installation and inspection of bolts) viewpoints. In the computer program which will be described in Chapter 6, equal spacing of the bolts is utilized to analyze the optimum bolting pattern and bolt tension.

5.2.2 Determination of Bolt Tension in Suspension Effect

The determination of adequate bolt tension in the immediate roof which is reinforced by suspension effect depends on the numbers of the bolted layers, the flexural rigidity of each layer, the number of bolts in each row, and the pattern in which roof bolts are installed.

The equations for the bolt tension of one to six bolts have been derived in Chapter 4 and Appendix I. However, in those equations the locations of bolts are variable. According to the results detailed in the previous section, it has been concluded that for any number of bolts, equal spacing will provide the best result. Therefore, the optimum bolt tension for any number of bolts can be determined by substituting equal spacings in the corresponding equations in Chapter 4 and Appendix I.

It should be pointed out that although the determination of bolt tension for any number of bolts has been made, how many bolts should be used is yet to be determined. Since the more bolts are installed, the more cost and labor will be required, it is advisable to choose the smaller number of bolts as long as the stability of the bolted roof strata is maintained. In the design of bolting system, a smaller number of bolts is tried first. If it can provide the stability of the roof strata, then it will be used. Otherwise, the next higher number of bolts will be tried. The more detailed procedure for determining the adequate number of bolts for any specific immediate roof will be described in Chapter 6.

5.3 Bolt Spacing and Bolt Tension in Friction Effect

For the immediate roofs which are reinforced by the friction effect, the bolt spacing in each row should be determined based on the "equal shear force" concept. The equation for determining the bolt spacing has been derived in Chapter 4 (see Equation 4.49). The equations for determining the bolt tension are given in Equations 4.50 through 4.53. It should be pointed out that for any specific immediate roof reinforced by friction effect, both the bolt spacing and bolt tension are dependent on the number of bolts for each row. However the number of bolts in each row is mainly controlled by the anchorage capacity of the rock. The higher the anchorage capacity the higher the bolt tension can be applied, which, in turn, means a smaller number of bolts is needed. As long as the number of bolts in each row is determined, the corresponding bolt spacing and bolt tension will also be found.

5.4 Determination of Row Spacing

The principle for determining the row spacing for specific bolting pattern is the same for suspension effect and friction effect. Therefore, the analysis of adequate row spacing for both reinforcing effects is carried out in this section.

From the analysis of reinforcement mechanism made in Chapter 4, it is found that the row spacing is not explicitly expressed in those derived equations. But it is directly related to the bolt tension and anchorage capacity. The larger the bolt tension, the smaller is the row spacing and vice versa. However, the bolt tension can't exceed the allowable anchorage capacity (i.e., 60% of anchorage capacity). Therefore, it is advisable to choose the allowable anchorage capacity as the adequate bolt tension, then find the adequate row spacing by the following equation

$$SA = \frac{P_A}{P_B} b \tag{5.1}$$

where SA = adequate (final) row spacing

P_A = allowable anchorage capacity

P_B = bolt tension

b = unit width of the beam, or the assumed row spacing

In the computer program which is developed for designing the bolting pattern and bolt tension, Equation 5.1 is adopted for determining the adequate row spacing for the immediate roof which is either reinforced by suspension effect or friction effect.

CHAPTER 6

PROCEDURE AND APPLICATION OF COMPUTER PROGRAM

6.1 General

One of the objectives of this research is to develop a computer program, from which the optimum roof bolting system with regard to bolting pattern and bolt tension for any specific coal mine roof can be obtained.

The reason for developing the computer program is obvious. First, during the analysis of the flexural behavior of the generalized immediate roof and reinforcement mechanisms of the mechanical roof bolting, many complicated equations have been derived. By using the computer, not only the computation time can be saved, but also the results of the analyses can be guaranteed with high accuracy. Second, due to the complicated conditions of the generalized immediate roof (such as arbitrary strata sequence, different material properties and strata thicknesses), variable geometrical information about the opening and multiple parameters of roof bolting (i.e., bolt spacing, bolt length and bolt tension), a complete analysis may not be feasible without utilizing the computer programming.

Based on the results of the analyses in Chapter 3 through Chapter 5, the computer program for the analysis of the flexural behavior of a generalized immediate roof and the design of optimum roof bolting system is developed. The program is written in FORTRAN IV language, which can be applied to most types of computer.

The characteristic of this program lies in its simplicity for the users. As long as the geological and geometrical information about any immediate roof is used as the input, the desired output information, i.e., either an optimum bolting pattern and bolt tension or a stable unbolted roof, can be obtained.

6.2 Procedure and Description of the Program

In order to apply this computer program, it is necessary to understand the general procedure adopted in the program. The general procedure of the computer program is shown in Fig. 6.1. The whole program is given in Appendix II. It can be seen from Fig. 6.1 that this computer program consists of three major parts: (1) analysis of the flexural behavior of the immediate roof, (2) reinforcement by suspension effect, and (3) reinforcement by friction effect. The procedure of analysis of the flexural behavior of the immediate roof has been depicted in Chapter 3. The procedures about the reinforcements by suspension effect and friction effect will be described in the following sections.

6.2.1 Procedure for Reinforcement by Suspension Effect

The general procedure for reinforcement by suspension effect is shown in Fig. 6.2. As shown in this figure, three subprograms are used; namely, COE123, COE45 and COE67. Subprogram COE123 is to carry out the reinforcement analysis by one, two, and three bolts. Subprogram COE45 is to analyze the reinforcement by four and five bolts. Subprogram COE67 is utilized for the reinforcement analysis

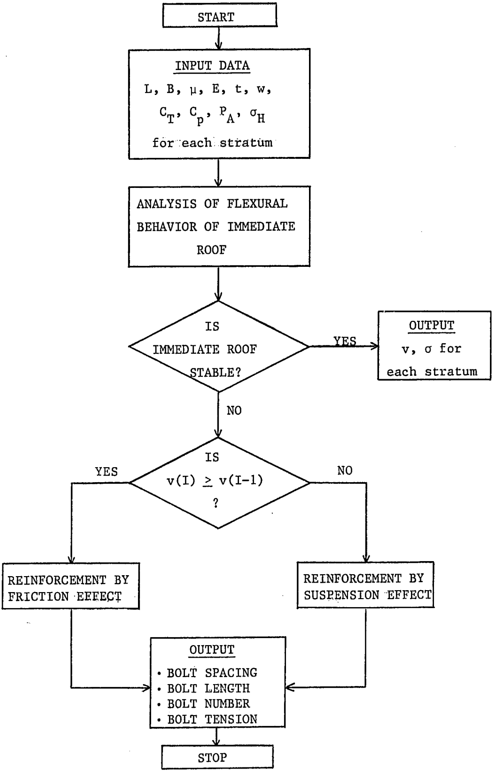

Fig. 6.1. Flow chart of general procecure of computer program.

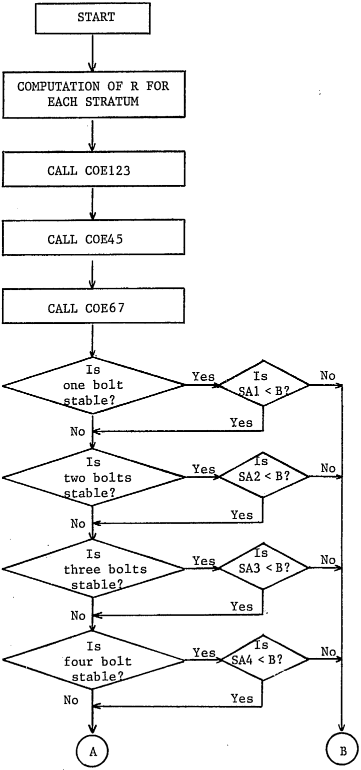

NOTE:

1. SA1, SA2, ... SA5 are row spacings for one bolt, two bolts, ... five bolts, respectively.
2. B = Assigned row spacing

(continued)

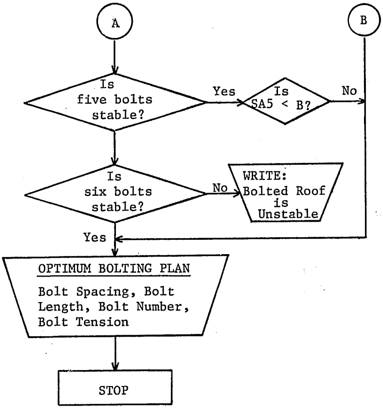

Fig. 6.2. Flow chart of procedure of suspension effect.

by six and seven bolts. In this research, however, only six bolts are considered in subprogram COE67. The reason for six bolts is that the width of the entry (or opening) in the United States is seldom larger than 20 ft. (6.1 m) (56). Under this condition, even if six bolts are installed, the spacing between the bolts will probably be smaller than 3 ft. (0.91 m). Since the current 4 x 4-ft. (122 x 1.22-m) pattern is in many cases overdesigned, it is, therefore, determined to consider at most six bolts for the reinforcement by suspension effect.

It can also be seen from this figure that the procedure for evaluation of stability of the bolted roof starts from one bolt to six bolts. The reason can be explained as follows: As long as the requirement for the stability of the bolted roof is met, the less is the number of bolts installed, the more cost will be reduced. Throughout all the analysis of reinforcement by roof bolting, this principle is adopted.

With regard to the spacing between the rows of bolts (or row spacing), an adequate value, B, is assumed in the beginning. After the reinforcement analysis is done, the calculated row spacing, SA, will be compared with B. Whenever the value of SA is smaller than that of B, the number of bolts will be changed to the next higher one. Therefore, the final (or optimum) bolting plan will be determined only when both stability condition and adequate row spacing are satisfied. It should also be noted that the spacing of bolts in each row is determined within the analysis of the reinforcement itself.

6.2.2 Procedure for Reinforcement by Friction Effect

The general procedure for reinforcement by friction effect is shown in Fig. 6.3. There are three subprograms used in this part of reinforcement analysis; namely, FRIC1, FRICM and FRSPAC. The subprogram FRIC1 is utilized for the analysis of friction effect when the immediate roof is of strata type C, i.e., each stratum deflects more than that of its underlying stratum and combined into one equivalent stratum. The subprogram FRICM is used to carry out the reinforcement analysis of friction effect when the strata sequence of the immediate roof is of such an order that the deflections of all the strata are equal and therefore multiple strata instead of one combined stratum need to be reinforced by friction effect. It should be pointed out that the reinforcement mechanism is the same for FRIC1 and FRICM. The major difference is the different number of layers involved and the corresponding determination of the neutral axis, statical moment of area, and moment of inertia for the bolted strata. The subprogram FRSPAC is used for determining the bolt spacing in each row based on the "equal shear force" concept which has been described in Section 4.2.1. The principle for determining the row spacing is basically the same as that for suspension effect; i.e., the row spacing obtained should be larger than or equal to that of the assigned adequate spacing, B.

6.3 Application of Computer Program

After the general procedure and description of the computer program, the next step is to know how to apply it. To this end,

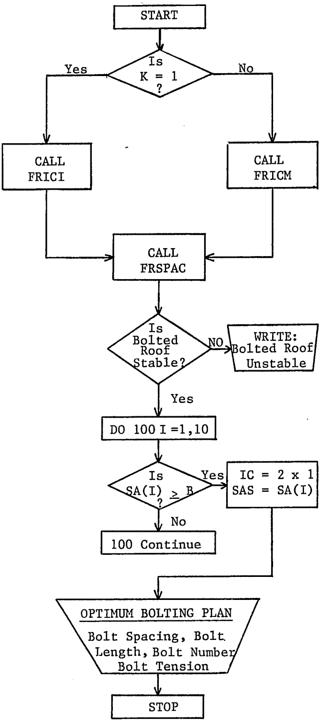

Fig. 6.3. Flow chart of procedure of friction effect.

the easiest way is to describe how the data is inputted and what is the result of the output. After that, illustrative examples will be demonstrated to show what are the input and output.

6.3.1 Description of Input Data and Output Result

The first card in the input data is the number of layers in the immediate roof to be reinforced. Since it is essential to know how many layers in the immediate roof so that the proper bolting pattern and bolt tension can be determined. In the computer program, it is represented by the variable N and read in with the format I2. The second card reads in the variables, XL, B, and US, which represent the roof span, assigned row spacing and coefficient of friction in the interface, respectively. Those three data are read in with the format 3F10.4. The next card to be read in is the information about each stratum. They are: (1) Young's modulus, E, (2) thickness, t, (3) unit weight, w, (4) in-situ horizontal stress, HS, (5) tensile strength, TENSH, (6) compressive strength, COMSH, and (7) allowable anchorage capacity (if any), P_A. Those seven data are read in with the format E10.3 and 6F10.4. The number of cards for each stratum depends on how many number of strata is read in the first card. For example, if the immediate roof is made up of six strata, then six cards need to be read in. The reading sequence starts from the lowest stratum. These are all the necessary input data to be read in for the determination of optimum bolting plan for any specific immediate roof.

The output of this computer program consists of two major parts. The first part shows the information of input data and the results of analysis of the flexural behavior of the immediate roof, from which the user can check the input data and understand what is the flexural behavior of the immediate roof in terms of deflection and bending stress. If the strata combination procedure occurs, it will also be shown in this part. The second part is the result of reinforcement analysis through roof bolting. The result depends on the type of reinforcement mechanism. If it is for suspension effect, the parameters and coefficients employed in the analysis are first listed. Next to that is the optimum bolting system including number of bolts per row, bolt spacing along the span and along the entry (or row spacing), bolt length and bolt tension. If the bolted roof fails, then instead of the bolting plan, the statement "Bolted roof is unstable" and the corresponding stresses are printed out. If it is for friction effect, the printout includes the neutral axis, the number of the stratum that requires the largest shear flow, and the bolt spacing based on "equal shear force" concept, followed, in the last part, by the optimum bolting plan or the failure condition, which is of the same form as that for suspension effect.

It should also be mentioned that the unit of both input data and output result are expressed in English System because it is most commonly used in the United States.

6.3.2 Illustrative Examples

In this section, two examples are used to illustrate what is the input data and output result for two immediate roofs reinforced by suspension and friction effect, respectively.

(1) Example 1 - reinforcement by suspension effect

Table 6.1 shows the strata sequence and material properties for, and in-situ horizontal stress in the immediate roof for a hypothetical underground coal mine A. The width of the opening is 20 ft. (6.1 m). If the designed row spacing is 4 ft. (1.22 m), what is the proper bolting pattern and bolt tension at which the roof bolts should be installed?

First, the necessary input data are read into the computer. The first card reads in N = 3. The second card reads in XL = 240.0 in. (6.1 m), B = 48.0 in. (1.22 m), and US = 0.0. The third through the fifth card read in the following information, respectively.

	E		t		w	
	x 10^6 psi	(x 10^3 MPa)	in.	(cm)	lb/in^3	(g/cm^3)
Card 3	0.72	(4.96)	18	(45.6)	0.0652	(1.80)
Card 4	0.90	(6.21)	24	(60.8)	0.0932	(2.58)
Card 5	2.19	(15.10)	48	(121.6)	0.0982	(2.72)

	HS		TENSH		COMSH		PA	
	psi	(MPa)	psi	(MPa)	psi	(MPa)	lbs	(kg)
Card 3	300	(2.1)	71.5	(0.5)	1447	(10.0)	7000	(3178)
Card 4	300	(2.1)	88	(0.6)	2133	(14.7)	7500	(3405)
Card 5	300	(2.1)	250	(1.7)	6270	(43.2)	8000	(3632)

Table 6.1. Strata Sequence and Material Properties for, and Horizontal Stress in the Immediate Roof, Hypothetical Mine A

Stratum Number	Thickness		Horizontal Stress		Young's Modulus		Unit Weight		Tensile Strength		Compressive Strength		Anchorage Capacity	
	in.	(cm)	psi	(MPa)	$\times 10^6$ psi	($\times 10^3$ MPa)	lb/in^3	(g/cm^3)	psi	(MPa)	psi	(MPa)	lbs	(Kg)
3	48	(121.6)	300	(2.1)	2.19	(15.10)	0.0982	(2.72)	250	(1.7)	6270	(43.2)	8000	(3632)
2	24	(60.8)	300	(2.1)	0.90	(6.21)	0.0932	(2.58)	88	(0.6)	2133	(14.7)	7500	(3405)
1	18	(45.6)	300	(2.1)	0.72	(4.96)	0.0652	(1.80)	71.5	(0.5)	1447	(10.0)	7000	(3178)

After the computer program is executed, the results (i.e., adequate bolting plan) are printed out (Table 6.2).

(2) Example 2 - reinforcement by friction effect

In this example, the strata sequence and material properties for, and in-situ horizontal stress in, the immediate roof for a hypothetical coal mine B is shown in Table 6.3. The width of the opening is 20 ft. (6.1 m). The coefficient of friction is 0.8 along the interfaces of the bedding planes. If the row spacing is designed to be 3 ft. (1.22 m), what is the proper bolting pattern and bolt tension for the roof bolting system to be used in this mine?

At first, the necessary input data are read in. The first card reads in N = 4. The second card reads in XL = 240.0 in. (6.1 m), B = 36.0 in. (0.91 m), and US = 0.8. The third through the sixth card read in the following information, respectively.

	E		t		w	
	x 10^6 psi	(x 10^3 MPa)	in.	(cm)	lb/in^3	(g/cm^3)
Card 3	1.00	(6.90)	12	(30.5)	0.0982	(2.72)
Card 4	0.90	(6.21)	10	(25.4)	0.0961	(2.66)
Card 5	0.72	(4.96)	12	(30.5)	0.0961	(2.66)
Card 6	0.86	(5.92)	8	(20.3)	0.0961	(2.66)

	HS		TENSH		COMSH		PA	
	psi	(MPa)	psi	(MPa)	psi	(MPa)	lbs	(Kg)
Card 3	300	(2.1)	250	(1.7)	6270	(43.2)	8000	(3632)
Card 4	300	(2.1)	71.5	(0.5)	1447	(10.0)	7000	(3178)
Card 5	300	(2.1)	71.5	(0.5)	1447	(10.0)	7000	(3178)
Card 6	300	(2.1)	151.5	(1.1)	1800	(12.4)	7500	(3405)

Table 6.2. Adequate Bolting Plan for Hypothetical Mine A

No. of Bolts Along the Span	4
Bolt Spacing Along the Span, in.	48.00
Bolt Spacing Along the Entry, in.	57.59
Bolt Length, in.	66.00
Bolt Tension, lbs.	8000.00

Table 6.3. Strata Sequence and Material Properties for, and Horizontal Stress in the Immediate Roof, Hypothetical Mine B

Stratum Number	Thickness		Horizontal Stress		Young's Modulus		Unit Weight		Tensile Strength		Compressive Strength		Anchorage Capacity	
	in.	(cm)	psi	(MPa)	$\times 10^6$ psi	($\times 10^3$ MPa)	lb/in^3	(g/cm^3)	psi	(MPa)	psi	(MPa)	lbs	(Kg)
4	8	(20.3)	300	(2.1)	0.86	(5.92)	0.0961	(2.66)	151.5	(1.1)	1800	(12.4)	7500	(3405)
3	12	(30.5)	300	(2.1)	0.72	(4.96)	0.0961	(2.66)	71.5	(0.5)	1447	(10.0)	7000	(3178)
2	10	(25.4)	300	(2.1)	0.90	(6.21)	0.0961	(2.66)	71.5	(0.5)	1447	(10.0)	7000	(3178)
1	12	(30.5)	300	(2.1)	1.00	(6.90)	0.0982	(2.72)	250	(1.7)	6270	(43.2)	8000	(1632)

The proper bolting plan for this hypothetic mine is printed out as shown in Table 6.4.

Table 6.4. Adequate Bolting Plan for Hypothetical Mine B

No. of Bolts Along the Span	12					
Bolt Location from the Center, in.	34.64	60.00	77.46	91.65	103.9	114.9
Row Spacing, in.	41.02					
Bolt Length, in.	42.00					
Bolt Tension, lbs.	7500.00					

CHAPTER 7

DEVELOPMENT OF DESIGN CRITERIA FOR ADEQUATE BOLTING PATTERN AND BOLT TENSION

7.1 Development of Nomographs for Determining the Adequate Bolting Pattern and Bolt Tension

Based on the results in previous chapters, a computer program has been developed for the determination of proper bolting pattern and bolt tension under which the mechanical roof bolts should be installed to reinforce the immediate roof. As stated in Chapter 6, there are several major characteristics in this computer program, such as simplicity of input data, higher accuracy, and wide ranging applications. With the application of this computer program, proper bolting pattern and bolt tension for most underground coal mines can be determined. From now on the practice of roof bolting systems with regard to bolting pattern and bolt tension can be accomplished scientifically rather than by the empirical rules.

Although the computer program developed in this research is efficient and powerful, there still exists a need to develop the nomographs for the determination of proper bolting pattern and bolt tension. The reason is quite simple. Because in order to use the computer program, a computer must be available. However, for many small coal mines, it may not be feasible to utilize the computer. Under this condition, it is desirable to use design nomographs for quick yet still accurate estimation. In the following sections, the nomographs for determining the proper bolting pattern and bolt tension are presented. It should be noted that some assumptions have been made in deriving these nomographs, which should be understood and satisfied in the application to the prototype so that accurate results can be obtained.

7.1.1 Nomographs for the Strata Types Reinforced by Suspension Effect

For the strata type to which the suspension effect applies, several nomographs are derived for the determination of proper bolting pattern and bolt tension. Figure 7.1 is for the evaluation of the stability of the unbolted strata. This nomograph is derived based on Equations 3.24 and 3.25. Figure 7.2 and Figure 7.3 are used for the determination of maximum bending stress in the bolted strata for the supported and supporting (or anchoring) strata, respectively. These two nomographs are derived based on Equations 4.21, 4.36 and 4.37. Figure 7.4 shows the nomograph for the determination of proper bolt number and bolt tension. This nomograph is derived based on Equation 4.9. In order to apply these nomographs, Table 7.1, Figures 3.14, 3.15 and some of the Figures 7.5 through 7.10 are used. In addition, Equation 4.35 is used to determine the R value for each stratum.

The procedure for applying these nomographs is described as follows:

Step 1: Determine the maximum bending stress of unbolted stratum from Fig. 7.1 by following the dotted line

Table 7.1. α for Various Number of Bolts, Equal Bolt Spacing

No. of Bolt	1	2	3	4	5	6	7	8
α	0.5	0.333	0.25	0.2	0.167	0.143	0.125	0.111

Note: α values are calculated based on equations in Appendix I.

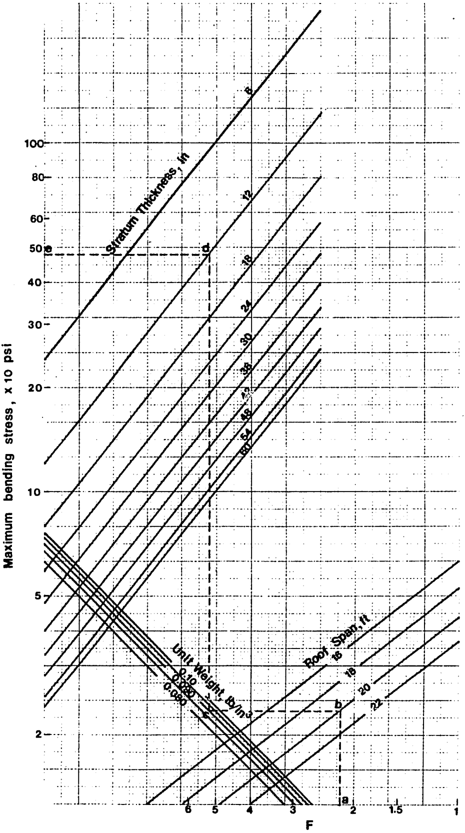

Fig. 7.1. Nomograph for the determination of maximum bending stress in the unbolted strata.

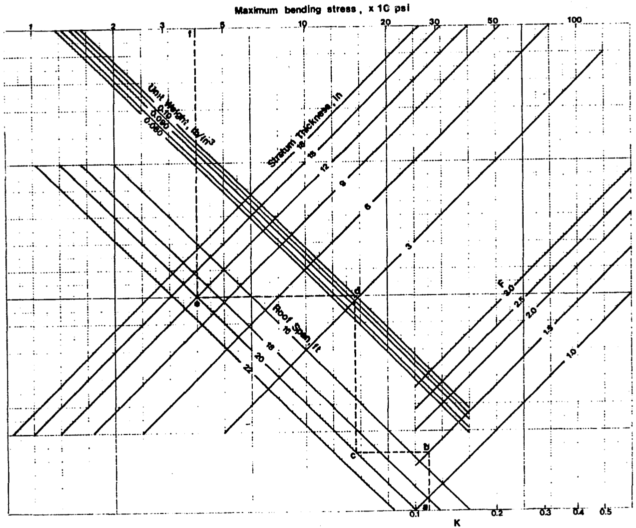

Fig. 7.2. Nomograph for the determination of maximum bending stress in the bolted roof - supported data.

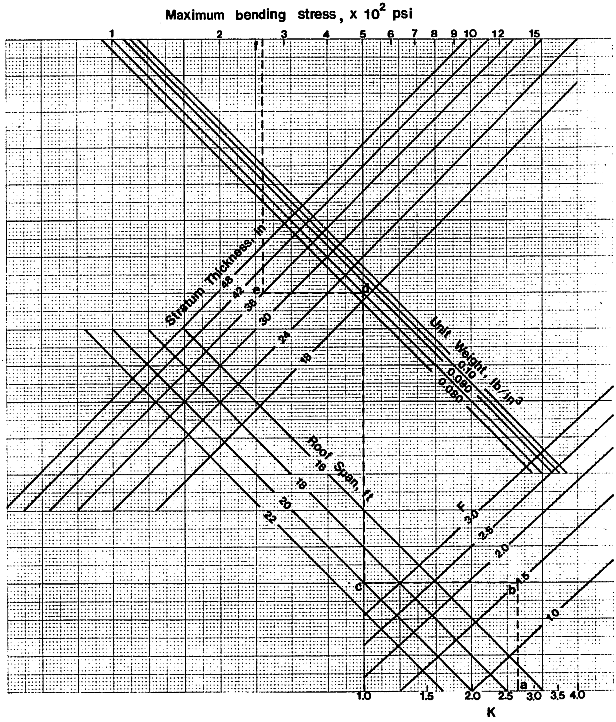

Fig. 7.3. Nomograph for the determination of maximum bending stress in the bolted roof - supporting strata.

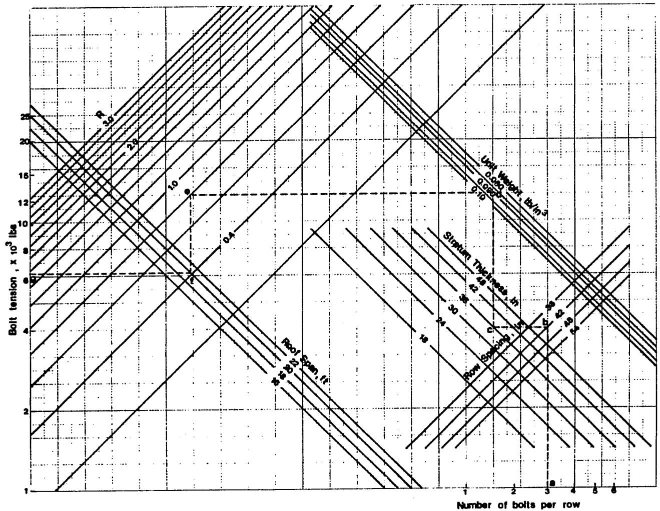

Fig. 7.4. Nomograph for the determination of proper bolt number and the tension - suspension effect.

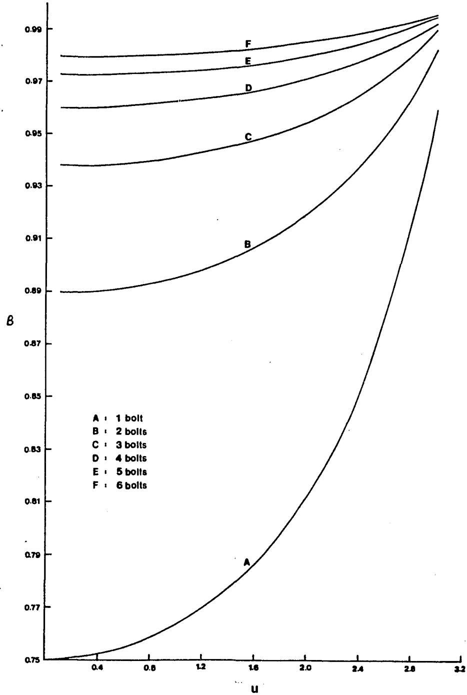

Fig. 7.5. Relationship between β and u for various number of bolts.

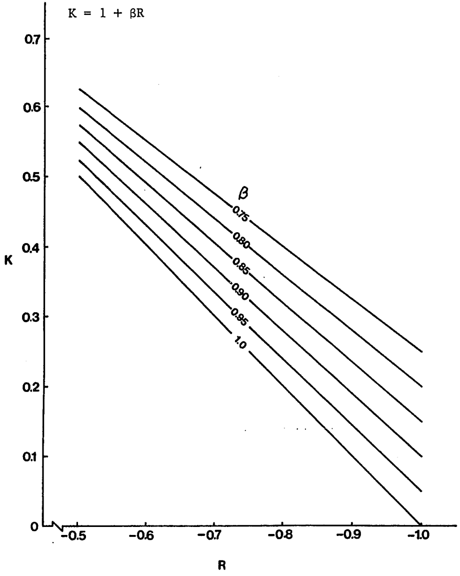

Fig. 7.6. Relationship between K and R for various β values for supported strata.

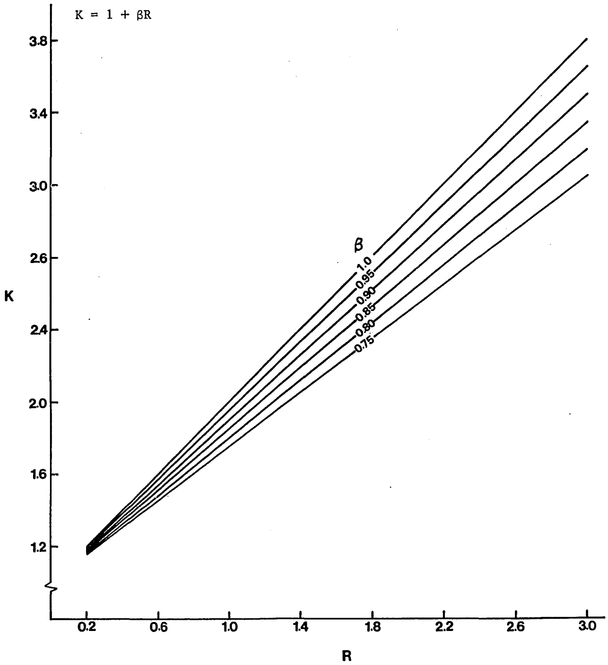

Fig. 7.7. Relationship between K and R for various β values for supporting data.

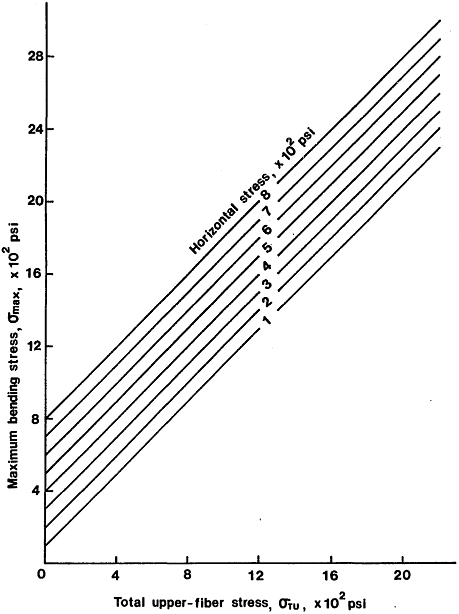

Fig. 7.8. Relationship between maximum bending stress and total upper-fiber stress for various horizontal stresses.

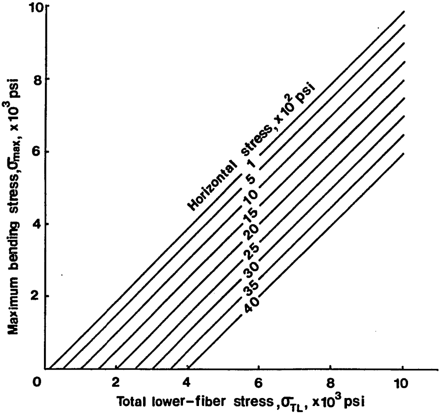

Fig. 7.9. Relationship between maximum bending stress and total lower-fiber stress.

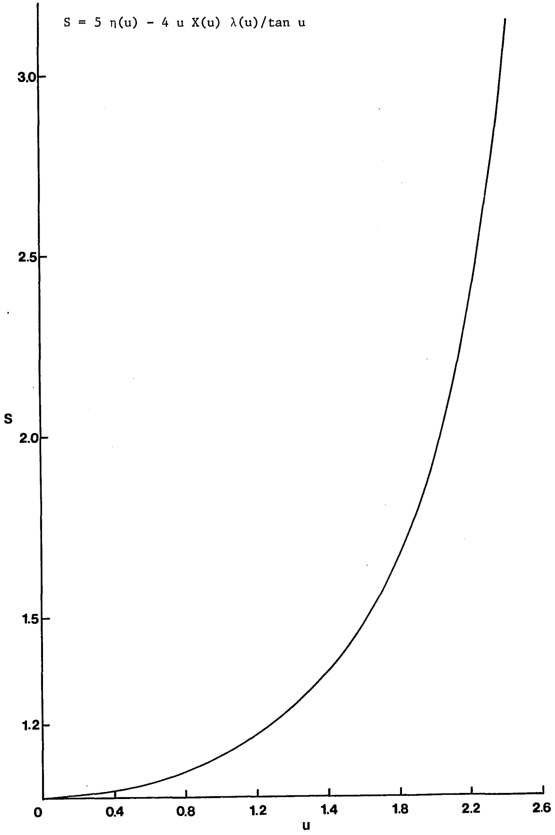

Fig. 7.10. Relationship between u and S.

abcde (the u factor and F factor can be found from Figures 3.14 and 3.15, respectively).

Step 2: Based on the result of Step 1, find the total upper-fiber stress and total lower-fiber stress of each stratum from Fig. 7.8 and Fig. 7.9, respectively.

Step 3: Compare the total upper-fiber stress with the tensile strength of the rock and compare the total lower-fiber stress with the compressive strength of the rock. If the strengths are larger than stresses then the stratum is stable; otherwise, the stratum will fail. If the stratum is stable, there is no need to install any roof bolt; if the stratum will fail, roof bolts are necessary to reinforce the roof. In the latter case, go to the next step.

Step 4: Find the maximum bending stress of the bolted stratum from the nomographs in Fig. 7.2 and Fig. 7.3 for the supported and supporting strata, respectively. It is obtained by following the dotted line abcdef. In this step the determination of K factor is very important (see the definition of K in p. 76). In order to determine K, Fig. 7.6 and Fig. 7.7 are used for the supported and supporting strata, respectively. In these two figures, the R values are determined from Equation 4.35. In order to determine R, S factor must be found first, which can be determined from

Fig. 7.10. It should be noted that in order to determine the proper number of bolts this step must be repeated for various number of bolts starting from one bolt.

Step 5: The same as that in Step 2 except that the maximum bending stress in this step is for the bolted stratum.

Step 6: Compare the total outer-fiber stresses with the strengths of the rock. When the stresses are less than the strengths, the stratum is stable. Choose the smallest number of bolts which can provide the stability.

Step 7: From the result of Step 6, find the corresponding bolt tension in Fig. 7.4 by following the dotted line abcdefg. Compare the bolt tension with the anchorage capacity. If the former is less than the latter, the bolt number is adequate; otherwise, try the next larger number of bolts. The final selection of bolt number is obtained when the corresponding bolt tension is less than the anchorage capacity.

An example is given below to illustrate these procedures.

<u>Example Problem</u>

An immediate roof is made up of three layers. The roof span is 20 ft. The physical and mechanical properties for these three layers are listed as follows:

Stratum Number	E ($\times 10^6$ psi)	t (in)	w (lb/in^3)	H_s (psi)	C_T (psi)	C_p (psi)	P_A (lbs)
3	2.19	36	0.0982	300	250	6270	8000
2	0.90	12	0.0932	300	88	2133	7500
1	0.72	6	0.090	300	72	1447	7500

The stratum number increases from the lower to the upper strata. Is this roof stable without roof bolting? If not, what is the proper bolt number in each row? Assuming the bolt tension is equal to the anchorage capacity of the uppermost layer, i.e., 8000 lbs. Also, the row spacing is assumed to be 4 ft.

Step 1: From Fig. 3.14, find u values for the three layers. They are $u_1 = 1.41$, $u_2 = 0.63$, $u_3 = 0.14$. From Fig. 3.15, find F values for the three layers. They are $F_1 = 1.17$, $F_2 = 1.03$, $F_3 = 1.00$. Then from Fig. 7.1, find the maximum bending stress for the three layers. They are 500 psi, 230 psi and 80 psi, respectively.

Step 2: Based on the result of Step 1, find the total upper-fiber stresses for the three layers from Fig. 7.8, i.e., 200 psi, 70 psi, and -220 psi, and find the total lower-fiber stresses for the three layers from Fig. 7.9, i.e., 800 psi, 530 psi, and 380 psi, respectively.

Step 3: Compare the result from Step 2 with the strengths of the three layers. It is found that tensile failure will occur for the lowest layer. Therefore, it is necessary to install the roof bolts.

Step 4: Find S values for the three layers from Fig. 7.10, i.e., 1.25, 1.04, and 1.00. Then from Equation 4.35 determine the R values for the lowest and highest layers, i.e., -0.988 and 0.446. Next, from Fig. 7.5 through Fig. 7.7 find the K values for these two layers for various number of bolts. Finally, from Fig. 7.2 and Fig. 7.3 find the maximum bending stresses of both layers for various number of bolts.

Step 5 &
Step 6: Based on the result of Step 4 and Fig. 7.8 and Fig. 7.9, it is found that the roof strata are stable when only one bolt is installed.

Step 7: In Fig. 7.4, starting from one bolt, find the corresponding bolt tension. It is found that although one bolt can provide the roof stability, the bolt load, 9080 lbs, is larger than the anchorage capacity, i.e., 8000 lb. When two bolts are installed the bolt load is 6060 lbs, which is less than the anchorage capacity. Therefore two bolts in a row is adequate for this case.

Although by using these nomographs, the proper bolt tension and bolt number (or bolt spacing) can be obtained immediately, it cannot deal with any type of strata with the same accuracy. For strata type A, i.e., each stratum deflects independently, it can yield very accurate results. But for strata type B, i.e., some strata need to be combined to one equivalent stratum, these nomographs can barely give approximate estimation.

7.1.2 Nomographs for the Strata Type Reinforced by Friction Effect

The reinforcement mechanism by friction effect has been investigated in Section 4.2. The basic concept in this function is to build up a single thick layer from individual thin layers, resulting in decreased bending stress of the "welded" layer and, thus increasing the stability of the roof strata.

In order to determine the proper bolt number (or bolt spacing) and bolt tension for the strata type which is reinforced by the friction effect, two nomographs are used (Fig. 7.1 and Fig. 7.11). As stated in the previous section, Fig. 7.1 is derived based on Equations 3.24 and 3.25. But Fig. 7.11 is based on the following equation:

$$C_x = \frac{x}{L/2} = \frac{2\ P_B\ \mu}{\gamma\ w\ b\ L^2} \tag{7.1}$$

Equation 7.1 is derived based on Equations 4.39, and 4.50 through 4.53.

The procedure for applying these nomographs is described as follows:

Step 1 through Step 3: These are the same as those for suspension effect.

Step 4: Based on the summation of the strength and horizontal stress, determine the required stratum thickness that will not fail. The procedure is by following

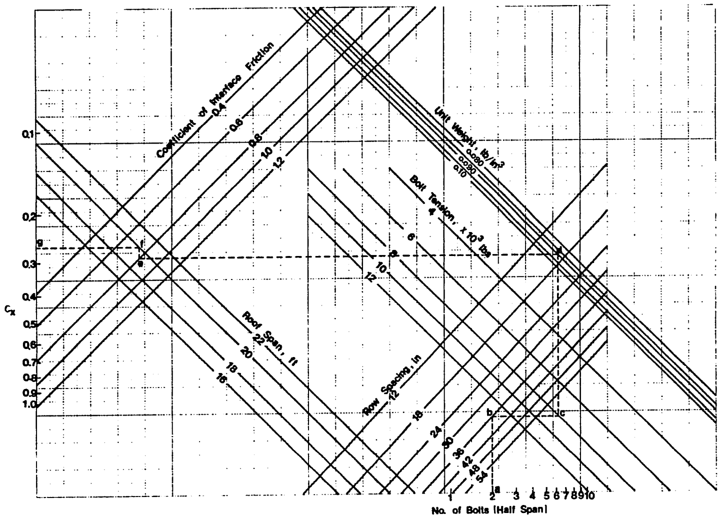

Fig. 7.11. Nomograph for the determination of proper bolt number and bolt spacing - friction effect.

the dotted line ed and abcd in Fig. 7.1. The intersection of these two dotted lines is the required stratum thickness, i.e., the thickness of thick stratum which is welded by individual thin layers. From this thickness, the number of layers which need to be welded can be obtained by dividing it with the average thickness of the thin layer. It should be pointed out that in this case, the maximum bending stress in Fig. 7.1 is actually the allowable maximum bending stress.

Step 5: Fig. 7.11 is used to find the bolt spacing by following the dotted line abcdefg. In this figure, the horizontal axis represents the γ value, which is dependent on the bolt spacing and bolt number. For bolt number ranging from one to ten (consider only the half span) the corresponding γ values are given in Table 7.2. The vertical axis in Fig. 7.11 represents the C_x value, which is the obtained ratio of the distance of the farthest segment of equal shear force (see Equation 4.48) to the half span. First, start with one bolt in the half span. By following the dotted line abcdefg, the corresponding C_x value is obtained.

Step 6: Compare the C_x value from Step 5 with the C_B values in Table 7.3. C_B is the ratio of the distance of the

Table 7.2. γ for Various Number of Bolts

Bolt No.	1	2	3	4	5	6	7	8	9	10
γ	0.375	0.265	0.216	0.188	0.168	0.153	0.142	0.133	0.125	0.119

Table 7.3. C_B for Various Number of Bolts

Bolt No.	1	2	3	4	5	6	7	8	9	10
C_B	1.0	0.707	0.577	0.5	0.557	0.408	0.378	0.354	0.333	0.316

farthest segment of equal shear force to the half span (C_B values for one through ten bolts in half span are listed in Table 7.3). If C_x is less than the corresponding C_B, then try two bolts. This procedure is repeated until C_x is larger than or equal to the corresponding C_B.

Step 7: From the final C_B in Step 6, the corresponding number of bolts can be determined. Also, the corresponding bolt spacing can be determined from Equation 4.49.

An example is given below to illustrate these steps.

Example Problem

An immediate roof is made up of two thin layers. Each layer is of same thickness and material property. The physical and mechanical properties for each layer are: $E = 0.9 \times 10^6$ psi, $t = 6.0$ in., $w = 0.090$ lb/in^3, $H_s = 300$ psi, $L = 240$ in., $P_A = 8000$ lbs, $C_T = 88$ psi, and $C_p = 2133$ psi. Find out: (a) are these two layers stable (i.e., no failure) without roof bolting? (b) if not stable, how many bolts in a row should be installed? Assume row spacing to be 36 in. and bolt tension to be 8000 lbs.

Step 1: First, from Fig. 3.14, find $u = 1.27$, and find $F = 1.13$ in Fig. 3.15. Then from Fig. 7.1, find maximum bending stress which is 490 psi.

Step 2: From Fig. 7.8, find the total upper-fiber stress which is 190 psi. From Fig. 7.9, find the total lower-fiber stress which is 790 psi.

Step 3: Comparing 190 psi with C_T = 88 psi and 790 psi with C_p = 2133 psi it is found that tensile failure will occur at the upper fiber. In order to prevent the failure, roof bolting is required.

Step 4: The summation of tensile strength of the rock and the horizontal stress is 388 psi. Based on this, find the required thickness of combined roof layers from Fig. 7.1 which is about 9 in. Since the total thickness of the two thin layers is 12 in., these two layers will be stable if they are reinforced by roof bolts.

Step 5 through Step 7: In Fig. 7.11, starting from one bolt, find the C_x value and compare it with the corresponding C_B value in Table 7.3. Find the smallest number of bolts that can provide the roof stability, i.e., six bolts (in half span). This can be seen from the result listed below (the results of one through four bolts are omitted)

Bolt No.	5	6
C_x	0.437	0.484
C_B	0.447	0.408

Therefore, based on the above-mentioned procedures, it is found that the roof strata are unstable without roof bolting. The proper bolt numbers in a row is 12 in order to achieve successful reinforcement.

It should be noted that in the above-mentioned procedure, the anchorage capacity, unit weight of rock stratum, row spacing, and coefficient of friction along the interfaces must be known in advance. Also, there are two assumptions made in this approach: First, the equivalent unit weight of all bolted strata is adopted. The equation for the equivalent unit weight is shown in Equation 4.55. Second, the material property (mainly Young's modulus), is assumed to be the same for all the bolted strata. Since in the nomograph, it's almost impossible to consider the transformed cross section for various layers made from different material properties.

7.2 Influence of Strata Sequence on Bolting Pattern and Bolt Tension

In Chapter 3, the effect of strata sequence on the flexural behavior of the immediate roof has been investigated and in Chapter 4, it has shown that the strata sequence plays a very important role in the reinforcement mechanism for roof bolting. In this section, the influence of the strata sequence on the determination of bolting pattern and bolt tension will be analyzed.

As stated before, the strata sequence of the immediate roofs can be divided into three strata types. Therefore, three types of strata sequence are used in this analysis. The same models which were used in Chapter 3 are adopted. The material properties and strata sequence of the three models are shown in Table 3.1. A horizontal stress of 300 psi (2.1 MPa) is uniformly applied to each stratum. The total outer-fiber stresses in the lowest layer for the three models and the corresponding strengths are shown in Table 7.4. It can be seen in this table that among the three strata types, type A is the only one that will fail. In order to prevent failure in this strata type, a proper roof bolting system is necessary. By using the computer program developed, the proper bolting pattern and bolt tension are determined and shown in Table 7.5.

In strata type A, the anchoring horizon (or layer) is at the uppermost location in the strata sequence. What will be the difference in bolting pattern and bolt tension if this layer is not in the uppermost location, i.e., in the lower levels of the strata sequence? Three models are analyzed for this purpose. The material properties and strata sequence for the three models are shown in Table 7.6. The proper bolt number, bolt spacing, and row spacing for the three models are shown in Fig. 7.12 through Fig. 7.14, respectively. It should be pointed out that the bolt tension is the same for all three models, i.e., 8000 lbs (3632 Kg). From these figures it can be seen that for the strata type which is reinforced by suspension effect the strata sequence influences greatly on the bolt number, bolt spacing, and row spacing. Furthermore, when the anchoring horizon is closer to the roofline, the proper bolt number is decreased while both bolt spacing and row spacing are increased.

For the immediate roof which is composed of thinly laminated layers, the reinforcement mechanism is by friction effect. The proper bolting pattern and bolt tension in this case is illustrated

Table 7.4. Total Outer-Fiber Stresses and Strengths for Three Strata Types

Strata Type	σ_{Tu} psi	C_T psi	σ_{TL} psi	C_p psi	Stable	Unstable
A	237	71.5	-837	1447		√
B	-56	71.5	-544	1447	√	
C	-131	250	-470	6270	√	

Table 7.5. Proper Bolting Pattern and Bolt Tension for Strata Type A

No. of bolts along the span	5
Bolt spacing along the span, in.	40.00
Bolt spacing along the entry, in.	49.00
Bolt length, in.	60.00
Bolt tension, lbs.	8000.00

Table 7.6. Material Properties and Strata Sequence for Three Models

Model	Stratum Number	Thickness in.	Thickness (cm)	Young's Modulus $\times 10^6$ psi	Young's Modulus ($\times 10^3$ MPa)	Unit Weight lb/in^3	Unit Weight (g/cm^3)
A	6	36	(91.4)	2.19	(15.10)	0.0982	(2.72)
	5	12	(30.5)	2.19	(15.10)	0.0982	(2.72)
	4	12	(30.5)	0.90	(6.21)	0.0932	(2.58)
	3	12	(30.5)	0.72	(4.96)	0.0961	(2.66)
	2	6	(15.2)	0.90	(6.21)	0.0932	(2.58)
	1	6	(15.2)	0.72	(4.96)	0.0961	(2.66)
B	6	12	(30.5)	2.19	(15.10)	0.0982	(2.72)
	5	36	(91.4)	2.19	(15.10)	0.0982	(2.72)
	4	12	(30.5)	0.90	(6.21)	0.0932	(2.58)
	3	12	(30.5)	0.72	(4.96)	0.0961	(2.66)
	2	6	(15.2)	0.90	(6.21)	0.0932	(2.58)
	1	6	(15.2)	0.72	(4.96)	0.0961	(2.66)
C	6	12	(30.5)	2.19	(15.10)	0.0982	(2.72)
	5	12	(30.5)	0.90	(6.21)	0.0932	(2.58)
	4	36	(91.4)	2.19	(15.10)	0.0982	(2.72)
	3	12	(30.5)	0.72	(4.96)	0.0961	(2.66)
	2	6	(15.2)	0.90	(6.21)	0.0932	(2.58)
	1	6	(15.2)	0.72	(4.96)	0.0961	(2.66)

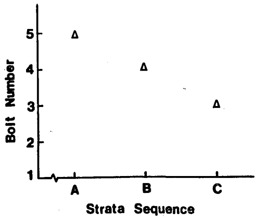

Fig. 7.12. Bolt number for different strata sequence.

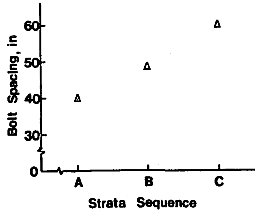

Fig. 7.13. Bolt spacing for different strata sequence.

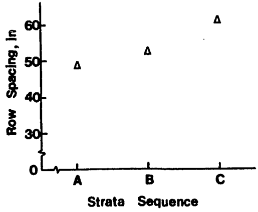

Fig. 7.14. Row spacing for different strata sequence.

by the following example. Assuming an immediate roof is made of six thin layers. The material properties for each layer are the same. They are: Young's modulus = 0.90×10^6 psi (6.21×10^3 MPa), thickness = 6 in. (15.2 cm), unit weight = 0.0932 lb/in^3 (2.58 g/cm^3), tensile strength = 88 psi (0.6 MPa), compressive strength = 2133 psi (14.7 MPa), and allowable anchorage capacity = 7500 lbs (3405 Kg). The coefficient of friction of the interfaces is assumed to be 0.8. The roof span is 20 ft. (6.1 m). A horizontal stress of 300 psi (2.1 MPa) is uniformly applied to each stratum. Under this condition, tensile failure will occur at each stratum if roof bolts are not installed. Because the total upper-fiber stress, 204 psi (2.4 MPa)(which can be obtained either from Fig. 7.1 or by the computer program) is larger than the tensile strength of the rock, 88 psi (0.6 MPa). Therefore reinforcement by roof bolting is necessary. By employing the analyses of friction effect, the proper bolting pattern and bolt tension are determined and shown in Table 7.7. From this table it can be seen that 16 bolts are needed in a row to achieve the friction effect, which, as compared to 5 bolts in Table 7.5, is obviously too large.

7.3 Comparison of Bolting Patterns by Suspension and Friction Effects

In order to confirm the concept that to achieve friction effect a large number of bolts is necessary, a comparison study is made in the following example.

Assume an immediate roof is made of three layers, of which the material properties and strata sequence are shown in Table

Table 7.7. Proper Bolting Pattern and Bolt Tension for a Hypothetical Coal Mine

No. of bolts along the span	16				
Bolt location from the center, in.	30.0	52.0	67.1	79.4	90.0
	99.5	100.2	116.2		
Row spacing, in.	53.65				
Bolt length, in.	36.00				
Bolt tension, lbs.	7500.00				

7.8. It can be seen that the lower two layers are of the same material properties while the third (or the uppermost) layer is thick and competent. In the first case, only the lower two layers are bolted by friction effect. Since the third layer is thick and strong, it can support itself without roof bolting. In the second case, all three layers are bolted by suspension effect with the anchorage at the third layer. Table 7.9 shows the comparison of bolting pattern and bolt tension between the two cases. It can be seen that if the immediate roof is supported by suspension effect only one bolt is necessary. But if the immediate roof is reinforced by friction effect, 12 bolts are needed. Also, the row spacing is larger while the bolt length is longer for the former.

Based on the results of these analyses, it is concluded that in order to achieve the reinforcement by friction effect it is necessary to install a larger number of bolts. This was also confirmed by other investigators (30, 32, 57). Since more bolts are needed, more time and cost will be spent. Therefore, it is cheaper to reinforce the mine roof by suspension effect if competent layer is within the distance of bolt length.

7.4 Case Study

To illustrate the practical application of the design criteria developed, nine field cases from 8 mines are discussed in this section. They are: Moss No. 4; McClure No. 2; Splashdam No. 1; White Pine Unit 44 and Unit 12; Keystone #5 Mine C; and Meigs No. 2; and Nemacolin. Table 7.10 lists the actual and predicted bolting patterns and bolt tensions.

Table 7.8. Material Properties and Strata Sequence for a Hypothetical Mine

Stratum Number	Thickness in.	(cm)	Young's Modulus $\times 10^6$ psi	($\times 10^3$ MPa)	Unit Weight lb/in^3	(g/cm^3)
3	36	(91.4)	2.19	(15.10)	0.0982	(2.72)
2	6	(15.2)	0.90	(6.21)	0.090	(2.49)
1	6	(15.2)	0.90	(6.21)	0.090	(2.49)

Table 7.9. Comparisons of Bolting Pattern and Bolt Tension in Two Cases

Case No.	Bolt No.	Row Spacing in.	(cm)	Bolt Tension lbs	(Kg)	Bolt Length in.	(cm)
2	1	62.58	(159)	8000	(3632)	30	(76)
1	12	39.51	(100)	8000	(3632)	12	(30.5)

Table 7.10. Actual and Predicted Bolting Patterns and Bolt Tensions for Nine Cases

Mine Name	Seam Depth (ft)	Entry Width (ft)	Bolt Spacing, in.		Row Spacing, in.		Bolt Tension, lbs.		Bolt Length, in.		Reference
			Actual	Predicted	Actual	Predicted	Actual	Predicated	Actual	Predicted	
Moss No. 4	900	20	48	48	48	48.3	6000-8000	6800	> 48	50	58
McClure No. 2	700	20	48	120	48	174.6	6000-8000	6800	> 48	74	58
Splashdam No. 1	800	20	60 & 30[a]	60	48	48.57	6000-8000	6800	> 43	61	58
White Pine											
Unit 12	1475	20	48	f[d]	48	f	6000-8000[b]	f	72	f	59
Unit 44	1200	20	48	f	48	f	6000-8000[b]	f	72	f	59
Keystone #5	650	20	48	120	48	117.0	6000-8000	6800	30 & 48	17	60
Mine C	300[b]	22	60 & 12[c]	37.7	48	32.8	6000-8000[b]	6400	72	59	61
Meigs No. 2	234	20	48	60	48	55.7	2500-11800	7200	48 & 96	84	62
Nemacolin	450	18	48 & 36[e]	60	48	58.2	5000-6800	6000	72	33	64

[a] central three bolts are 60 in.-spaced and two rib bolts are 30 in. from ribs

[b] assumed data

[c] central three bolts are 60 in.-spaced and two rib bolts are 12 in. from ribs and inclined at 45°

[d] bolted roof fail

[e] central three bolts are 48 in.-spaced and two rib bolts are 36 in. from ribs

It should be pointed out that data collection is a big job. After exhaustive search in the published literature and personal communications with some mining engineers, the data for these nine cases are obtained. However, some information are still lacking. For example, the in-situ horizontal stress is only available for White Pine case. In order to carry out this study, however, the in-situ horizontal stresses for other cases are assumed to be 3 times the vertical stresses (6,32,63), which are much larger than those estimated by the Poisson's effect of the overburden weight. Because in most active underground coal mines, the measured large horizontal stresses (usually using borehole deformation gage) reflect the active tectonic forces associated with the mountain building process. In addition, the anchorage capacities ranging from 7000 to 12000 lbs (3178 to 5448 Kg) are assumed for different rocks in the anchoring horizons (1). With these assumptions in mind, the results should not be considered to be absolutely correct. Nevertheless, it demonstrates the validity of the criteria developed.

It can be seen from Table 7.10 that in most cases, the actual bolt spacing and row spacing are less than that of the predicted values except Mine C. In other words, the general 4 x 4-ft. (1.22 x 1.22-m) spacing are a little overdesigned. For Mine C, the predicted bolt spacing and row spacing are less than that of the actual data. This may be due to the fact that two inclined bolts are anchored above the abutments. With regard to bolt tension and bolt length, the predicted values are largely very close to the actual data. Only for Keystone #5 and Nemacolin the predicted bolt lengths are a little shorter than those of actual values. The reason is that in the computer program the bolt length is only required to be 12 inches (30.5 cm) anchored at the anchoring horizon. But in real installation, the bolts are seldom of these short lengths.

The results of White Pine deserve more attention. In this mine due to the high in-situ horizontal stress, 4000 psi (28 MPa), cracks appear close to the ribs in the roof (which resemble shear failure), although the roof bolts are installed (59). This is also confirmed by the predicted results. Therefore there is no bolting pattern and bolt tension for the predicted values.

In conclusion, the common practices of bolting pattern are generally a little overdesigned as compared to the predicted results from the design criteria developed on the condition that no geological defects exist in the immediate roof strata.

CHAPTER 8

CONCLUSIONS

For the first time, the design criteria for mechanical roof bolting system with regard to bolting pattern and bolt tension have been developed. The practice of roof bolting system will no longer be based on empirical rules. The proper bolt spacing, row spacing, bolt length and bolt tension for any immediate roof in horizontally bedded strata can be obtained immediately either by using the computer program or nomographs developed in this dissertation. Since mechanical roof bolting systems are widely used in underground coal mines, it is hoped that this development can lead to maximum safety with minimum cost.

In order to reinforce the mine roof safely and economically, the flexural behavior of a generalized immediate roof should first be understood. Based on the strata sequence, the strata in the immediate roof are divided into three types (see Chapter 3). The flexural behavior of the three strata types are investigated in terms of the following effects: roof span, horizontal stress, thickness and Young's modulus of the lowest stratum. The results of this investigation not only gives us a clear picture of the flexural behavior of the unbolted roof, it also provides the basis for the analysis of the reinforcement mechanism by mechanical roof bolting in the immediate roof. For some strata (such as strata type A), it must be reinforced by roof bolting; otherwise roof failure will occur. On the other hand, there is no need to install any roof bolt for some other strata (such as strata type C) because it is strong enough to support itself. A nomograph (Fig. 7.1) is derived, from which the stability of any roof stratum can be evaluated. The step-by-step procedure for roof bolting design is described in Section 7.1.1.

In some underground openings where high in-situ horizontal stress exists, the buckling of thin strata is apt to occur. A nomograph (Fig. 3.14) is derived, from which any roof stratum whether buckles or not can be determined. If the buckling of roof stratum does occur, then reinforcement by roof bolting alone cannot overcome this problem. Rather it may be necessary to cut away that stratum or support with other methods or change the mine layout.

The reinforcement mechanism by mechanical roof bolting in horizontally bedded strata is either by suspension effect or friction effect depending on the strata sequence of the immediate roof. If the strata sequence of the immediate roof is of such an order that each stratum deflects more than that of its upper stratum, the suspension effect is valid. If the strata sequence of the immediate roof is of such an order that the deflection of each stratum is larger than or equal to its underlying stratum, then the friction effect is valid. However, it should be noted that the strata sequence mentioned earlier is not limited to the original sequence only. It can also be applied to the strata after strata combination as long as the final sequence meets the requirement.

In the immediate roof which is reinforced by suspension effect, the major function of roof bolting is to transfer parts of the weights of the weaker (or thinner) strata to the competent (or thicker) ones. Through proper bolt tension, all the bolted strata are constrained to have equal deflections at the bolt locations. The equations for the deflection, maximum bending stress, transferred bolt load, etc. are derived based on the beam-column theory. All the equations related to suspension effect are shown in Section 4.1 and Appendix I. In any immediate roof which is reinforced by suspension effect, the maximum bending stress and deflection of the supported stratum are decreased, whereas those of the supporting (or anchoring) stratum are increased. The extent of decrease (or increase) depends not only on the flexural rigidity of the stratum itself but also on those of other strata within the bolt length. This phenomenon can be seen from Equations 4.3, 4.9 and 4.21. An important factor, R, which represents the relative flexural rigidity of the stratum in question to other bolted strata, is derived in Equation 4.9. If R is negative, the stratum will receive support from other competent stratum. In other words, parts of the weight of this stratum will be transferred to the competent stratum through roof bolting. Under this condition both the maximum bending stress and deflection are decreased (see Equations 4.21 and 4.3, respectively). If R is positive, the stratum will offer (or provide) support to other weak stratum. In other words, parts of the load (or weight) from other weak strata will be transferred to this stratum, increasing the maximum bending stress and deflection of this stratum. It is important to point out that the load (or weight) transfer is limited. Because whenever the maximum bending stress of the competent stratum is increased to such an extent that the total outer-fiber stress of this stratum is larger than the inherent strength of the roof rock, the stratum will fail and the suspension effect disappears.

The basic concept in the reinforcement mechanism by friction effect is to build up a single thick layer from several thin layers. Since the maximum bending deflection of any stratum is inversely proportional to the square of beam thickness, and the bending stress is inversely proportional to the thickness, the deflection and bending stress of the "welded" thick stratum are decreased, thereby increasing the strata stability. In order to build up a single thick layer, the slip between the interfaces of all the thin layers must be prevented. In mechanical roof bolting, this is made by the clamping force due to the tensioning of the roof bolts.

With regard to proper bolting pattern and bolt tension for any specific immediate roof, the following conclusions are made based on the analysis in Chapter 5:

For the immediate roof which is reinforced by suspension effect, the bolt length should be anchored at least 12 in. in the anchoring horizon and the bolt spacing should be of equal distance. For the immediate roof which is reinforced by the friction effect, the bolt spacing should be based on the "equal shear force" concept, i.e., each bolt is subject to equal shear force on both sides. The actual location of each bolt can be determined from Equation 4.49. With regards to row spacing, there is no difference between suspension and friction effects. It is mainly controlled by the anchorage capacity, with larger row spacing for higher anchorage capacity. The bolt tension for both suspension and friction effects can be determined from the computer program developed. However, the bolt tension cannot exceed the anchorage capacity. Therefore, it is advisable to choose allowable anchorage capacity as the maximum bolt tension.

An efficient computer program as well as several design nomographs have been developed for the determination of proper bolting pattern and bolt tension. The application of the computer program is described in Chapter 6 while the procedures of using the nomographs are illustrated in Chapter 7.

The strata sequence of the immediate roof not only affects the flexural behavior but also influences the bolting pattern and bolt tension. Figure 7.12 through Figure 7.14 show the influence of different strata sequence on the bolt number, bolt spacing, and row spacing for three models. As it can be seen from these figures when the anchoring horizon is closer to the roofline, the bolt number is decreased while both bolt spacing and row spacing are increased. Since the strata sequence in real situation can be arbitrary, the corresponding bolting pattern and bolt tension may also be changed.

Table 7.9 shows the result of the comparisons in bolting pattern and bolt tension between suspension and friction effects. It seems that it is unfeasible to reinforce the immediate roof by friction effect because it needs a much larger number of bolts than that by suspension effect to achieve the reinforcement. Therefore, it is suggested that reinforcement by friction effect is only applicable when the immediate roof is made up of very thin layers and there is no competent layer located within the bolt length.

Case studies from nine sites in 8 mines are made. The results indicate that most bolting patterns used in general practice are a little overdesigned. In order to obtain an optimum design of roof bolting system with regard to bolting pattern and bolt tension, the required information such as detailed geologic column, anchorage capacity, and the material properties (e.g., tensile and compressive strengths) should be obtained first. In addition, any geologic anomaly and the in-situ horizontal stress should be determined so that mine layout may be modified in advance. Otherwise roof failure may occur even roof bolts are installed.

Although the developed design criteria developed in this dissertation are very helpful and efficient in the determination of the roof bolting systems in terms of bolting pattern and bolt tension. There are some limitations which should be understood and satisfied in their applications. For example, all bolts are of equal lengths and are vertically installed into the roof. For futher research is is advisable to carry out the analysis in which the roof bolts are of unequal lengths, i.e., roof bolts are not anchored at the same horizon, which is advisable for preventing anchorage failure for the whole bolted strata. Also, the inclined bolts anchored above the abutments seem to have better reinforcement in preventing the shear failure at the ribs and need more detailed study. With regard to friction effect, the coefficient of friction is assumed to be constant for all the interfaces. In reality, it may not be true, hence it is also recommended to perform further research in which different coefficients of friction exist for interfaces between different roof strata.

REFERENCES

1. Peng, S. S. Coal Mine Ground Control, John Wiley and Sons, Inc., New York, 1978, pp. 130-173.

2. Smelser, T. W., dar, S. M., Pettibone, H. C., and Bolstad, D. D. "Modeling and Field Verification of Roof-Bolt Systems," presented at the SME-AIME Annual Meeting, Dallas, Texas, February 1982, 11 pp.

3. Karabin, G. J., and Debevec, W. J. "Comparative Evaluation of Conventional and Resin Bolting Systems," U. S. Department of Interior, MESA, IR 1033, 1976, 22 pp.

4. Fairhurst, C., and Singh, B. "Roofbolting in Horizontally Laminated Rock," Engineering and Mining Journal, February 1974, pp. 80-90.

5. Tang, H. Y., and Peng, S. S. "Effects of Strata Sequence on the Flexural Behavior of the Immediate Roof," Proceedings First Conference on Use of Computers in the Coal Industry, West Virginia University, August 1983, pp. 518-532.

6. Aggson, J. R., and Curran, J. "Coal Mine Ground Control Problems Associated with a High Horizontal Stress Field," 1978 AIME Annual Meeting, Denver, CO, 1978, 19 pp.

7. Duvall, W. I. "General Principles of Underground Opening Design in Competent Rock," presented at 17th Symposium on Rock Mechanics, Utah, 1976, pp. 101-111.

8. Wright, F. D. "Lateral Thrust, Bedding, and Jointing in Roof Stability Calculations," U. S. Bureau of Mines, Department of the Interior, Information Circular, IC 8630, 1974, pp. 86-91.

9. Lang, T. A., Bischoff, J. A., and Wagner, P. L. A Program Plan for Determining Optimum Roof Bolt Tension, Theory and Application of Rock Reinforcement Systems in Coal Mines, Leeds, Hill, and Jewett, Inc., a contract report submitted to U. S. Bureau of Mines, March 1979, Vol. 1, 255 pp.

10. Lang, T. A. "Theory and Practice of Rock Bolting," Trans. AIME, Vol. 220, 1961, pp. 333-348.

11. American Society for Testing and Materials. "Standard Specifications for Roof and Rock Bolts and Accessories," ASTM Standard No. F432-76a, 1976, 14 pp.

12. Moss, K. J. "Rock Bolts in Current Use in Australia," Symposium on Rock Bolting, The Australasian Institute of Mining and Metallurgy, Illawarra Branch, Paper No. 5, February 1971, 15 pp.

13. Shutack, J. B., and Hanna, N. E. "Evaluation of the Explosive-Anchored Rock Bolt," U. S. Bureau of Mines, RI 7163, 1968, 15 pp.

14. Shell Lock II with 3M "No Mix Resin" Mine Roof Bolt Anchoring Systems, Frazer & Jones Co. with New Business Ventures Division/ 3M, U. S. Patent No. 4,253,566.

15. Panek, L. A., and McCormick, J. A. "Roof/Rock Bolting," in SME Mining Engineering Handbook, Cummins, A. B. and Given, I. A. (eds.), AIME, New York, 1973, pp. 13-125 to 13-134.

16. Karabin, G. J., and Hoch, M. T. "An Operational Analysis of Point Resin-Anchored Bolting System," U. S. Department of Interior, MESA, IR 1100, 1979, 14 pp.

17. Mitchell, D. W., and Debevec, W. J. "A New Look at Roof Bolts," Coal Mining and Processing, February 1970, pp. 34-36.

18. Foster, B. E., Snyder, S. D., and McClung, R. W. "Development of Nondestructive Evaluation Techniques for Large Rock Specimens," Oak Ridge National Laboratories, Oak Ridge, TN. Report No. ORNL-TM-4899, June 1975, 69 pp.

19. Stefanko, R., and de la Cruz, R. V. "Mechanisms of Load Loss in Roof Bolts," Proceedings 6th Symposium on Rock Mechanics, University of Missouri-Rolla, October 1964, pp. 293-309.

20. Sawyer, S. G., Karabin, G. J., and Debevec, W. J. "Investigation of the Effects of Thrust and Hardened Washers on the Installed Tension of a Roof Bolt," U. S. Mine Safety and Health Administration, IR 1031, 1976, 189 pp.

21. Stefanko, R. "Underground Stress Instrumentation and Support Evaluation," Ph.D. Dissertation, The Penn State University, 1961, 158 pp.

22. Obert, L., and Duvall, W. I. Rock Mechanics and the Design of Structures in Rock, Wiley, New York, 1967, pp. 612-638.

23. Merrill, R. H. "Roof-Span Studies in Limestone," U. S. Bureau of Mines, RI 5348, 1957, 38 pp.

24. Panek, L. A. "The Effect of Suspension in Bolting Bedded Mine Roof," U. S. Bureau of Mines, RI 6138, 1962, 59 pp.

25. Panek, L. A. "Use of Vertical Roof Bolts to Reinforce An Arbitrary Sequence of Beds," Proceedings International Symposium on Mining Research, University of Missouri, 1961, V. 2, pp. 499-508.

26. Panek, L. A. "Design for Bolting Stratified Roof," Trans. Society of Mining Engineers, AIME, June 1964, pp. 113-119.

27. Agapito, J. F. T., Mitchell, S. J., Hardy, M. P., and Hoskins, W. N. "Determination of In-Situ Horizontal Rock Stress on Both a Mine-Wide and District-Wide Basis," U. S. Bureau of Mines, Contract No. J0285020, Tosco Research Inc., Denver, CO, March 1980, 174 pp.

28. Panek, L. A. "Theory of Model Testing as Applied to Roof Bolting," U. S. Bureau of Mines, RI 5154, 1956, 11 pp.

29. Panek, L. A. "Design of Bolting Systems to Reinforce Bedded Mine Roof," U. S. Bureau of Mines, RI 5155, 1956, 16 pp.

30. Panek, L. A. "Principles of Reinforcing Bedded Mine Roof with Bolts," U. S. Bureau of Mines, RI 5156, 1956, 26 pp.

31. Panek, L. A. "The Combined Effects of Friction and Suspension in Bolting Bedded Mine Roof," U. S. Bureau of Mines, RI 6139, 1962, 31 pp.

32. Janak, D. "Finite Element Investigation of Bolted Mine Roof Structures," Ph.D. Dissertation, University of Missouri-Rolla, 1976, 122 pp.

33. Van Ham, F., and Tsur-Lavie, Y. "Reinforcement Effect and Action of Perpendicular and Inclined Roofbolts in Layered Rock Formations," Proceedings 2nd Congress of ISRM, Beograd, 1970, V. 2, pp. 457-467.

34. Gerdeen, J. C., et al. "Design Criteria for Roof Bolting Plans Using Fully Resin-Grouted Nontensioned Bolts to Reinforce Bedded Mine Roof," U. S. Bureau of Mines, Contract No. J0366004, Michigan Technological University, 1977, Vol. IV, 79 pp.

35. Lang, T. A. "Rock Bolting Speeds Snowy Mountains Project," Civil Engineering, February 1958, pp. 40-42.

36. Gardner, F. J. "History of Rock Bolting," Symposium on Rock Bolting, The Australasian Institute of Mining and Metallurgy, Illawarra Branch, Paper No. 2, February 1971, 11 pp.

37. Dejean, M., and Raffoux, J. F. "Mining Drifts and Tunnels-Role of Rockbolting and Parameters in Its Selection," Tunnelling, Jones, M. J. (ed.), London, IMM, 1976, pp. 321-327.

38. Tincelin, E. "Roof-Bolting Recommendations," Exploration and Exploitation of Mineral Deposits and Mineral Processing, Parley of Co-operation and Industrial Promotion, Sydney, May 1970, 32 pp.

39. Alexander, L. G., and Hosking, A. D. "Principles of Rock Bolting Formation of a Support Medium," Symposium on Rock Bolting, The Australasian Institute of Mining and Metallurgy, Illawarra Branch, Paper No. 1, February 1971, 21 pp.

40. Anderson, R. B. "Use of Resin-Anchored Roof Bolts in Adverse Conditions," Mining Engineering Journal, January 1974, pp. 37-40.

41. Foundation Sciences, Inc. "Test of Inclined Roof Bolts and Analysis of Their Effectiveness in Roof Control in Coal Mines," U. S. Bureau of Mines Contract No. H0252071, 1976.

42. Timoshenko, S. P., and Gere, J. M. Theory of Elastic Stability, McGraw-Hill Book Co., Inc., 2nd ed., New York, 1961, pp. 1-45, 521-529.

43. Tincelin, E., and Sinou, P. "The Functioning and Practical of Strata Bolting," French "Rock Bolting," 1980, pp. 96-117.

44. Timoshenko, S. P. Strength of Materials, Part I, D. Van Nostrand Company, Inc., Tenth printing, 1978, pp. 125-129.

45. Gerdeen, J. C., et al. "Design Criteria for Roof Bolting Plans Using Fully Resin-Grouted Nontensioned Bolts to Reinforce Bedded Mine Roof," U. S. Bureau of Mines, Contract No. J0366004, Michigan Technological University, 1977, Vol. V, 126 pp.

46. Rajaram, V., and Singh, M. M. "Rationale for the Design of Rock Reinforcement Systems," presented at the SME-AIME Annual Meeting, Atlanta, GA, 1983, 10 pp.

47. Popov, E. P. Mechanics of Materials, Prentice-Hall, Inc., 1970, pp. 113-139, 342-349.

48. Merrill, R. H. "Design of Underground Mine Openings, Oil-Shale Mine, Rifle, CO," U. S. Bureau of Mines, RI 5089, 1954, 56 pp.

49. Caudle, R. D. "Mine Roof Stability," U. S. Bureau of Mines, Department of the Interior, Information Circular, IC 8630, 1974, pp. 79-85.

50. Adler, L., and Sun, M. C. Ground Control in Bedded Formations, Virginia Polytechnic Institute, Research Division, 1968, 266 pp.

51. Chen, W. F. Theory of Beam Columns, McGraw-Hill, Inc., New York, 1976, pp. 1-91.

52. Dunham, R. K. "Model Studies of Resin-Anchored Bolting Reinforcement," Colliery Guardian, Vol. 224, N. 11, November 1976, pp. 593-598.

53. Stimpson, B. "The Influence of Rock Bolt Location on the Reinforcement of Horizontally Bedded Roofs by Full Column Grouted Bolts," presented at the International Symposium on Rock Bolting, Theory and Application in Mining and Underground Construction, Sweden, 1983.

54. Jeffery, R. G., and Daemen, J. K. "Analysis of Rockbolt Reinforcement of Layered Rock Using Beam Equations," presented at the International Symposium on Rock Bolting, Theory and Application in Mining and Underground Construction, Sweden, 1983.

55. U. S. Government, 1969 Coal Mine Health and Safety Act, in Code of Federal Regulations 30, Mineral Resources, Rev. 1981, pp. 462-467.

56. Bieniawski, Z. T. "Improved Design of Room and Pillar Coal Mining," Final Technical Report, The Pennsylvania State University, June 1982, 165 pp.

57. Stephansson, O. "Stability of Single Openings in Horizontally Bedded Rock," Engineering Geology, 5, 1971, pp. 5-71.

58. Glover, R. Personal Communication, 1983.

59. White Pine Copper Co. "Comparisons of Uniform Four-Foot Length, Fully-Grouted Resin Roof Bolts and Alternating Four- and Six-Foot Length, Fully-Grouted Resin Roof Bolts," U. S. Bureau of Mines Contract No. H0242029, December 1975, 313 pp.

60. McGolden, M. Personal Communication, 1983.

61. Thomas, E., Barry, A. J., and Metcalfe, A. "Suspension Support," Progress Report, U. S. Bureau of Mines, IC 7533, 13 pp.

62. Langland, R. T. "Analytical Modeling of Coal Mine Roof Behavior," Lawrence Livermore Laboratory, October 1978, 93 pp.

63. Brown, E. T., and Hoek, E. "Trends in Relationships Between Measured In-Situ Stresses and Depth," International Journal of Rock Mechanics, Mining Science & Geomech. Abstracts, V. 15, 1978, pp. 211-215.

64. Grayson, R. L. Personal communication, 1984.

APPENDIX I

DERIVATION OF EQUATIONS FOR SUSPENSION EFFECT

1. Introduction

As stated in Chapter 4, the deflection of a bolted roof stratum, v_B, is equal to the sum of the deflection of the unbolted stratum, v, and the additional deflection due to bolting, Δv,

$$v_B = v + \Delta v \qquad (A.1.1)$$

While the deflection of the unbolted stratum is constant for each specific stratum (because the self weight of each stratum is constant), the additional deflection due to bolting varies with the number of bolts, location of bolts, and bolt load for each bolt.

2. Deflection and Moment for Unbolted Stratum

The deflection of an unbolted roof stratum subjected to uniform transverse loading (due to self weight) and axial loading (due to horizontal stress) is found by superimposing the deflection produced by the uniform load and the deflection produced by the two equal moments applied at the ends (42) (Fig. 3.1)

$$v = \frac{q\ L^4}{16\ E\ I\ u^4}\left[\frac{\cos(u - 2ux/L)}{\cos u} - 1\right] - \frac{q\ L^2}{8\ E\ I\ u^2}\ x(L - x)$$

$$+ \frac{M_o\ L^2}{8\ E\ I}\ \frac{2}{u^2 \cos u}\left[\cos\left(u - \frac{2\ u\ x}{L}\right) - \cos u\right] \qquad (A.1.2)$$

For a fixed-end beam subject to uniform transverse loading and axial loading, the bending moment at both ends is (42):

$$M_o = -\frac{q\,L^2}{12}\,\frac{X(u)}{\tan u/u} \qquad (A.1.3)$$

where $$X(u) = \frac{3(\tan u - u)}{u^3} \qquad (A.1.4)$$

Let m = x/L and substituting Equation A.1.3 into Equation A.1.2 and rearranging, the following equation is obtained

$$v = \frac{q\,L^4}{384\,E\,I}\left[5\,\eta_x(u) - \frac{4\,u\,X(u)\,\lambda_x(u)}{\tan u}\right] \qquad (A.1.5)$$

$$= \frac{q\,L^4}{384\,E\,I}\,S_x \qquad (A.1.6)$$

where

$$\eta_x(u) = \frac{12[2\cos(u - 2um)\sec u - 2 - 4\,u^2(m - m^2)]}{5\,u^4} \qquad (A.1.7)$$

$$\lambda_x(u) = \frac{2[\cos(u - 2\,um) - \cos u]}{u^2\cos u} \qquad (A.1.8)$$

$$S_x = 5\,\eta_x(u) - \frac{4\,u\,X(u)\,\lambda_x(u)}{\tan u} \qquad (A.1.9)$$

At the center of the span, i.e., x = L/2 Equation A.15 and A.16 can be represented as

$$v = \frac{q\,L^4}{384\,E\,I}\left[5\,\eta(u) - \frac{4\,u\,X(u)\,\lambda(u)}{\tan u}\right] \qquad (A.1.10)$$

$$= \frac{q\,L^4}{384\,E\,I}\,S \qquad (A.1.11)$$

3. Deflection and Moment and Transferred Bolt Load for the Bolted Roof Stratum

3.1 One Bolt at the Center of the Roof Span

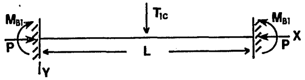

Fig. A.1

The deflection of a fixed-end beam subject to a concentrated bolt load at the mid-span and a horizontal force (p) simultaneously is (42) (Fig. A.1):

$$v = \frac{T_{1c}\ L^3 \sin 2um}{16\ E\ I\ u^3 \cos u} - \frac{T_{1c}\ L^3\ m}{8\ E\ I\ u^2} + \frac{M_{B1}\ L^2}{8\ E\ I}\ \frac{2}{u^2 \cos u}$$

$$[\cos(u - 2um) - \cos u] \qquad \text{(A.1.12)}$$

The bending moment M_{B1} at the built-in ends is obtained from the condition that the rotation of the ends produced by the concentrated load is eliminated by the moments acting at the ends, i.e., the slope at the ends is zero (42).

$$\frac{T_{1c}\ L^2}{16\ E\ I}\ \lambda(u) + \frac{M_{B1}\ L}{2\ E\ I}\ \frac{\tan u}{u} = 0 \qquad \text{(A.1.13)}$$

From Equation A.1.13, M_{B1} is obtained,

$$M_{B1} = - \frac{T_{1c} L}{8} \frac{\lambda(u)}{\tan u/u} \tag{A.1.14}$$

where $$\lambda(u) = \frac{2(1 - \cos u)}{u^2 \cos u} \tag{A.1.15}$$

By substituting Equation A.1.14 into Equation A.1.12 and rearranging,

$$v = \frac{T_{1c} L^3}{192 E I} [4 X_x(u) - 3 \frac{\lambda_x(u) \lambda(u)}{\tan u/u}] \tag{A.1.16}$$

$$= \frac{T_{1c} L^2}{192 E I} G_x \tag{A.1.17}$$

where

$$G_x = 4 X_x(u) - 3 \frac{\lambda_x(u) \lambda(u)}{\tan u/u} \tag{A.1.18}$$

$$X_x(u) = \frac{3(\frac{\sin 2um}{\cos u} - 2um)}{u^3} \tag{A.1.19}$$

At the center of the roof span, i.e., x = L/2, the following equations are obtained based on Equations A.1.16 through A.1.19.

At x = L/2,

$$v = \frac{T_{1c} L^3}{192 E I} [4 X(u) - \frac{3[\lambda(u)]^2}{\tan u/u}] \tag{A.1.20}$$

$$= \frac{T_{1c} L^3}{192 E I} G \tag{A.1.21}$$

where

$$G = 4\ X(u) - \frac{3[\lambda(u)]^2}{\tan u/u} \qquad \text{(A.1.22)}$$

It is found that at $x = L/2$, G is equal to S in Equation A.1.11. This can be proven easily by proper substitution. The transferred bolt load for one bolt at the center of the roof span has already been presented in Chapter 4. Therefore, it will not be repeated here.

3.2 Two Bolts at Symmetric Locations

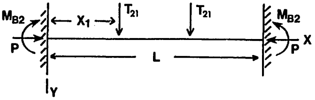

Fig. A.2

The deflection of a fixed-end beam subject to two concentrated bolt loads at symmetric locations and a horizontal force simultaneously is (Fig. A.2):

$$v = \frac{T_{21}\ L^3}{E\ I}\left[\frac{\sin(2\ uml)\ \cos(2um - u)}{8\ u^3\ \cos u} - \frac{ml}{4\ u^2}\right]$$

$$+ \frac{M_{B2}\ L^2}{8\ E\ I}\ \frac{2}{u^2\ \cos u}[\cos(u - 2\ um) - \cos u] \qquad (A.1.23)$$

The slope (rotation) of the ends produced by the two concentrated loads is eliminated by the moments acting at the ends, i.e.,

$$\frac{T_{21}\ \sin 2\ u(1 - ml)}{P\ \sin 2\ u} - \frac{T_{21}(1 - ml)}{P} + \frac{T_{21}\ \sin(2\ uml)}{P\ \sin 2\ u}$$

$$- \frac{T_{21}\ ml}{P} + \frac{M_{B2}}{2\ E\ I}\ \frac{\tan u}{u} = 0 \qquad (A.1.24)$$

Rearranging Equation A.1.24,

$$M_{B2} = - \frac{T_{21}\ L}{2\ u\ \tan u}\left[\frac{\cos(u - 2\ uml) - \cos u}{\cos u}\right] \qquad (A.1.25)$$

Substituting Equation A.1.25 into Equation A.1.23 and rearranging,

$$v = \frac{T_{21} L^3}{E I}\left[\frac{\sin(2\ uml)\ \cos(2um - u)}{8\ u^3\ \cos u} - \frac{ml}{4\ u^2}\right]$$

$$- \frac{T_{21} L^3}{4\ E\ I\ u^3\ \sin 2\ u}[\cos(u - 2\ uml) - \cos u]$$

$$[\cos\ (u - 2\ um) - \cos u] \qquad (A.1.26)$$

The deflection at the mid-span can be obtained by substituting $m = 1/2$ into Equation A.1.26

$$v = \frac{T_{21} L^3}{E I}\left[\frac{\sin(2\ uml)}{8\ u^3\ \cos u} - \frac{ml}{4\ u^2}\right] - \frac{T_{21} L^3}{4\ E\ I\ u^3\ \sin 2\ u}$$

$$[\cos(u - 2\ uml) - \cos u][1 - \cos u] \qquad (A.1.27)$$

The transferred bolt load for two bolts at symmetric locations is discussed as follows:

First, determine the deflection at the bolt locations. Based on Equation A.1.26, it is obtained that

$$v_{21} = \frac{T_{21} L^3}{E I}\left[\frac{\sin(2\ uml)\ \cos(2\ uml - u)}{8\ u^3\ \cos u} - \frac{ml}{4\ u^2}\right]$$

$$- \frac{T_{21} L^3}{4\ E\ I\ u^3\ \sin 2\ u}[\cos(u - 2\ uml) - \cos u]^2 \qquad (A.1.28)$$

According to Equations 4.2 to 4.4, the deflection at the bolt location due to bolt load is equal to the deflection due to the self weight of the roof stratum multiplied by R. Therefore, from Equations A.1.16 and A.1.28, the following equation is obtained.

$$\frac{R\ q\ L^4\ S_{21}}{384\ E\ I} = \frac{T_{21}\ L^3}{E\ I}\{\frac{\sin(2\ uml)\ \cos(2\ uml - u)}{8\ u^3\ \cos u} - \frac{ml}{4\ u^2} - \frac{[\cos(8 - 2\ uml) - \cos u]^2}{4\ u^3\ \sin u}\} \tag{A.1.29}$$

where S_{21} is the S_x value for x at x = xl.

From Equation A.1.29, T_{21} is determined,

$$T_{21} = (\frac{R\ q\ L\ S_{21}}{384})/(\frac{\sin(2\ uml)\ \cos(2\ uml - u)}{8\ u^3\ \cos u} - \frac{ml}{4\ u^2} - \frac{[\cos(u - 2\ uml) - \cos u]^2}{4\ u^3\ \sin 2\ u}) \tag{A.1.30}$$

Based on Equation 4.9, the α value under this condition is obtained as

$$\alpha_{21} = (\frac{S_{21}}{384})/(\frac{\sin(2\ uml)\ \cos(2\ uml - u)}{8\ u^3\ \cos u} - \frac{ml}{4\ u^2} - \frac{[\cos(u - 2\ uml) - \cos u]^2}{4\ u^3\ \sin 2\ u}) \tag{A.1.31}$$

3.3 Three Bolts; One Bolt at Center, Two Bolts at Symmetric Locations

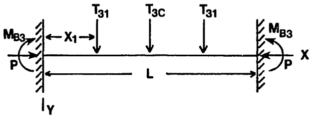

Fig. A.3

The deflection of a fixed-end beam subject to a concentrated bolt load at the center, two bolt loads at symmetric locations and a horizontal force simultaneously is (Fig. A.3):

$$v = \frac{T_{3c}\ L^3}{E\ I}\left(\frac{\sin(2\ um)}{16\ u^3\ \cos u} - \frac{m}{8\ u^2}\right) + \frac{T_{31}\ L^3}{E\ I}\left[\frac{\sin(2\ uml)\ \cos(2\ um - u)}{8\ u^3\ \cos u} - \frac{ml}{4\ u^2}\right] + \frac{M_{B3}\ L^2}{8\ E\ I}\ \frac{2}{u^2\ \cos u}[\cos(u - 2\ um) - \cos u] \tag{A.1.32}$$

The slope at the ends produced by three concentrated loads is eliminated by the moments at the ends, i.e.,

$$\frac{T_{3c}\ L^2}{16\ E\ I}\ \lambda(u) + \frac{T_{31}}{P}\left[\frac{\cos(u - 2\ uml) - \cos u}{\cos u}\right] + \frac{M_{B3}\ L}{2\ E\ I}\ \frac{\tan u}{u} = 0 \tag{A.1.33}$$

By rearranging Equation A.1.29, M_{B3} is obtained as follows:

$$M_{B3} = - \frac{L}{4\ u \sin u}[T_{3c}(1 - \cos u) - 2\ T_{31}(\cos u - \cos(u - 2\ uml))] \qquad (A.1.34)$$

Substituting Equation A.1.34 into Equation A.1.32 and rearranging

$$v = \frac{T_{3c}\ L^3}{E\ I}\left(\frac{\sin(2\ um)}{16\ u^3 \cos u} - \frac{m}{8\ u^2}\right) + \frac{T_{31}\ L^3}{E\ I}\left[\frac{\sin(2\ uml)\ \cos(2\ um - u)}{8\ u^3 \cos u} - \frac{ml}{4\ u^2}\right] + \frac{L^3}{8\ u^3\ E\ I \sin u}[2\ T_{31}(\cos u - \cos(u - 2\ um) - T_{3c}(1 - \cos u)] - [\cos(u - 2\ um) - \cos u]$$

(A.1.35)

The deflection at the mid-span can be obtained by letting $m = 1/2$ in Equation A.1.35 and rearranging

$$v = \frac{L^3}{8\ E\ I\ u^3}\{T_{3c}[\frac{\tan u - u}{2} - \frac{(1 - \cos u)^2}{\sin 2\ u} + T_{31}[\frac{\sin(2\ uml)}{\cos u} - 2\ uml + \frac{2(\cos u - \cos(u - 2\ uml))(1 - \cos u)}{\sin 2\ u}]\} \qquad (A.1.36)$$

The derivation of equations for the transferred bolt loads is presented as follows:

First, find the deflections at the bolt locations due to transferred bolt loads, i.e., v_{31} and v_{3c}. Since v_{3c} has already been derived in Equation A.1.36, only v_{31} need to be determined. Based on Equation A.1.35, v_{31} is obtained as

$$v_{31} = \frac{T_{3c}\ L^3}{E\ I}\left[\frac{\sin(2\ uml)}{16\ u^3\ \cos u} - \frac{ml}{8\ u^2}\right] + \frac{T_{31}\ L^3}{E\ I}\left[\frac{\sin(2\ uml)\ \cos(2\ uml - u)}{8\ u^3\ \cos u}\right.$$

$$\left. - \frac{ml}{4\ u^2}\right] + \frac{L^3}{8\ u^3\ E\ I\ \sin 2\ u}[2\ T_{31}(\cos u - \cos(u - 2uml)$$

$$- T_{3c}(1 - \cos u)][\cos(u - 2\ uml) - \cos u] \quad \text{(A.1.37)}$$

Then, based on Equations 4.2 through 4.4 and Equations A.1.36 through A.1.37, the following equations are obtained.

$$\frac{R\ q\ L^4\ S_{31}}{384\ E\ I} = \frac{L^3}{8\ E\ I\ u^3}\{T_{3c}\left[\frac{\sin(2\ uml)}{2\ \cos u} - uml\right.$$

$$\left. - \frac{(1 - \cos u)[\cos(u - 2\ uml) - \cos u]}{\sin 2\ u}\right]$$

$$+ T_{31}\left[\frac{\sin(2\ uml)\ \cos(2\ uml - u)}{\cos u} - 2\ uml\right.$$

$$\left. - \frac{2[\cos(u - 2\ uml) - \cos u]^2}{\sin 2\ u}\right]\} \quad \text{(A.1.38)}$$

$$\frac{R\ q\ L^4\ S}{384\ E\ I} = \frac{L^3}{8\ E\ I\ u^3}\{T_{3c}\left[\frac{\tan u - u}{2} - \frac{(1 - \cos u)^2}{\sin 2\ u}\right]$$

$$+ T_{31}\left[\frac{\sin(2\ uml)}{\cos u} - 2\ uml\right.$$

$$\left. + \frac{2[\cos u - \cos(u - 2\ uml)](1 - \cos u)}{\sin 2\ u}\right]\} \quad \text{(A.1.39)}$$

Based on the Cramer's rule, T_{31} and T_{3c} can be determined by solving two simultaneous Equations A.1.38 and A.1.39.

$$T_{31} = R\ q\ L(A1 \cdot K2 - A2 \cdot K1)/(A1 \cdot B2 - A2 \cdot B1) \tag{A.1.40}$$

$$T_{3c} = R\ q\ L(K1 \cdot B2 - K2 \cdot B1)/(A1 \cdot B2 - A2 \cdot B1) \tag{A.1.41}$$

$$\alpha_{31} = (A1 \cdot K2 - A2 \cdot K1)/(A1 \cdot B2 - A2 \cdot B1) \tag{A.1.42}$$

$$\alpha_{3c} = (K1 \cdot B2 - K2 \cdot B1)/(A1 \cdot B2 - A2 \cdot B1) \tag{A.1.43}$$

where

$$A1 = \frac{1}{u^3}\left(\frac{\tan u - u}{2} - \frac{(1 - \cos u)^2}{\sin u}\right)$$

$$A2 = \frac{1}{u^3}\left[\frac{\sin(2\ uml)}{2 \cos u} - uml - \frac{(1 - \cos u)[\cos(u - 2\ uml) - \cos u]}{\sin 2u}\right]$$

$$B1 = \frac{1}{u^3}\left[\frac{\sin(2\ uml)}{\cos u} - 2\ uml + \frac{2[\cos u - \cos(u - 2\ uml)](1 - \cos u)}{\sin 2u}\right]$$

$$B2 = \frac{1}{u^3}\left[\frac{\sin(2\ uml)\ \cos(2\ uml - u)}{\cos u} - 2\ uml - \frac{2[\cos u - \cos(u - 2\ uml)]^2}{\sin 2u}\right]$$

$$K1 = \frac{S}{48}$$

$$K2 = \frac{S_{31}}{48}$$

3.4 Four Bolts at Symmetric Locations

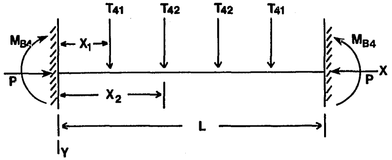

Fig. A.4

The deflection of a fixed-end beam subject to four bolt loads at symmetric locations and a horizontal force simultaneously is (Fig. A.4):

$$v = \frac{T_{41}\ L^3}{E\ I}\left[\frac{\sin(2\ uml)\ \cos(2\ um - u)}{8\ u^3\ \cos u} - \frac{ml}{4\ u^2}\right]$$

$$+ \frac{T_{42}\ L^3}{E\ I}\left[\frac{\sin(2\ um2)\ \cos(2\ um - u)}{8\ u^3\ \cos u} - \frac{m2}{4\ u^2}\right]$$

$$+ \frac{M_{B4}\ L^2}{8\ E\ I}\ \frac{2}{u^2\ \cos u}[\cos(u - 2\ um) - \cos u] \qquad (A.1.44)$$

The slope at the ends produced by four concentrated loads is eliminated by the moments acting at the ends, i.e.,

$$\frac{T_{41} \sin 2u(1 - m1)}{P \sin 2u} - \frac{T_{41}(1 - m1)}{P} + \frac{T_{41} \sin(2 um1)}{P \sin 2u}$$

$$- \frac{T_{41} m1}{P} + \frac{T_{42} \sin 2u(1 - m2)}{P \sin 2u} - \frac{T_{42}(1 - m2)}{P}$$

$$+ \frac{T_{42} \sin(2 um2)}{P \sin 2u} - \frac{T_{42} m2}{P} + \frac{M_{B4}}{2 E I} \frac{\tan u}{u} = 0 \qquad \text{(A.1.45)}$$

Rearranging Equation A.1.45, M_{B4} is obtained as

$$M_{B4} = - \frac{L}{2 u \tan u}[T_{41}(\frac{\cos(u - 2 um1) - \cos u}{\cos u})$$

$$+ T_{42}(\frac{\cos(u - 2 um2) - \cos u}{\cos u})] \qquad \text{(A.1.46)}$$

Substituting Equation A.1.46 into Equation A.1.44 and rearranging

$$v = \frac{L^3}{8 E I} \{T_{41}[\frac{\sin(2 um1) \cos(2 um - u)}{u^3 \cos u} - \frac{2m1}{u^2}$$

$$- \frac{2[\cos(u - 2 um1) - \cos u][\cos(u - 2 um) - \cos u]}{u^3 \sin 2u}]$$

$$+ T_{42}[\frac{\sin(2 um2) \cos(2 um - u)}{u^3 \cos u} - \frac{2 m2}{u^2}$$

$$- \frac{2[\cos(u - 2 um2) - \cos u][\cos(u - 2 um) - \cos u]}{u^3 \sin 2u}]\}$$

(A.1.47)

The deflection at the mid-span can be found by letting $m = 1/2$ in Equation A.1.47,

$$v = \frac{L^3}{8\,E\,I}\{T_{41}[\frac{\sin(2\,um1)}{u^3\cos u} - \frac{2\,m2}{u^2}$$

$$- \frac{2[\cos(u - 2\,um1) - \cos u][1 - \cos u]}{u^3\sin 2\,u}]$$

$$+ T_{42}[\frac{\sin(2\,um2)}{u^3\cos u} - \frac{2\,m2}{u^2}$$

$$- \frac{2[\cos(u - 2\,um2) - \cos u][1 - \cos u]}{u^3\cos u}]\} \qquad (A.1.48)$$

With the same procedure as for the case of three bolts, the transferred bolt loads, i.e., T_{41} and T_{42} are derviced as follows:

$$T_{41} = R\,q\,L(K1\cdot B2 - K2\cdot B1)/(A1\cdot B2 - A2\cdot B1) \qquad (A.1.49)$$

$$T_{42} = R\,q\,L(A1\cdot K2 - A2\cdot K1)/(A1\cdot B2 - A2\cdot B1) \qquad (A.1.50)$$

$$\alpha_{41} = (K1\cdot B2 - K2\cdot B1)/(A1\cdot B2 - A2\cdot B1) \qquad (A.1.51)$$

$$\alpha_{42} = (A1\cdot K2 - A2\cdot K1)/(A1\cdot B2 - A2\cdot B1) \qquad (A.1.52)$$

where

$$A1 = \frac{1}{u^3}[\frac{\sin(2\,um1)\cos(u - 2\,um1)}{\cos u} - 2\,um1$$

$$- \frac{2[\cos(u - 2\,um1) - \cos u]^2}{\sin 2\,u}]$$

$$A2 = \frac{1}{u^3}\left[\frac{\sin(2\ um1)\ \cos(u - 2\ um2)}{\cos\ u} - 2\ um1 - \frac{2[\cos(u - 2\ um1) - \cos\ u][\cos(u - 2\ um2) - \cos\ u]}{\sin\ 2\ u}\right]$$

$$B1 = \frac{1}{u^3}\left[\frac{\sin(2\ um1)\ \cos(u - 2\ um2)}{\cos\ u} - 2\ um1 - \frac{2[\cos(u - 2\ um1) - \cos\ u][\cos(u - 2\ um2) - \cos\ u]}{\sin\ 2\ u}\right]$$

$$B2 = \frac{1}{u^3}\left[\frac{\sin(2\ um2)\ \cos(u - 2\ um2)}{\cos\ u} - 2\ um2 - \frac{2[\cos(u - 2\ um2) - \cos\ u]^2}{\sin\ 2\ u}\right]$$

$$K1 = \frac{S_{41}}{48}$$

$$K2 = \frac{S_{42}}{48}$$

S_{41}, S_{42} = S_x factors for the first bolt and second bolt, respectively.

3.5 Five Bolts; One Bolt at Center, Four Bolts at Symmetric Locations

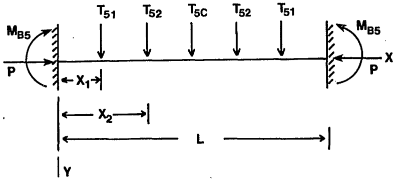

Fig. A.5

The deflection of a fixed-end beam subject to one bolt load at the center, four bolt loads at symmetric locations and a horizontal force simultaneously is (Fig. A.5):

$$v = \frac{T_{5c}\ L^3}{E\ I}\left[\frac{\sin(2\ um)}{16\ u^3\ \cos u} - \frac{m}{8\ u^2}\right] + \frac{T_{51}\ L^3}{E\ I}\left[\frac{\sin(2\ um1)\ \cos(2\ um - u)}{8\ u^3\ \cos u}\right.$$

$$\left. - \frac{m1}{4\ u2}\right] + \frac{T_{52}\ L^3}{E\ I}\left[\frac{\sin(2\ um2)\ \cos(2\ um - u)}{8\ u^3\ \cos u} - \frac{m2}{4\ u^2}\right]$$

$$+ \frac{M_{B5}\ L^2}{8\ E\ I}[\cos(u - 2\ um) - \cos u] \qquad \text{(A.1.53)}$$

The slope at the ends produced by five concentrated loads is eliminated by the moments at the ends, i.e.,

$$\frac{T_{5c}\,L^2}{16\,E\,I}\,\lambda(u) + \frac{T_{51}}{P}\left[\frac{\cos(u - 2\,um1) - \cos u}{\cos u}\right]$$

$$+ \frac{T_{52}}{P}\left[\frac{\cos(u - 2\,um2) - \cos u}{\cos u}\right]$$

$$+ \frac{M_{B5}\,L}{2\,E\,I}\,\frac{\tan u}{u} = 0 \qquad \text{(A.1.54)}$$

Rearranging Equation A.1.54, M_{B5} can be obtained as

$$M_{B5} = -\frac{L}{4\,u\,\sin u}[T_{5c}(1 - \cos u) - 2\,T_{51}(\cos u - \cos(u - 2\,um1))$$

$$- 2\,T_{52}(\cos u - \cos(u - 2\,um2))] \qquad \text{(A.1.55)}$$

Substituting Equation A.1.55 into Equation A.1.54 and rearranging

$$v = \frac{T_{5c}\,L^3}{E\,I}\left[\frac{\sin(2\,um)}{16\,u^3\,\cos u} - \frac{m}{8\,u^2}\right] + \frac{T_{51}\,L^3}{E\,I}\left[\frac{\sin(2\,um1)\,\cos(2\,um - u)}{8\,u^3\,\cos u}\right.$$

$$\left. - \frac{m1}{4\,u^2}\right] + \frac{T_{52}\,L^3}{E\,I}\left[\frac{\sin(2\,um2)\,\cos(2\,um - u)}{8\,u^3\,\cos u} - \frac{m2}{4\,u^2}\right]$$

$$+ \frac{L^3}{8\,u^3\,E\,I\,\sin 2\,u}[2\,T_{51}(\cos u - \cos(u - 2\,um1))$$

$$+ 2\,T_{52}(\cos u - \cos(u - 2\,um2)) - T_{5c}(1 - \cos u)]$$

$$\text{(A.1.56)}$$

The deflection at the mid-span can be obtained by substituting $m = 1/2$ into Equation A.1.56 and rearranging

$$v = \frac{L^3}{8\ E\ I\ u^3}\ \{T_{5c}[\frac{\tan\ u - u}{2} - \frac{(1 - \cos\ u)^2}{\sin\ 2\ u}]$$

$$+\ T_{51}[\frac{\sin(2\ um1)}{\cos\ u} - 2\ um1 + \frac{2(\cos\ u - \cos(u - 2\ um1))(1 - \cos\ u)}{\sin\ 2\ u}]$$

$$+T_{52}[\frac{\sin(2\ um2)}{\cos\ u} - 2\ um2 + \frac{2(\cos\ u - \cos(u - 2\ um2))(1 - \cos\ u)}{\sin\ 2\ u}]\}$$

(A.1.57)

The derivation of the equations for the transferred bolt loads in this case can be done by following the similar procedure as for the case of three bolts and four bolts, except that three simultaneous equations, instead of two, need to be solved.

$$T_{5c} = R\ q\ L\{[K1(B2\cdot C3 - B3\cdot C2) - K2(B1\cdot C3 - B3\cdot C1)$$
$$+ K3(B1\cdot C2 - B2\cdot C1)]/[A1(B2\cdot C3 - B3\cdot C2)$$
$$- A2(B1\cdot C3 - B3\cdot C1) + A3(B1\cdot C2 - B2\cdot C1)]\} \qquad (A.1.58)$$

$$T_{51} = R\ q\ L\{[A1(K2\cdot C3 - K3\cdot C2) - A2(K1\cdot C3 - K3\cdot C1)$$
$$+ A3(K1\cdot (2 - K2\cdot C1)]/[A1(B2\cdot C3 - B3\cdot C2)$$
$$- A2(B1\cdot C3 - B3\cdot C1) + A3(B1\cdot (2 - B2\cdot C1)]\} \qquad (A.1.59)$$

$$T_{52} = R\ q\ L\{[A1(B2\cdot K3 - B3\cdot K2) - A2(B1\cdot K3 - B3\cdot K1)$$
$$+ A3(B1\cdot K2 - B2\cdot K1)]/[A1(B2\cdot C3 - B3\cdot C2)$$
$$- A2(B1\cdot (3 - B3\cdot C1) + A3(B1\cdot C2 - B2\cdot C1)]\} \qquad (A.1.60)$$

$$\alpha_{5c} = [K1(B2 \cdot C3 - B3 \cdot C2) - K2(B1 \cdot C3 - B3 \cdot C1)$$

$$+ K3(B1 \cdot C2 - B2 \cdot C1)]/C5D \qquad (A.1.61)$$

$$\alpha_{51} = [A1(K2 \cdot C3 - K3 \cdot C2) - A2(K1 \cdot C3 - K3 \cdot C1)$$

$$+ A3(K1 \cdot C2 - K2 \cdot C1)]/C5D \qquad (A.1.62)$$

$$\alpha_{52} = [A1(B2 \cdot K3 - B3 \cdot K2) - A2(B1 \cdot K3 - B3 \cdot K1)$$

$$+A3(B1 \cdot K2 - B2 \cdot K1)]/C5D \qquad (A.1.63)$$

where

$$C5D = A1(B2 \cdot C3 - B3 \cdot C2) - A2(B1 \cdot C3 - B3 \cdot C1) + A3(B1 \cdot C2 - B2 \cdot C1)$$

$$A1 = \frac{1}{u^3}\left[\frac{\tan u - u}{2} - \frac{(1 - \cos u)^2}{\sin 2u}\right]$$

$$A2 = \frac{1}{u^3}\left[\frac{\sin(2\,uml)}{2\cos u} - uml - \frac{(1 - \cos u)[\cos(u - 2\,uml) - \cos u]}{\sin 2u}\right]$$

$$A3 = \frac{1}{u^3}\left[\frac{\sin(2\,um2)}{2\cos u} - um2 - \frac{(1 - \cos u)[\cos(u - 2\,um2) - \cos u]}{\sin 2u}\right]$$

$$B1 = \frac{1}{u^3}\left[\frac{\sin(2\,uml)}{\cos u} - 2\,uml + \frac{2[\cos u - \cos(u - 2\,uml)](1 - \cos u)}{\sin 2u}\right]$$

$$B2 = \frac{1}{u^3}\left[\frac{\sin(2\,uml)\cos(u - 2\,uml)}{\cos u} - 2\,uml\right.$$

$$\left. - \frac{2[\cos(u - 2\,uml) - \cos u]^2}{\sin 2u}\right]$$

$$B3 = \frac{1}{u^3}\left[\frac{\sin(2\ um1)\ \cos(u - 2\ um2)}{\cos u} - 2\ um1\right.$$

$$\left. - \frac{2[\cos(u - 2\ um1) - \cos u][\cos(u - 2\ um2) - \cos u]}{\sin 2\ u}\right]$$

$$C1 = \frac{1}{u^3}\left[\frac{\sin(2\ um2)}{\cos u} - 2\ um2 + \frac{2[\cos u - \cos(u - 2\ um2)](1 - \cos u)}{\sin 2\ u}\right]$$

$$C2 = \frac{1}{u^3}\left[\frac{\sin(2\ um1)\ \cos(u - 2\ um2)}{\cos u} - 2\ um1\right.$$

$$\left. - \frac{2[\cos(u - 2\ um2) - \cos u][\cos(u - 2\ um1) - \cos u]}{\sin 2\ u}\right]$$

$$C3 = \frac{1}{u^3}\left[\frac{\sin(2\ um2)\ \cos(u - 2um2)}{\cos u} - 2\ um2\right.$$

$$\left. - \frac{2[\cos(u - 2\ um2) - \cos u]^2}{\sin 2\ u}\right]$$

$$K1 = \frac{S}{48}$$

$$K2 = \frac{S_{51}}{48}$$

$$K3 = \frac{S_{52}}{48}$$

S_{51}, S_{52} = S_x factors for the first bolt and second bolt, respectively.

3.6 Six Bolts at Symmetric Locations

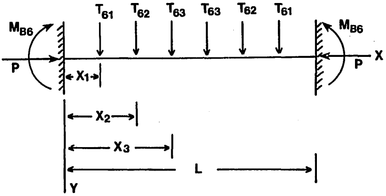

Fig. A.6

The deflection of a fixed-end beam subject to six concentrated bolt loads and a horizontal force simultaneously is (Fig. A.6):

$$v = \frac{T_{61}\ L^3}{E\ I}\left[\frac{\sin(2\ um1)\ \cos(2\ um - u)}{8\ u^3\ \cos u} - \frac{m1}{4\ u^2}\right]$$

$$+ \frac{T_{62}\ L^3}{E\ I}\left[\frac{\sin(2\ um2)\ \cos(2\ um - u)}{8\ u^3\ \cos u} - \frac{m2}{4\ u^2}\right]$$

$$+ \frac{T_{63}\ L^3}{E\ I}\left[\frac{\sin(2\ um3)\ \cos(2\ um - u)}{8\ u^3\ \cos u} - \frac{m3}{4\ u^2}\right]$$

$$+ \frac{M_{B6}\ L^2}{8\ E\ I}\ \frac{2}{u^2\ \cos u}[\cos(u - 2\ um) - \cos u] \qquad (A.1.64)$$

The slope at the ends produced by six concentrated loads is eliminated by the moments acting at the ends, i.e.,

$$\frac{T_{61} \sin 2 u(1 - m1)}{P \sin 2 u} - \frac{T_{61}(1 - m1)}{P} + \frac{T_{61} \sin(2 um1)}{P \sin 2 u} - \frac{T_{61} m1}{P}$$

$$+ \frac{T_{62} \sin 2 u(1 - m2)}{P \sin 2 u} - \frac{T_{62}(1 - m2)}{P} + \frac{T_{63} \sin 2 u(1 - m3)}{P \sin 2 u}$$

$$- \frac{T_{63}(1 - m3)}{P} + \frac{T_{63} \sin(2 um3)}{P \sin 2 u} - \frac{T_{63} m3}{P}$$

$$+ \frac{M_{B6}}{2 E I} \frac{\tan u}{u} = 0 \qquad (A.1.65)$$

Rearranging Equation A.1.65, M_{B6} is obtained as

$$M_{B6} = - \frac{L}{2 u \tan u}[T_{61}(\frac{\cos(u - 2 um1) - \cos u}{\cos u})$$

$$+ T_{62}(\frac{\cos(u - 2 um2) - \cos u}{\cos u})$$

$$+ T_{63}(\frac{\cos(u - 2 um3) - \cos u}{\cos u})] \qquad (A.1.66)$$

Substituting Equation A.1.66 into Equation A.1.64 and rearranging,

$$v = \frac{L^3}{8 E I} \{T_{61}[\frac{\sin(2 um1) \cos(2 um - u)}{u^3 \cos u} - \frac{2 m1}{u^2}$$

$$- \frac{2[\cos(u - 2 um1) - \cos u][\cos(u - 2 um) - \cos u]}{u^3 \sin 2 u}]$$

$$+ T_{62}[\frac{\sin(2 um2) \cos(2 um - u)}{u^3 \cos u} - \frac{2 m2}{u^2}$$

$$- \frac{2[\cos(u - 2 um2) - \cos u][\cos(u - 2 um) - \cos u]}{u^3 \sin 2 u}]$$

$$+ T_{63}\left[\frac{\sin(2\,um3)\,\cos(2\,um - u)}{u^3\,\cos u} - \frac{2\,m3}{u^2}\right.$$

$$\left.- \frac{2[\cos(u - 2\,um3) - \cos u][\cos(u - 2\,um) - \cos u]}{u^3\,\sin 2\,u}\right]\Big\}$$

(A.1.67)

The deflection at the mid-span is obtained by substituting $m = 1/2$ into Equation A.1.67,

$$v = \frac{L^3}{8\,E\,I}\Big\{T_{61}\left[\frac{\sin(2\,um1)}{u^3\,\cos u} - \frac{2\,m1}{u^2} - \frac{2[\cos(u - 2\,um1) - \cos u][1 - \cos u]}{u^3\,\sin 2\,u}\right]$$

$$+ T_{62}\left[\frac{\sin(2\,um2)}{u^3\,\cos u} - \frac{2\,m2}{u^2} - \frac{2[\cos(u - 2\,um2) - \cos u][1 - \cos u]}{u^3\,\sin 2\,u}\right]$$

$$+ T_{63}\left[\frac{\sin(2\,um3)}{u^3\,\cos u} - \frac{2\,m3}{u^2} - \frac{2[\cos(u - 2\,um3) - \cos u][1 - \cos u]}{u^3\,\sin 2\,u}\right]\Big\}$$

(A.1.68)

The derivation of the transferred bolt loads in this case can be obtained by following the same procedure as for the case of five bolts in the previous section.

$$T_{61} = R\,q\,L\{[K1(B2\cdot C3 - B3\cdot C2) - K2(B1\cdot C3 - B3\cdot C1)$$

$$+ K3(B1\cdot C2 - B2\cdot C1)]/[A1(B2\cdot C3 - B3\cdot C2)$$

$$- A2(B1\cdot C3 - B3\cdot C1) + A3(B1\cdot C2 - B2\cdot C1)]\} \qquad \text{(A.1.69)}$$

$$T_{62} = R\ q\ L\{[A1(K2 \cdot C3 - K3 \cdot C2) - A2(K1 \cdot C3 - K3 \cdot C1) + A3(K1 \cdot C2 - K2 \cdot C1)]/[A1(B2 \cdot C3 - B3 \cdot C2) - A2(B1 \cdot C3 - B3 \cdot C1) + A3(B1 \cdot C2 - B2 \cdot C1)]\} \tag{A.1.70}$$

$$T_{63} = R\ q\ L\{[A1(B2 \cdot K3 - B3 \cdot K2) - A2(B1 \cdot K3 - B3 \cdot K1) + A3(B1 \cdot K2 - B2 \cdot K1)]/[A1(B2 \cdot C3 - B3 \cdot C2) - A2(B1 \cdot C3 - B3 \cdot C1) + A3(B1 \cdot C2 - B2 \cdot C1)]\} \tag{A.1.71}$$

$$\alpha_{61} = [K1(B2 \cdot C3 - B3 \cdot C2) - K2(B1 \cdot C3 - B3 \cdot C1) + K3(B1 \cdot C2 - B2 \cdot C1)]/C6D \tag{A.1.72}$$

$$\alpha_{62} = [A1(K2 \cdot C3 - K3 \cdot C2) - A2(K1 \cdot C3 - K3 \cdot C1) + A3(K1 \cdot C2 - K2 \cdot C1)]/C6D \tag{A.1.73}$$

$$\alpha_{63} = [A1(B2 \cdot K3 - B3 \cdot K2) - A2(B1 \cdot K3 - B3 \cdot K1) + A3(B1 \cdot K2 - B2 \cdot K1)]/C6D \tag{A.1.74}$$

where

$$C6D = A1(B2 \cdot C3 - B3 \cdot C2) - A2(B1 \cdot C3 - B3 \cdot C1) + A3(B1 \cdot C2 - B2 \cdot C1)$$

$$A1 = \frac{1}{u^3}\left[\frac{\sin(2\ uml)\ \cos(2\ uml - u)}{\cos u} - 2\ uml - \frac{2[\cos(u - 2\ uml) - \cos u]^2}{\sin 2\ u}\right]$$

$$A2 = \frac{1}{u^3}\left[\frac{\sin(2\ um1)\ \cos(2\ um2 - u)}{\cos\ u} - 2\ um1 - \frac{2[\cos(u - 2\ um1) - \cos\ u][\cos\ (u - 2\ um2) - \cos\ u]}{\sin\ 2\ u}\right]$$

$$A3 = \frac{1}{u^3}\left[\frac{\sin(2\ um1)\ \cos(2\ um3 - u)}{\cos\ u} - 2\ um1 - \frac{2[\cos(u - 2\ um1) - \cos\ u][\cos(u - 2\ um3) - \cos\ u]}{\sin\ 2\ u}\right]$$

$$B1 = \frac{1}{u^3}\left[\frac{\sin(2\ um1)\ \cos(2\ um2 - u)}{\cos\ u} - 2\ um1 - \frac{2[\cos(u - 2\ um1) - \cos\ u][\cos(u - 2\ um2) - \cos\ u]}{\sin\ 2\ u}\right]$$

$$B2 = \frac{1}{u^3}\left[\frac{\sin(2\ um2)\ \cos(2\ um2 - u)}{\cos\ u} - 2\ um2 - \frac{2[\cos(u - 2\ um2) - \cos\ u]^2}{\sin\ 2\ u}\right]$$

$$B3 = \frac{1}{u^3}\left[\frac{\sin(2\ um2)\ \cos(2\ um3 - u)}{\cos\ u} - 2\ um2 - \frac{2[\cos(u - 2\ um2) - \cos\ u][\cos(u - 2\ um3) - \cos\ u]}{\sin\ 2\ u}\right]$$

$$C1 = \frac{1}{u^3}\left[\frac{\sin(2\ um1)\ \cos(2\ um3 - u)}{\cos\ u} - 2\ um1 - \frac{2[\cos(u - 2\ um1) - \cos\ u][\cos(u - 2\ um3) - \cos\ u]}{\sin\ 2\ u}\right]$$

$$C2 = \frac{1}{u^3}\left[\frac{\sin(2\ um2)\ \cos(2\ um3 - u)}{\cos\ u} - 2\ um2 - \frac{2[\cos(u - 2\ um3) - \cos\ u][\cos(u - 2\ um2) - \cos\ u]}{\sin\ 2\ u}\right]$$

$$C3 = \frac{1}{u^3}\left[\frac{\sin(2\ um3)\ \cos(2\ um3 - u)}{\cos u} - 2\ um3 - \frac{2[\cos(u - 2\ um3) - \cos u]^2}{\sin 2u}\right]$$

$$K1 = \frac{S_{61}}{48}$$

$$K2 = \frac{S_{62}}{48}$$

$$K3 = \frac{S_{63}}{48}$$

S_{61}, S_{62}, S_{63} = S_x factors for the first, second and third bolt, respectively.

APPENDIX II

COMPUTER PROGRAM FOR THE REINFORCEMENT ANALYSIS OF MECHANICAL ROOF BOLTING

```
C     ****************************************************************
C     *                                                              *
C     *  DEVELOPMENT OF DESIGN CRITERIA FOR MECHANICAL ROOF BOLTING  *
C     *                                                              *
C     ****************************************************************
C
C
C
C     XL=ROOF SPAN, IN
C     B=WIDTH OF ROOF LAYER OR BOLT SPACING, IN
C     US=COEFFICIENT OF FRICTION ALONG THE BEDDING PLANE
C     N=LAYER NUMBERS OF IMMEDIATE ROOF
C     E=YOUNG'S MODULUS OF EACH LAYER,PSI
C     T=THICKNESS OF EACH LAYER, IN
C     W=UNIT WEIGHT OF EACH LAYER, LB/CU. IN
C     Q=LINE LOAD OF EACH LAYER, LB/IN
C     HS=IN-SITU HORIZONTAL STRESS, PSI
C     XI=MOMENT OF INERTIA OF EACH LAYER,
C     HSET,ZETA,X,ALMDA,S,F=PARAMETER WITH HORIZONTAL STRESS
C     TAU1=MAXIMUM SHEAR STRESS AT THE END
C     XMO=MAXIMUM BENDING MOMENT AT THE END
C     SIGM1=MAXIMUM BENDING STRESS AT THE END OF THE BEAM, UNBOLTED ROOF
C     , PSI
C     SIGMTU=TOTAL UPPER-FIBER STRESS AT THE END OF THE BEAM, UNBOLTED ROOF
C     , PSI
C     SIGMTL=TOTAL LOWER-FIBER STRESS AT THE END OF THE BEAM, UNBOLTED ROOF
C     , PSI
C     V2L=MAXIMUM DEFLECTION AT MID-SPAN OF THE BEAM, IN.
C     TENSH=TENSILE STRENGTH OF THE ROCK, PSI
C     TENSHU=TENSILE STRENGTH OF THE TOP STRATUM, PSI
C     COMSH=COMPRESSIVE STRENGTH OF THE ROCK, PSI
C     COMSHL=COMPRESSIVE STRENGTH OF THE BOTTOM STRATUM, PSI
C     PA=ANCHORAGE CAPACITY OF THE STRATUM, LB
C     PAU=ANCHORAGE CAPACITY OF THE ANCHORING STRATUM, IB
C     VO=SHEAR FORCE AT THE END OF THE BEAM, LB
C     QS1=SHEAR FLOW,LB/IN
C     SIGBU=MAXIMUM BENDING STRESS OF THE UPPER FIBER, BOLTED ROOF DUE TO
C     FRICTION EFFECT, PSI
C     SIGBL=MAXIMUM BENDING STRESS OF THR LOWER FIBER, BOLTED ROOF DUE TO
C     FRICTION EFFECT, PSI
C     SIGTU=TOTAL UPPER-FIBER STRESS OF BOLTED ROOF, PSI
C     SIGTL=TOTAL LOWER-FIBER STRESS OF BOLTED ROOF, PSI
C     SIGB5,SIGB4,ETC.=MAXIMUM BENDING STRESS OF BOLTED ROOF DUE TO
C     SUSPENSION EFFECT, 5 BOLTS, 4 BOLTS, ETC.
C     NB=NUMBER OF BOLTS EACH ROW ALONG THE SPAN
C     SA=SPACING BETWEEN BOLT SETS ALONG THE OPENING, IN.
C     SB=BOLT SPACING ALONG THE SPAN DUE TO SUSPENSION EFFECT, IN.
C     XB=BOLT SPACING ALONG THE SPAN DUE TO FRICTION EFFECT, IN.
C     BL=BOLT LENGTH, IN.
C
      DOUBLE PRECISION EIS(10),M(10),HS(10),SIGMTU(10),C1CS(10,10),A1(10
     1),SIGMTL(10),P31(10,1),P32(10,10),R(10),Q(10),XI(10),E(10),TY12,T(
     110),W(10),SIGM1(10),COMSH(10),QA(10),WA(10),H(10),TENSH(10),PA(10)
     2,V2L2(10),V2L(10),HSET(10),U(10),ZETA(10),ALMDA(10),D1(10,10),SC(1
     30),G(10),X(10),F(10),VC(10),S(10),IQM32(10),PB4(10),SIGM42(10),XMO
     4(10),TAU1(10),SEIS(10),SUMQ,SUMEIS,XM(10),UM(10,10),ZETAX(10,10),A
     5LMDAX(10,10),SX(10,10),XX(10,10),G1X(10,10),C1X(10,10),G2X(10,10),
     6C2X(10,10),C2T(10,10),XK3C(10),XK31(10,10),A2(10,10),B1(10,10),B2(
     710,10),C3C(10,10),C31(10,10),C3T(10,10),UM1(10,10),UM2(10,10),ZETA
     8X1(10,10),ALMDA1(10,10),ALMDA2(10,10),ZETAX2(10,10),S41(10,10),S42
     9(10,10),A41(10,10),B41(10,10,10),A42(10,10,10),B42(10,10),XK41(10,
     A10),XK42(10,10),CE4(10,10,10),C41(10,10,10),C42(10,10,10),C4T(10,1
     A0,10),C4MP(10,10,10),S5C(10),S51(10,10),S52(10,10),A51(10),B51(10,
     A10),D51(10,10),A52(10,10),B52(10,10),D52(10,10,10),A53(10,10),B53(
     A10,10,10),D53(10,10),XK51(10),XK52(10,10),XK53(10,10),CE5(10,10,10
     A),C5C(10,10,10),C51(10,10,10),C52(10,10,10),C5T(10,10,10),C5MC1(10
     A,10,10),C5MC2(10,10,10),Q1C(10,10),V1C(10,10),W1C(10,10),R1C(10,10
```

```
     A),W1CS(10,10),V1CX(10,10),W1CX(10,10),R1CX(10,10),W1CXS(10,10)
      DOUBLE PRECISION V3C(10,10),W3C(10,10),R3C(10,10),W3CS(10,10),R3CS
     A(10,10),Z,C21S(10,10),Q21(10,10),V21(10,10),W21(10,10),R21(10,10),
     AW21S(10,10),R21S(10,10),V21C(10,10),Q21C(10,10),W21C(10,10),R21C(1
     A0,10),W21CS(10,10),R21CS(10,10),C31S(10,10),Q31(10,10),C3CS(10,10)
     A,Q3C(10,10),V31(10,10),W31(10,10),R31(10,10),W31S(10,10),R31S(10,1
     A0),R1CXS(10,10),R1CS(10,10),TT(10),VCS(10),EI(10),B,CDC(10,10),Q41
     AC(10,10),Q42C(10,10),XM1(10),XM2(10),C3MP(10,10)
      DOUBLE PRECISION C41S(10,10,10),Q41(10,10,10),C42S(10,10,10),Q42(1
     10,10,10),Q4T(10,10,10),V41(10,10,10),W41(10,10,10),R41(10,10,10),W
     241S(10,10,10),R41S(10,10,10),V42(10,10,10),W42(10,10,10),R42(10,10
     3,10),W42S(10,10,10),R42S(10,10,10),V42C(10,10,10),W42CS(10,10,10),
     4R42CS(10,10,10),C51S(10,10,10),Q51(10,10,10),C52S(10,10,10),Q52(10
     5,10,10),C5CS(10,10,10),Q5C(10,10,10),V5C(10,10,10),W5C(10,10,10),R
     65C(10,10,10),W5CS(10,10,10),R5CS(10,10,10),V51(10,10,10),W51(10,10
     7,10),R51(10,10,10),W51S(10,10,10),R51S(10,10,10),V52(10,10,10),W52
     8(10,10,10),R52(10,10,10),W52S(10,10,10),R52S(10,10,10),Q2T(10,10),
     9Q3T(10,10),Q5T(10,10,10),XMB1(10,10),XMB2(10,10),XMB3(10,10),XMB4(
     A10,10,10),XMB5(10,10,10),SIGO(10),XMB10(10,10),XMB20(10,10),XMB30(
     A10,10),XMB40(10,10,10),XMB50(10,10,10),SIGB1(10,10),SIGB2(10,10),S
     AIGB3(10,10),SIGB4(10,10,10),SIGB5(10,10,10),QT(10),RQ1T(10),SIGTU1
     A(10),SIGTL1(10),SIGTU2(10),SIGTL2(10),SIGTU3(10),SIGTL3(10),SIGTU4
     A(10),SIGTL4(10),SIGTU5(10),SIGTL5(10),SB,SA,ET(10),TENSHU,COMSHL
      DOUBLE PRECISION SUMTT1(10),TT1(10),SUMTF1,BE1(10),ET1(10),AE1(10)
     A,YD1(10),AY1(10),SUMA1,SUMAY1,SUME1,YC1,SMIZC1,YF1(10),XIA1(10),IZ
     AC1(10),SUMIA1,X1(10),V0,V1(10),QS1(10),QSM1(10),VS1(10),TB1(10),US
     A,U1,XMB,SIGBL,SIGBU,V2L1,CB1(10),SMETT1,F1,S1,XF1,ZETA1,ALDA1
      DOUBLE PRECISION PAU,SUMTT(10),SUMTF,BE(10),EC(10),AE(10),YD(10),A
     AY(10),SUMA,SUMAY,SUME,YC,SUMIZC,YF(10),XIA(10),IZC(10),SUMIA,SUMET
     AT,SIGTU,SIGTL,SA1(10),TBS,SAS
      DOUBLE PRECISION XB(10,10),XL,CB2(10),SUMQT,BL,S61(10,10),T121,S62
     9(10,10),A61(10,10),B61(10,10,10),A62(10,10,10),B62(10,10),XK61(10,
     A10),XK62(10,10),XK63(10,10),XM3(10),UM3(10,10),ZETAX3(10,10),TW,AL
     AMDA3(10,10),S63(10,10),D61(10,10,10),D62(10,10,10),A63(10,10,10),B
     A63(10,10,10),D63(10,10),C61(10,10,10,10),C62(10,10,10,10),C63(10,1
     A0,10,10),C6T(10,10,10,10),C6M12(10,10,10,10),C6M13(10,10,10,10),CE
     A6(10,10,10,10),C61S(10,10,10,10),C62S(10,10,10,10),C63S(10,10,10,1
     A0),Q61(10,10,10,10),Q62(10,10,10,10),T123,TT456,Q6T(10,10,10,10),V
     A61(10,10,10,10),W61(10,10,10,10),R61(10,10,10,10),V62(10,10,10,10)
     A,W62(10,10,10,10),R62(10,10,10,10),V63(10,10,10,10),W63(10,10,10,1
     A0),R63(10,10,10,10),Q61C(10,10),Q62C(10,10),Q63C(10,10),V6C(10,10,
     A10,10),W6C(10,10,10,10),R6C(10,10,10,10),XMB6(10,10,10,10),XMB60(1
     A0,10,10,10),SIGB6(10,10,10,10),SIGTU6(10),SIGTL6(10),Q63(10,10,10,
     A10),BETA1(10,10),BETA2(10,10),BETA3(10,10),BETA4(10,10,10),BETA5(1
     A0,10,10),BETA6(10,10,10,10)
C
C     FLEXURAL BEHAVIOR OF IMMEDIATE ROOF
C
C     INPUT OF MATERIAL PROPERTIES,GEOMETRY AND HORIZONTAL STRESS OF
C     IMMEDIATE ROOF
C
      READ(5,80) N
   80 FORMAT(I2)
      READ(5,79) XL,B,US
   79 FORMAT(3F10.4)
      READ(5,80) N
   80 FORMAT(I2)
      WRITE(6,86) N
   86 FORMAT(1H1,3X,'LAYER NUMBERS',2X,I2)
      N1=N
      DO 55 I=1,N
      READ(5,33) E(I),T(I),W(I),HS(I),TENSH(I),COMSH(I),PA(I)
   33 FORMAT(E10.3,6F10.4)
      Q(I)=W(I)*B*T(I)
      QT(I)=Q(I)
      TT(I)=T(I)
      ET(I)=E(I)*T(I)
```

```
      ET1(I)=E(I)
      TT1(I)=T(I)
      XI(I)=B*T(I)**3/12.
      EI(I)=E(I)*XI(I)
C
C     CALCULATION OF PARAMETERS WITH HORIZONTAL STRESS
C
      HSET(I)=3.*HS(I)/(E(I)*T(I)**2)
      U(I)=XL*DSQRT(HSET(I))
      IF(U(I).GT.3.00) U(I)=3.00
      ZETA(I)=12.*(2./DCOS(U(I))-2.-U(I)**2)/(5.*U(I)**4)
      X(I)=3.*(DTAN(U(I))-U(I))/(U(I)**3)
      ALMDA(I)=2.*(1.-DCOS(U(I)))/(U(I)**2*DCOS(U(I)))
      S(I)=5.*ZETA(I)-4.*U(I)*X(I)*ALMDA(I)/DTAN(U(I))
      EIS(I)=E(I)*XI(I)/S(I)
      F(I)=X(I)*U(I)/DTAN(U(I))
C
C     CALCULATION OF TAU1,XMO,SIGM1,SIGMTU,SIGMTL,V2L OF EACH LAYER
C     BEFORE COMBINATION
C
      TAU1(I)=(3.*W(I)*XL)/4.
      XMO(I)=Q(I)*XL**2/12.*F(I)
      SIGM1(I)=W(I)*XL**2/(2.*T(I))*F(I)
      SIGMTU(I)=-1.*HS(I)+SIGM1(I)
      SIGMTL(I)=-1.*HS(I)-SIGM1(I)
      V2L(I)=Q(I)*XL**4/(384.*EIS(I))
   55 CONTINUE
      TENSHU=TENSH(N)
      COMSHL=COMSH(1)
      PAU=PA(N)
      WRITE(6,54)
   54 FORMAT(1H0,2X,'E',12X,'T',12X,'W',12X,'Q',12X,'EIS',10X,'TENSH',8X
     1,'COMSH',8X,'PA')
      WRITE(6,61) (E(I),T(I),W(I),Q(I),EIS(I),TENSH(I),COMSH(I),PA(I),I=
     11,N)
   61 FORMAT(1H0,3X/8(D11.4,2X))
      WRITE(6,87)
   87 FORMAT(1H0,2X,'XMO',10X,'SIGM1',8X,'TAU1',9X,'V2L',10X,'F',12X,'SI
     1GMTU',7X,'SIGMTL')
      WRITE(6,62)(XMO(I),SIGM1(I),TAU1(I),V2L(I),F(I),SIGMTU(I),SIGMTL(I
     1),I=1,N)
   62 FORMAT(1H0,3X,/7(D11.4,2X))
      WRITE(6,57)
   57 FORMAT(1H0,2X,'HS',11X,'U',12X,'ZETA',9X,'X',12X,'ALMDA',9X,'S')
      WRITE(6,12) (HS(I),U(I),ZETA(I),X(I),ALMDA(I),S(I),I=1,N)
   12 FORMAT(1H0,/6(D11.4,2X))
      WRITE(6,718) US
  718 FORMAT(1H0,2X,'US',2X,D11.4)
C
C     STRATA COMBINING PROCESS
C
C     KC=NUMBER OF COMBINATION FOR WHOLE ROOF STRATA
      KC=1
   10 K=1
      J=1
      L=1
      M(1)=1
      EC(1)=E(1)
      IF(KC.EQ.1) QA(1)=Q(1)
      IF(KC.EQ.1) SEIS(1)=EIS(1)
      DO 20 I=2,N
      IF(V2L(I).LE.V2L(I-1)) GO TO 30
      J=J+1
      M(J)=I
      ID=K
C     FIRST COMBINING OR NOT
      IF(J-2)40,50,40
```

```
C       CONSECUTIVE COMBINING OR NOT
   40   IF(M(J)-M(J-1)-1)50,60,50
C
C       CALCULATION OF DEFLECTION OF COMBINED LAYER
C
   50   SUMQ=QT(I-1)
        SUMT=TT(I-1)
        SUMEI=EI(I-1)
        SUMET=ET(I-1)
        IF(KC.EQ.1) SUMEIS=EIS(I-1)
        IF(KC.GT.1) SUMEIS=SEIS(I-1)
        SUMV=V2L(I-1)
   60   SUMQ=SUMQ+QT(I)
        SUMT=SUMT+TT(I)
        SUMEI=SUMEI+EI(I)
        SUMET=SUMET+ET(I)
        IF(KC.EQ.1)SUMEIS=SUMEIS+EIS(I)
        IF(KC.GT.1)SUMEIS=SUMEIS+SEIS(I)
        SUMV=SUMQ*XL**4/(384.*SUMEIS)
C
C       CALCULATION OF ADJUSTED LINE LOAD (GRAVITY) OF 1ST MEMBER OF
C       COMBINED LAYER
C
        EIS(ID)=EIS(I-1)
        QA(ID)=EIS(ID)*SUMQ/SUMEIS
        T(ID)=T(I-1)
        Q(ID)=Q(I-1)
C       ADJUSTED UNIT WEIGHT OF 1ST MEMBER OF COMBINED LAYER
        W(ID)=QA(ID)/(B*T(ID))
        HS(ID)=HS(I-1)
        TENSH(ID)=TENSH(I-1)
        COMSH(ID)=COMSH(I-1)
        PA(ID)=PA(I-1)
        F(ID)=F(I-1)
        EIS(I)=EIS(I-1)
        T(I)=T(I-1)
        HS(I)=HS(I-1)
        TENSH(I)=TENSH(I-1)
        COMSH(I)=COMSH(I-1)
        PA(I)=PA(I-1)
        Q(I)=Q(I-1)
        F(I)=F(I-1)
C       EQUIVALENT EIS OF COMBINED LAYER
        QT(ID)=SUMQ
        TT(ID)=SUMT
        EI(ID)=SUMEI
        ET(ID)=SUMET
        EC(ID)=ET(ID)/TT(ID)
        SEIS(ID)=SUMEIS
        V2L(ID)=SUMV
        WRITE(6,101) ID,T(ID),W(ID),QT(ID),Q(ID),QA(ID)
  101   FORMAT(1H0,1X,'ID',1X,I2,2X,'TID',D12.4,3X,'WID',1X,D12.4,1X,'QTID
       1',D12.4,1X,'QID',1X,D12.4,1X,'QAID',1X,D12.4)
        GO TO 20
C
C       UNCOMBINED LAYERS
C
   30   K=K+1
        Q(K)=Q(I)
        QT(K)=QT(I)
        TT(K)=TT(I)
        EC(K)=E(I)
        EI(K)=EI(I)
        EIS(K)=EIS(I)
        IF(KC.EQ.1) QA(K)=Q(I)
        IF(KC.GT.1)QA(K)=QA(I)
        IF(KC.EQ.1) SEIS(K)=EIS(I)
```

```
      IF(KC.GT.1)SEIS(K)=SEIS(I)
      V2L(K)=V2L(I)
      T(K)=T(I)
      HS(K)=HS(I)
      TENSH(K)=TENSH(I)
      COMSH(K)=COMSH(I)
      PA(K)=PA(I)
      F(K)=F(I)
      W(K)=W(I)
      WRITE(6,105) K,TT(K),W(K),QT(K),QA(K)
  105 FORMAT(1H0,1X,'K',2X,I2,2X,'T',1X,D13.4,4X,'W',1X,D13.4,1X,'QT',1X
     1,D13.4,1X,'QA',1X,D13.4)
   20 CONTINUE
      WRITE(6,65) K
   65 FORMAT(1H0,3X,'K',2X,I2)
      WRITE(6,63)
   63 FORMAT(1H0,'K',4X,'V2L',10X,'QT',12X,'W',11X,'SEIS',10X,'T',12X,'Q
     1A')
      WRITE(6,64) (I,V2L(I),QT(I),W(I),SEIS(I),TT(I),QA(I),I=1,K)
   64 FORMAT(1H0,3X/(I2,6(D11.4,2X)))
C     COMBINING OR NOT FOR WHOLE ROOF STRATA
      IF(K.EQ.N) GO TO 100
      IF(K.EQ.1) GO TO 100
      N=K
      DO 108 I=2,K
      IF(V2L(I).LE.V2L(I-1)) L=L+1
  108 CONTINUE
C
C     CHECK NEW LAYERS NEED COMBINING OR NOT
C
      IF(L.EQ.K) GO TO 100
      KC=KC+1
      GO TO 10
  333 KK=1
      DO 713 I=2,N
      IF(V2L(I).EQ.V2L(I-1)) KK=KK+1
  713 CONTINUE
      IF(KK.EQ.N) GO TO 777
      GO TO 89
C
C     CALCULATION OF TAUI,XMO,SIGM1,SIGMTU,SIGMTL,V2L OF LAYERS AFTER
C     COMBINATION
C
  100 DO 29 I=1,K
      TAU1(I)=(3.*W(I)*XL)/4.
      XMO(I)=QA(I)*XL**2/12.*F(I)
      SIGM1(I)=QA(I)*XL**2/(2.*B*T(I)**2)*F(I)
      SIGMTU(I)=-1.*HS(I)+SIGM1(I)
      SIGMTL(I)=-1.*HS(I)-SIGM1(I)
      V2L(I)=QT(I)*XL**4/(384.*SEIS(I))
   29 CONTINUE
      WRITE(6,66)
   66 FORMAT(1H0,3X,'TAU1',9X,'XMO',10X,'SIGM1',7X,'SIGMTU',7X,'SIGMTL',
     17X,'V2L')
      WRITE(6,13) (TAU1(I),XMO(I),SIGM1(I),SIGMTU(I),SIGMTL(I),V2L(I),I=
     11,K)
   13 FORMAT(1H0,3X/6(D11.4,2X))
C
C     FAILURE CRITERIA FOR UNBOLTED ROOF
C
      KC=0
      DO 41 I=1,N
      IF(TENSH(I).GE.SIGMTU(I).AND.COMSH(I).GE.DABS(SIGMTL(I))) GO TO 41
      IF(TENSH(I).LT.SIGMTU(I).AND.COMSH(I).GE.DABS(SIGMTL(I))) GO TO 81
      IF(TENSH(I).GE.SIGMTU(I).AND.COMSH(I).LT.DABS(SIGMTL(I))) GO TO 82
      IDCT=I
      WRITE(6,83) IDCT
```

```
   83 FORMAT(1H0,3X,'TENSILE FAILURE AT TOP FIBER, AND SHEAR FAILURE AT
     1BOTTOM',5X,'LAYER NO. ',2X,I2)
      GO TO 75
   81 IDT=I
      WRITE(6,84) IDT
   84 FORMAT(1H0,3X,'TENSILE FAILURE AT TOP FIBER',5X,'LAYER NO. ',2X,I2)
      GO TO 75
   82 IDC=I
      WRITE(6,85) IDC
   85 FORMAT(1H0,3X,'SHEAR FAILURE AT BOTTOM FIBER',5X,'LAYER NO. ',2X,I2
     1)
   75 WRITE(6,51)
   51 FORMAT(1H0,3X,'SIGMTU',15X,'TENSH',16X,'SIGMTL',16X,'COMSH')
      WRITE(6,58) SIGMTU(I),TENSH(I),SIGMTL(I),COMSH(I)
   58 FORMAT(1H0,2X,4(D11.4,10X))
      KC=KC+1
   41 CONTINUE
      IF(KC.NE.N) GO TO 42
      WRITE(6,52)
   52 FORMAT(1H1,//3X,'UNBOLTED ROOF IS STABLE')
      IF(K.EQ.1) GO TO 444
      GO TO 333
C
C     FRICTION EFFECT
C
C     FRICTION EFFECT FOR ONE EQUIVALENT LAYER
C
  444 CALL FRIC1(SUMTT1,TT1,N1,SUMTF1,BE1,ET1,B,AE1,YD1,AY1,SUMA1,SUMAY1
     A,SUME1,YC1,SMIZC1,YF1,XIA1,IZC1,IC1,SUMIA1,I,J,X1,VO,V1,QS1,QSM1,V
     AS1,TB1,US,U1,XMB,SIGBL,SIGBU,V2L1,SMETT1,CB1,F1,S1,XF1,ZETA1,ALDA1
     A,HS,QT,XL,XB,CB2,BL)
      CALL FRSPAC(J,XB,I,XL,CB1,CB2)
      SIGTU=-1.*HS(1)+SIGBU
      SIGTL=-1.*HS(1)-SIGBL
      IF(TENSHU.GE.SIGTU.AND.COMSHL.GE.DABS(SIGTL)) GO TO 715
      WRITE(6,424)
      WRITE(6,719) TENSHU,SIGTU,COMSHL,SIGTL
  719 FORMAT(1H0,2X,'TENSHU',1X,D11.4,1X,'SIGTU',1X,D11.4,1X,'COMSHL',1X
     1,D11.4,1X,'SIGTL',1X,D11.4)
      GO TO 717
  715 WRITE(6,716)
  716 FORMAT(1H1,//3X,'BOLTED ROOF IS STABLE')
      DO 520 J=1,10
      SA1(J)=PAU/TB1(J)*B
  520 CONTINUE
      DO 530 J=1,10
      IF(SA1(J).GE.B) GO TO 540
  530 CONTINUE
  540 J1=2*J
      TBS=TB1(J)
      SAS=SA1(J)
      WRITE(6,408) J1
      WRITE(6,409) (XB(J,I2),I2=1,J)
      WRITE(6,413) SAS
      WRITE(6,425) BL
      WRITE(6,423) PAU
      WRITE(6,580)
  580 FORMAT(1H0,2X,'SIGTU',10X,'SIGTL',9X,'V2L1',8X,'TENSHU',7X,'COMSHL
     1')
      WRITE(6,570) SIGTU,SIGTL,V2L1,TENSHU,COMSHL
  570 FORMAT(1H0,2X,5(D11.4,2X))
      WRITE(6,735)
  735 FORMAT(1H1)
  717 GO TO 415
C
C     FRICTION EFFECT FOR MULTIPLE LAYERS
C
```

```
  777 CALL FRICM(SUMTT,TT,K,SUMTF,BE,EC,B,AE,YD,AY,SUMA,SUMAY,SUME,YC,SU
     AMIZC,YF,XIA,IZC,IC,SUMIA,X1,VO,V1,QS1,QSM1,VS1,TB1,US,U1,XMB,SIGBL
     A,SIGBU,V2L1,I,J,CB1,SUMETT,F1,S1,XF1,ZETA1,ALDA1,HS,QT,XL,XB,CB2,S
     AUMQT,BL)
      CALL FRSPAC(J,XB,I,XL,CB1,CB2)
      SIGTU=-1.*HS(1)+SIGBU
      SIGTL=-1.*HS(1)-SIGBL
      IF(TENSHU.GE.SIGTU.AND.COMSHL.GE.DABS(SIGTL)) GO TO 715
      WRITE(6,424)
      WRITE(6,719) TENSHU,SIGTU,COMSHL,SIGTL
      GO TO 717
C
C     SUSPENSION EFFECT
C
   89 SUMQ=0.0
      SUMEIS=0.0
      DO 77 I=1,K
      SUMQ=SUMQ+QT(I)
      SUMEIS=SUMEIS+SEIS(I)
   77 CONTINUE
      SUMTT(1)=TT(1)
      DO 78 I=2,K
      SUMTT(I)=SUMTT(I-1)+TT(I)
   78 CONTINUE
      BL=SUMTT(K-1)+12.
      DO 88 I=1,K
      R(I)=(SUMQ/SUMEIS)/(QT(I)/SEIS(I))-1.
      RQ1T(I)=Q(I)/QT(I)
   88 CONTINUE
      WRITE(6,99) (I,R(I),RQ1T(I),I=1,K)
   99 FORMAT(1H-,3X,'I',I3,3X,'R',D12.5,3X,'RQ1T',D12.5)
      DO 24 I=1,K
      DO 24 J=1,9
C
C     COE123
C
      CALL COE123(XL,U,XM,UM,ZETAX,ALMDAX,X,SX,XX,G1X,C1X,G2X,C2X,C2T,XK
     13C,XK31,A1,A2,B1,B2,C3C,C31,C3T,UM1,UM2,ZETA,ALMDA,H1,ZETAX2,ALMDA
     22,S41,S42,A41,B41,A42,B42,XK41,XK42,CE4,C41,C42,C4T,C4MP,S5C,S51,S
     352,A51,B51,D51,A52,B52,D52,A53,D53,XK51,XK52,XK53,CE5,C5C,C51,C52,
     4C5T,C5MC1,C5MC2,SC,I,J,TT,EI,B,HS,CDC,C3MP,XMO,SIGO,QA,F,T)
      C1CS(I,J)=R(I)*0.5
      Q1C(I,J)=C1CS(I,J)*QT(I)*XL
      VC(I)=QT(I)*XL**4/(384.*EI(I))
      VCS(I)=QT(I)*XL**4/(384.*SEIS(I))
      V1C(I,J)=VCS(I)+Q1C(I,J)*XL**3/(192.*SEIS(I))
      W1C(I,J)=V1C(I,J)/VCS(I)
      R1C(I,J)=W1C(I,J)-1.
      W1CS(I,J)=V1C(I,J)/VC(I)
      R1CS(I,J)=W1CS(I,J)-1.
      XMB1(I,J)=Q1C(I,J)*XL/8.*ALMDA(I)*U(I)/DTAN(U(I))*RQ1T(I)
      XMB1O(I,J)=XMB1(I,J)/XMO(I)
      BETA1(I,J)=XMB1O(I,J)/R(I)
      SIGB1(I,J)=(1.+XMB1O(I,J))*SIGO(I)
      C21S(I,J)=R(I)*C2X(I,J)
      Q21(I,J)=C21S(I,J)*QT(I)*XL
      Q2T(I,J)=2.*Q21(I,J)
      V21(I,J)=VC(I)*SX(I,J)+Q21(I,J)*XL**3/(EI(I))*G2X(I,J)
      W21(I,J)=V21(I,J)/(VC(I)*SX(I,J))
      R21(I,J)=W21(I,J)-1.
      W21S(I,J)=V21(I,J)/VC(I)
      R21S(I,J)=W21S(I,J)-1.
      G21C(I,J)=DSIN(2.*UM(I,J))/(8.*U(I)**3*DCOS(U(I)))-XM(J)/(4.*U(I)*
     1*2)-(DCOS(U(I)-2.*UM(I,J))-DCOS(U(I)))*(1.-DCOS(U(I)))/(4.*U(I)**3
     2*DSIN(2.*U(I)))
      V21C(I,J)=VCS(I)+Q21(I,J)*XL**3/(EI(I))*G21C(I,J)
      W21C(I,J)=V21C(I,J)/(VC(I)*SX(I,J))
```

```
      R21C(I,J)=W21C(I,J)-1.
      XMB2(I,J)=Q21(I,J)*XL/(2.*U(I)*DTAN(U(I)))*((DCOS(U(I)-2.*UM(I,J))
     1-DCOS(U(I)))/DCOS(U(I)))*RQ1T(I)
      XMB20(I,J)=XMB2(I,J)/XMO(I)
      BETA2(I,J)=XMB20(I,J)/R(I)
      SIGB2(I,J)=(1.+XMB20(I,J))*SIGO(I)
      IF(CDC(I,J).EQ.0.0) GO TO 24
      C31S(I,J)=R(I)*C31(I,J)
      Q31(I,J)=C31S(I,J)*QT(I)*XL
      C3CS(I,J)=R(I)*C3C(I,J)
      Q3C(I,J)=C3CS(I,J)*QT(I)*XL
      Q3T(I,J)=2.*Q31(I,J)+Q3C(I,J)
      V31(I,J)=VC(I)*SX(I,J)+XL**3/(8.*EI(I))*(Q3C(I,J)*A2(I,J)+Q31(I,J)
     1*B2(I,J))
      W31(I,J)=V31(I,J)/(VC(I)*SX(I,J))
      R31(I,J)=W31(I,J)-1.
      W31S(I,J)=V31(I,J)/VC(I)
      R31S(I,J)=W31S(I,J)-1.
      V3C(I,J)=VCS(I)+XL**3/(8.*EI(I))*(Q3C(I,J)*A1(I)+Q31(I,J)*B1(I,J))
      W3C(I,J)=V3C(I,J)/(VCS(I))
      R3C(I,J)=W3C(I,J)-1.
      W3CS(I,J)=V3C(I,J)/VC(I)
      R3CS(I,J)=W3CS(I,J)-1.
      XMB3(I,J)=XL/(4.*U(I)*DSIN(U(I)))*(Q3C(I,J)*(1.-DCOS(U(I)))-2.*Q31
     1(I,J)*(DCOS(U(I))-DCOS(U(I)-2.*UM(I,J))))*RQ1T(I)
      XMB30(I,J)=XMB3(I,J)/XMO(I)
      BETA3(I,J)=XMB30(I,J)/R(I)
      SIGB3(I,J)=(1.+XMB30(I,J))*SIGO(I)
   24 CONTINUE
      WRITE(6,92) (XM(J),J=1,9)
   92 FORMAT(1H1,5X,'XM',1X,9(D11.4,1X))
      DO 34 I=1,K
      WRITE(6,599) I
  599 FORMAT(1H1,3X,'I',I3)
      WRITE(6,90)
   90 FORMAT(1H-,5X,'ZETAX',9X,'XX',12X,'ALMDAX',8X,'SX')
      WRITE(6,91) (ZETAX(I,J),XX(I,J),ALMDAX(I,J),SX(I,J),J=1,9)
   91 FORMAT(1H0,5X,4D12.5)
      WRITE(6,93) (C1X(I,J),J=1,9)
   93 FORMAT(1H-,5X,'C1X',9(D11.4,1X))
      WRITE(6,94) (C2X(I,J),J=1,9)
   94 FORMAT(1H-,5X,'C2X',9(D11.4,1X))
      WRITE(6,95) (C2T(I,J),J=1,9)
   95 FORMAT(1H-,5X,'C2T',9(D11.4,1X))
      WRITE(6,96) (C3C(I,J),J=1,9)
   96 FORMAT(1H-,5X,'C3C',9(D11.4,1X))
      WRITE(6,103) (C31(I,J),J=1,9)
  103 FORMAT(1H-,5X,'C31',9(D11.4,1X))
      WRITE(6,104) (C3T(I,J),J=1,9)
  104 FORMAT(1H-,5X,'C3T',9(D11.4,1X))
      WRITE(6,201) (C1CS(I,J),J=1,9)
  201 FORMAT(1H-,4X,'C1CS',9(D11.4,1X))
  202 FORMAT(1H-,5X,'Q1C',9(D11.4,1X))
  203 FORMAT(1H-,5X,'V1C',9(D11.4,1X))
      WRITE(6,204) (W1C(I,J),J=1,9)
  204 FORMAT(1H-,5X,'W1C',9(D11.4,1X))
      WRITE(6,205) (R1C(I,J),J=1,9)
  205 FORMAT(1H-,5X,'R1C',9(D11.4,1X))
      WRITE(6,206) (W1CS(I,J),J=1,9)
  206 FORMAT(1H-,4X,'W1CS',9(D11.4,1X))
      WRITE(6,207) (R1CS(I,J),J=1,9)
  207 FORMAT(1H-,4X,'R1CS',9(D11.4,1X))
      WRITE(6,213) (C21S(I,J),J=1,9)
  213 FORMAT(1H-,4X,'C21S',9(D11.4,1X))
  214 FORMAT(1H-,5X,'Q21',9(D11.4,1X))
  301 FORMAT(1H-,5X,'Q2T',9(D11.4,1X))
  215 FORMAT(1H-,5X,'V21',9(D11.4,1X))
```

```
      WRITE(6,216) (W21(I,J),J=1,9)
  216 FORMAT(1H-,5X,'W21',9(D11.4,1X))
      WRITE(6,217) (R21(I,J),J=1,9)
  217 FORMAT(1H-,5X,'R21',9(D11.4,1X))
      WRITE(6,218) (W21S(I,J),J=1,9)
  218 FORMAT(1H-,4X,'W21S',9(D11.4,1X))
      WRITE(6,219) (R21S(I,J),J=1,9)
  219 FORMAT(1H-,4X,'R21S',9(D11.4,1X))
  220 FORMAT(1H-,4X,'V21C',9(D11.4,1X))
      WRITE(6,221) (W21C(I,J),J=1,9)
  221 FORMAT(1H-,4X,'W21C',9(D11.4,1X))
      WRITE(6,222) (R21C(I,J),J=1,9)
  222 FORMAT(1H-,4X,'R21C',9(D11.4,1X))
      WRITE(6,225) (C31S(I,J),J=1,9)
  225 FORMAT(1H-,4X,'C31S',9(D11.4,1X))
  226 FORMAT(1H-,5X,'Q31',9(D11.4,1X))
      WRITE(6,227) (C3CS(I,J),J=1,9)
  227 FORMAT(1H-,4X,'C3CS',9(D11.4,1X))
  228 FORMAT(1H-,5X,'Q3C',9(D11.4,1X))
  302 FORMAT(1H-,5X,'Q3T',9(D11.4,1X))
  229 FORMAT(1H-,5X,'V31',9(D11.4,1X))
      WRITE(6,230) (W31(I,J),J=1,9)
  230 FORMAT(1H-,5X,'W31',9(D11.4,1X))
      WRITE(6,231) (R31(I,J),J=1,9)
  231 FORMAT(1H-,5X,'R31',9(D11.4,1X))
      WRITE(6,232) (W31S(I,J),J=1,9)
  232 FORMAT(1H-,4X,'W31S',9(D11.4,1X))
      WRITE(6,233) (R31S(I,J),J=1,9)
  233 FORMAT(1H-,4X,'R31S',9(D11.4,1X))
  234 FORMAT(1H-,5X,'V3C',9(D11.4,1X))
      WRITE(6,235) (W3C(I,J),J=1,9)
  235 FORMAT(1H-,5X,'W3C',9(D11.4,1X))
      WRITE(6,236) (R3C(I,J),J=1,9)
  236 FORMAT(1H-,5X,'R3C',9(D11.4,1X))
      WRITE(6,237) (W3CS(I,J),J=1,9)
  237 FORMAT(1H-,4X,'W3CS',9(D11.4,1X))
      WRITE(6,238) (R3CS(I,J),J=1,9)
  238 FORMAT(1H-,4X,'R3CS',9(D11.4,1X))
      WRITE(6,212) I,XMO(I)
  212 FORMAT(1H-,3X,'I',I3,2X,'XMO',2X,D12.5)
      WRITE(6,311) I,SIGO(I)
  311 FORMAT(1H-,3X,'I',I3,2X,'SIGO',2X,D12.5)
      WRITE(6,203) (V1C(I,J),J=1,9)
      WRITE(6,215) (V21(I,J),J=1,9)
      WRITE(6,220) (V21C(I,J),J=1,9)
      WRITE(6,229) (V31(I,J),J=1,9)
      WRITE(6,234) (V3C(I,J),J=1,9)
      WRITE(6,202) (Q1C(I,J),J=1,9)
      WRITE(6,214) (Q21(I,J),J=1,9)
      WRITE(6,301) (Q2T(I,J),J=1,9)
      WRITE(6,226) (Q31(I,J),J=1,9)
      WRITE(6,228) (Q3C(I,J),J=1,9)
      WRITE(6,302) (Q3T(I,J),J=1,9)
      WRITE(6,312) (XMB1(I,J),J=1,9)
  312 FORMAT(1H-,4X,'XMB1',9(D11.4,1X))
      WRITE(6,313) (XMB2(I,J),J=1,9)
  313 FORMAT(1H-,4X,'XMB2',9(D11.4,1X))
      WRITE(6,314) (XMB3(I,J),J=1,9)
  314 FORMAT(1H-,4X,'XMB3',9(D11.4,1X))
      WRITE(6,315) (XMB10(I,J),J=1,9)
  315 FORMAT(1H-,3X,'XMB10',9(D11.4,1X))
      WRITE(6,316) (XMB20(I,J),J=1,9)
  316 FORMAT(1H-,3X,'XMB20',9(D11.4,1X))
      WRITE(6,317) (XMB30(I,J),J=1,9)
  317 FORMAT(1H-,3X,'XMB30',9(D11.4,1X))
      WRITE(6,360) (BETA1(I,J),J=1,9)
  360 FORMAT(1H-,3X,'BETA1',9(D11.4,1X))
```

```
      WRITE(6,361) (BETA2(I,J),J=1,9)
  361 FORMAT(1H-,3X,'BETA2',9(D11.4,1X))
      WRITE(6,362) (BETA3(I,J),J=1,9)
  362 FORMAT(1H-,3X,'BETA3',9(D11.4,1X))
      WRITE(6,318) (SIGB1(I,J),J=1,9)
  318 FORMAT(1H-,3X,'SIGB1',9(D11.4,1X))
      WRITE(6,319) (SIGB2(I,J),J=1,9)
  319 FORMAT(1H-,3X,'SIGB2',9(D11.4,1X))
      WRITE(6,320) (SIGB3(I,J),J=1,9)
  320 FORMAT(1H-,3X,'SIGB3',9(D11.4,1X))
   34 CONTINUE
      DO 11 I=1,K
      DO 11 I1=1,8
      J2=I1+1
      DO 11 I2=J2,9
C
C     COE45
C
      CALL COE45(I,J,XL,U,XM1,XM2,UM1,UM2,ZETAX1,ALMDA1,ZETAX2,ALMDA2,X,
     1ALMDA,ZETA,S41,S42,A41,B41,A42,B42,XK41,XK42,CE4,C41,C42,C4T,C4MP,
     2S5C,S51,S52,A51,B51,D51,A52,B52,D52,A53,B53,D53,XK51,XK52,XK53,CE5
     3,C5C,C51,C52,C5T,C5MC1,C5MC2,TT,EI,I1,I2,B,HS,XMO,SIGO,QA,F,T)
      IF(CE4(I,I1,I2).EQ.O.) GO TO 177
      C41S(I,I1,I2)=C41(I,I1,I2)*R(I)
      Q41(I,I1,I2)=C41S(I,I1,I2)*QT(I)*XL
      C42S(I,I1,I2)=C42(I,I1,I2)*R(I)
      Q42(I,I1,I2)=C42S(I,I1,I2)*QT(I)*XL
      Q4T(I,I1,I2)=2.*(Q41(I,I1,I2)+Q42(I,I1,I2))
      VC(I)=QT(I)*XL**4/(384.*EI(I))
      V41(I,I1,I2)=VC(I)*S41(I,I1)+XL**3/(8.*EI(I))*(Q41(I,I1,I2)*A41(I,
     1I1)+Q42(I,I1,I2)*B41(I,I1,I2))
      W41(I,I1,I2)=V41(I,I1,I2)/(VC(I)*S41(I,I1))
      R41(I,I1,I2)=W41(I,I1,I2)-1.
      W41S(I,I1,I2)=W41(I,I1,I2)*S41(I,I1)
      R41S(I,I1,I2)=W41S(I,I1,I2)-1.
      V42(I,I1,I2)=VC(I)*S42(I,I2)+XL**3/(8.*EI(I))*(Q41(I,I1,I2)*A42(I,
     1I1,I2)+Q42(I,I1,I2)*B42(I,I2))
      W42(I,I1,I2)=V42(I,I1,I2)/(VC(I)*S42(I,I2))
      R42(I,I1,I2)=W42(I,I1,I2)-1.
      W42S(I,I1,I2)=W42(I,I1,I2)*S42(I,I2)
      R42S(I,I1,I2)=W42S(I,I1,I2)-1.
      Q41C(I,I1)=DSIN(2.*UM1(I,I1))/(8.*U(I)**3*DCOS(U(I)))-XM1(I1)/(4.*
     1U(I)**2)-(DCOS(U(I)-2.*UM1(I,I1))-DCOS(U(I)))*(1.-DCOS(U(I)))/(4.*
     2U(I)**3*DSIN(2.*U(I)))
      Q42C(I,I2)=DSIN(2.*UM2(I,I2))/(8.*U(I)**3*DCOS(U(I)))-XM2(I2)/(4.*
     1U(I)**2)-(DCOS(U(I)-2.*UM2(I,I2))-DCOS(U(I)))*(1.-DCOS(U(I)))/(4.*
     2U(I)**3*DSIN(2.*U(I)))
      V42C(I,I1,I2)=VCS(I)+Q41(I,I1,I2)*XL**3/EI(I)*Q41C(I,I1)+Q42(I,I1,
     2I2)*XL**3/EI(I)*Q42C(I,I2)
      W42CS(I,I1,I2)=V42C(I,I1,I2)/VC(I)
      R42CS(I,I1,I2)=W42CS(I,I1,I2)-1.
  177 IF(CE5(I,I1,I2).EQ.O.) GO TO 11
      C51S(I,I1,I2)=C51(I,I1,I2)*R(I)
      Q51(I,I1,I2)=C51S(I,I1,I2)*QT(I)*XL
      C52S(I,I1,I2)=C52(I,I1,I2)*R(I)
      Q52(I,I1,I2)=C52S(I,I1,I2)*QT(I)*XL
      C5CS(I,I1,I2)=C5C(I,I1,I2)*R(I)
      Q5C(I,I1,I2)=C5CS(I,I1,I2)*QT(I)*XL
      Q5T(I,I1,I2)=2.*(Q51(I,I1,I2)+Q52(I,I1,I2))+Q5C(I,I1,I2)
      V5C(I,I1,I2)=VCS(I)+XL**3/(8.*EI(I))*(Q5C(I,I1,I2)*A51(I)+Q51(I,I1
     1,I2)*B51(I,I1)+Q52(I,I1,I2)*D51(I,I2))
      W5C(I,I1,I2)=V5C(I,I1,I2)/VCS(I)
      R5C(I,I1,I2)=W5C(I,I1,I2)-1.
      W5CS(I,I1,I2)=V5C(I,I1,I2)/VC(I)
      R5CS(I,I1,I2)=W5CS(I,I1,I2)-1.
      V51(I,I1,I2)=VC(I)*S51(I,I1)+XL**3/(8.*EI(I))*(Q5C(I,I1,I2)*A52(I,
     1I1)+Q51(I,I1,I2)*B52(I,I1)+Q52(I,I1,I2)*D52(I,I1,I2))
```

```
      W51(I,I1,I2)=V51(I,I1,I2)/(VC(I)*S51(I,I1))
      R51(I,I1,I2)=W51(I,I1,I2)-1.
      W51S(I,I1,I2)=V51(I,I1,I2)/VC(I)
      R51S(I,I1,I2)=W51S(I,I1,I2)-1.
      V52(I,I1,I2)=VC(I)*S52(I,I2)+XL**3/(8.*EI(I))*(Q5C(I,I1,I2)*A53(I,
     1I2)+Q51(I,I1,I2)*B53(I,I1,I2)+Q52(I,I1,I2)*D53(I,I2))
      W52(I,I1,I2)=V52(I,I1,I2)/(VC(I)*S52(I,I2))
      R52(I,I1,I2)=W52(I,I1,I2)-1.
      W52S(I,I1,I2)=V52(I,I1,I2)/VC(I)
      R52S(I,I1,I2)=W52S(I,I1,I2)-1.
      XMB4(I,I1,I2)=XL/(2.*U(I)*DTAN(U(I)))*(Q41(I,I1,I2)*((DCOS(U(I)-2.
     2*UM1(I,I1))-DCOS(U(I)))/DCOS(U(I)))+Q42(I,I1,I2)*((DCOS(U(I)-2.*UM
     32(I,I2))-DCOS(U(I)))/DCOS(U(I))))*RQ1T(I)
      XMB5(I,I1,I2)=XL/(4.*U(I)*DSIN(U(I)))*(Q5C(I,I1,I2)*(1.-DCOS(U(I))
     4)-2.*Q51(I,I1,I2)*(DCOS(U(I))-DCOS(U(I)-2.*UM1(I,I1)))-2.*Q52(I,I1
     5,I2)*(DCOS(U(I))-DCOS(U(I)-2.*UM2(I,I2))))*RQ1T(I)
      XMB40(I,I1,I2)=XMB4(I,I1,I2)/XMO(I)
      XMB50(I,I1,I2)=XMB5(I,I1,I2)/XMO(I)
      BETA4(I,I1,I2)=XMB40(I,I1,I2)/R(I)
      BETA5(I,I1,I2)=XMB50(I,I1,I2)/R(I)
      SIGB4(I,I1,I2)=(1.+XMB40(I,I1,I2))*SIGO(I)
      SIGB5(I,I1,I2)=(1.+XMB50(I,I1,I2))*SIGO(I)
   11 CONTINUE
      DO 37 I=1,K
      DO 37 I1=1,8
      J=I1+1
      WRITE(6,199) I,I1,XM1(I1)
  199 FORMAT(1H1,3X,'I',I3,3X,'I1',I3,3X,'XM1',2X,D10.3//)
      WRITE(6,240) (C41(I,I1,I2),I2=J,9)
  240 FORMAT(1H-,5X,'C41',1X,8(D11.4,1X))
      WRITE(6,241) (C42(I,I1,I2),I2=J,9)
  241 FORMAT(1H-,5X,'C42',1X,8(D11.4,1X))
      WRITE(6,242) (C4T(I,I1,I2),I2=J,9)
  242 FORMAT(1H-,5X,'C4T',1X,8(D11.4,1X))
      WRITE(6,243) (C5C(I,I1,I2),I2=J,9)
  243 FORMAT(1H-,5X,'C5C',1X,8(D11.4,1X))
      WRITE(6,244) (C51(I,I1,I2),I2=J,9)
  244 FORMAT(1H-,5X,'C51',1X,8(D11.4,1X))
      WRITE(6,245) (C52(I,I1,I2),I2=J,9)
  245 FORMAT(1H-,5X,'C52',1X,8(D11.4,1X))
      WRITE(6,246) (C5T(I,I1,I2),I2=J,9)
  246 FORMAT(1H-,5X,'C5T',1X,8(D11.4,1X))
      WRITE(6,247) (C41S(I,I1,I2),I2=J,9)
  247 FORMAT(1H-,4X,'C41S',1X,8(D11.4,1X))
      WRITE(6,248) (C42S(I,I1,I2),I2=J,9)
  248 FORMAT(1H-,4X,'C42S',1X,8(D11.4,1X))
  249 FORMAT(1H-,5X,'Q41',1X,8(D11.4,1X))
  250 FORMAT(1H-,5X,'Q42',1X,8(D11.4,1X))
  251 FORMAT(1H-,5X,'Q4T',1X,8(D11.4,1X))
  252 FORMAT(1H-,5X,'V41',1X,8(D11.4,1X))
      WRITE(6,253) (R41(I,I1,I2),I2=J,9)
  253 FORMAT(1H-,5X,'R41',1X,8(D11.4,1X))
  254 FORMAT(1H-,5X,'V42',1X,8(D11.4,1X))
      WRITE(6,255) (R42(I,I1,I2),I2=J,9)
  255 FORMAT(1H-,5X,'R42',1X,8(D11.4,1X))
      WRITE(6,256) (R41S(I,I1,I2),I2=J,9)
  256 FORMAT(1H-,4X,'R41S',1X,8(D11.4,1X))
      WRITE(6,257) (R42S(I,I1,I2),I2=J,9)
  257 FORMAT(1H-,4X,'R42S',1X,8(D11.4,1X))
  258 FORMAT(1H-,4X,'V42C',1X,8(D11.4,1X))
      WRITE(6,259) (R42CS(I,I1,I2),I2=J,9)
  259 FORMAT(1H-,3X,'R42CS',1X,8(D11.4,1X))
      WRITE(6,260) (C51S(I,I1,I2),I2=J,9)
  260 FORMAT(1H-,4X,'C51S',1X,8(D11.4,1X))
      WRITE(6,261) (C52S(I,I1,I2),I2=J,9)
  261 FORMAT(1H-,4X,'C52S',1X,8(D11.4,1X))
      WRITE(6,262) (C5CS(I,I1,I2),I2=J,9)
```

```
262 FORMAT(1H-,4X,'C5CS',1X,8(D11.4,1X))
263 FORMAT(1H-,5X,'Q51',1X,8(D11.4,1X))
264 FORMAT(1H-,5X,'Q52',1X,8(D11.4,1X))
265 FORMAT(1H-,5X,'Q5C',1X,8(D11.4,1X))
303 FORMAT(1H-,5X,'Q5T',1X,8(D11.4,1X))
266 FORMAT(1H-,5X,'V5C',1X,8(D11.4,1X))
    WRITE(6,267) (R5C(I,I1,I2),I2=J,9)
267 FORMAT(1H-,5X,'R5C',1X,8(D11.4,1X))
    WRITE(6,268) (R5CS(I,I1,I2),I2=J,9)
268 FORMAT(1H-,4X,'R5CS',1X,8(D11.4,1X))
    WRITE(6,269) (R51S(I,I1,I2),I2=J,9)
269 FORMAT(1H-,4X,'R51S',1X,8(D11.4,1X))
    WRITE(6,270) (R52S(I,I1,I2),I2=J,9)
270 FORMAT(1H-,4X,'R52S',1X,8(D11.4,1X))
271 FORMAT(1H-,5X,'V51',1X,8(D11.4,1X))
    WRITE(6,272) (R51(I,I1,I2),I2=J,9)
272 FORMAT(1H-,5X,'R51',1X,8(D11.4,1X))
    WRITE(6,274) (R52(I,I1,I2),I2=J,9)
274 FORMAT(1H-,5X,'R52',1X,8(D11.4,1X))
275 FORMAT(1H-,5X,'V52',1X,8(D11.4,1X))
    WRITE(6,252) (V41(I,I1,I2),I2=J,9)
    WRITE(6,254) (V42(I,I1,I2),I2=J,9)
    WRITE(6,258) (V42C(I,I1,I2),I2=J,9)
    WRITE(6,271) (V51(I,I1,I2),I2=J,9)
    WRITE(6,275) (V52(I,I1,I2),I2=J,9)
    WRITE(6,266) (V5C(I,I1,I2),I2=J,9)
    WRITE(6,249) (Q41(I,I1,I2),I2=J,9)
    WRITE(6,250) (Q42(I,I1,I2),I2=J,9)
    WRITE(6,251) (Q4T(I,I1,I2),I2=J,9)
    WRITE(6,263) (Q51(I,I1,I2),I2=J,9)
    WRITE(6,264) (Q52(I,I1,I2),I2=J,9)
    WRITE(6,265) (Q5C(I,I1,I2),I2=J,9)
    WRITE(6,303) (Q5T(I,I1,I2),I2=J,9)
    WRITE(6,321) (XMB4(I,I1,I2),I2=J,9)
321 FORMAT(1H-,4X,'XMB4',1X,8(D11.4,1X))
    WRITE(6,322) (XMB5(I,I1,I2),I2=J,9)
322 FORMAT(1H-,4X,'XMB5',1X,8(D11.4,1X))
    WRITE(6,323) (XMB40(I,I1,I2),I2=J,9)
323 FORMAT(1H-,3X,'XMB40',1X,8(D11.4,1X))
    WRITE(6,324) (XMB50(I,I1,I2),I2=J,9)
324 FORMAT(1H-,3X,'XMB50',1X,8(D11.4,1X))
    WRITE(6,363) (BETA4(I,I1,I2),I2=J,9)
363 FORMAT(1H-,3X,'BETA4',1X,8(D11.4,1X))
    WRITE(6,364) (BETA5(I,I1,I2),I2=J,9)
364 FORMAT(1H-,3X,'BETA5',1X,8(D11.4,1X))
    WRITE(6,325) (SIGB4(I,I1,I2),I2=J,9)
325 FORMAT(1H-,3X,'SIGB4',1X,8(D11.4,1X))
    WRITE(6,326) (SIGB5(I,I1,I2),I2=J,9)
326 FORMAT(1H-,3X,'SIGB5',1X,8(D11.4,1X))
 37 CONTINUE
    DO 15 I=1,K
    DO 15 I1=1,7
    J1=I1+1
    DO 15 I2=J1,8
    J2=I1+2
    DO 15 I3=J2,9
C
C   COE67
C
    CALL COE67(I,J,XL,U,XM1,XM2,UM1,UM2,ZETAX1,ALMDA1,ZETAX2,ALMDA2,X,
   1ALMDA,ZETA,S61,S62,A61,B61,A62,B62,XK61,XK62,CE6,C61,C62,C6T,XM3,U
   2M3,ZETAX3,ALMDA3,S63,D61,D62,A63,B63,D63,XK63,C63,I3,C6M12,C6M13,T
   3T,EI,I1,I2,B,HS,XMO,SIGO,QA,F,T)
    IF(CE6(I,I1,I2,I3).EQ.0.) GO TO 15
    VC(I)=QT(I)*XL**4/(384.*EI(I))
    VCS(I)=QT(I)*XL**4/(384.*SEIS(I))
    C61S(I,I1,I2,I3)=C61(I,I1,I2,I3)*R(I)
```

```
      C62S(I,I1,I2,I3)=C62(I,I1,I2,I3)*R(I)
      C63S(I,I1,I2,I3)=C63(I,I1,I2,I3)*R(I)
      Q61(I,I1,I2,I3)=C61S(I,I1,I2,I3)*QT(I)*XL
      Q62(I,I1,I2,I3)=C62S(I,I1,I2,I3)*QT(I)*XL
      Q63(I,I1,I2,I3)=C63S(I,I1,I2,I3)*QT(I)*XL
      Q6T(I,I1,I2,I3)=2.*(Q61(I,I1,I2,I3)+Q62(I,I1,I2,I3)+Q63(I,I1,I2,I3
     1))
      V61(I,I1,I2,I3)=VC(I)*S61(I,I1)+XL**3/(8.*EI(I))*(Q61(I,I1,I2,I3)*
     1A61(I,I1)+Q62(I,I1,I2,I3)*B61(I,I1,I2)+Q63(I,I1,I2,I3)*D61(I,I1,I3
     2))
      W61(I,I1,I2,I3)=V61(I,I1,I2,I3)/(VC(I)*S61(I,I1))
      R61(I,I1,I2,I3)=W61(I,I1,I2,I3)-1.
      V62(I,I1,I2,I3)=VC(I)*S62(I,I2)+XL**3/(8.*EI(I))*(Q61(I,I1,I2,I3)*
     1A62(I,I1,I2)+Q62(I,I1,I2,I3)*B62(I,I2)+Q63(I,I1,I2,I3)*D62(I,I2,I3
     2))
      W62(I,I1,I2,I3)=V62(I,I1,I2,I3)/(VC(I)*S62(I,I2))
      R62(I,I1,I2,I3)=W62(I,I1,I2,I3)-1.
      V63(I,I1,I2,I3)=VC(I)*S63(I,I3)+XL**3/(8.*EI(I))*(Q61(I,I1,I2,I3)*
     1A63(I,I1,I3)+Q62(I,I1,I2,I3)*B63(I,I2,I3)+Q63(I,I1,I2,I3)*D63(I,I3
     2))
      W63(I,I1,I2,I3)=V63(I,I1,I2,I3)/(VC(I)*S63(I,I3))
      R63(I,I1,I2,I3)=W63(I,I1,I2,I3)-1.
      G61C(I,I1)=DSIN(2.*UM1(I,I1))/(8.*U(I)**3*DCOS(U(I)))-XM1(I1)/(4.*
     1U(I)**2)-(DCOS(U(I)-2.*UM1(I,I1))-DCOS(U(I)))*(1.-DCOS(U(I)))/(4.*
     2U(I)**3*DSIN(2.*U(I)))
      G62C(I,I2)=DSIN(2.*UM2(I,I2))/(8.*U(I)**3*DCOS(U(I)))-XM2(I2)/(4.*
     1U(I)**2)-(DCOS(U(I)-2.*UM2(I,I2))-DCOS(U(I)))*(1.-DCOS(U(I)))/(4.*
     2U(I)**3*DSIN(2.*U(I)))
      G63C(I,I3)=DSIN(2.*UM3(I,I3))/(8.*U(I)**3*DCOS(U(I)))-XM3(I3)/(4.*
     1U(I)**2)-(DCOS(U(I)-2.*UM3(I,I3))-DCOS(U(I)))*(1.-DCOS(U(I)))/(4.*
     2U(I)**3*DSIN(2.*U(I)))
      V6C(I,I1,I2,I3)=VCS(I)+Q61(I,I1,I2,I3)*XL**3/EI(I)*G61C(I,I1)+Q62(
     1I,I1,I2,I3)*XL**3/EI(I)*G62C(I,I2)+Q63(I,I1,I2,I3)*XL**3/EI(I)*G63
     2C(I,I3)
      W6C(I,I1,I2,I3)=V6C(I,I1,I2,I3)/VCS(I)
      R6C(I,I1,I2,I3)=W6C(I,I1,I2,I3)-1.
      XMB6(I,I1,I2,I3)=XL/(2.*U(I)*DTAN(U(I)))*(Q61(I,I1,I2,I3)*((DCOS(U
     1(I)-2.*UM1(I,I1))-DCOS(U(I)))/DCOS(U(I)))+Q62(I,I1,I2,I3)*((DCOS(U
     2(I)-2.*UM2(I,I2))-DCOS(U(I)))/DCOS(U(I)))+Q63(I,I1,I2,I3)*((DCOS(U
     3(I)-2.*UM3(I,I3))-DCOS(U(I)))/DCOS(U(I))))*RQ1T(I)
      XMB60(I,I1,I2,I3)=XMB6(I,I1,I2,I3)/XMO(I)
      BETA6(I,I1,I2,I3)=XMB60(I,I1,I2,I3)/R(I)
      SIGB6(I,I1,I2,I3)=(1.+XMB60(I,I1,I2,I3))*SIGO(I)
   15 CONTINUE
      DO 38 I=1,K
      DO 38 I1=1,7
      J1=I1+1
      WRITE(6,366) I,I1,I2,XM1(I1)
  366 FORMAT(1H1,3X,'I',I3,3X,'I1',I3,3X,'I2',I3,3X,'XM1',2X,D10.3//)
      DO 38 I2=J1,8
      J2=I1+2
      WRITE(6,531) (C61(I,I1,I2,I3),I3=J2,9)
  531 FORMAT(1H-,3X,'C61',1X,7(D11.4,1X))
      WRITE(6,532) (C62(I,I1,I2,I3),I3=J2,9)
  532 FORMAT(1H-,3X,'C62',1X,7(D11.4,1X))
      WRITE(6,533) (C63(I,I1,I2,I3),I3=J2,9)
  533 FORMAT(1H-,3X,'C63',1X,7(D11.4,1X))
      WRITE(6,534) (C6T(I,I1,I2,I3),I3=J2,9)
  534 FORMAT(1H-,3X,'C6T',1X,7(D11.4,1X))
      WRITE(6,535) (V61(I,I1,I2,I3),I3=J2,9)
  535 FORMAT(1H-,3X,'V61',1X,7(D11.4,1X))
      WRITE(6,547) (R61(I,I1,I2,I3),I3=J2,9)
  547 FORMAT(1H-,3X,'R61',1X,7(D11.4,1X))
      WRITE(6,536) (V62(I,I1,I2,I3),I3=J2,9)
  536 FORMAT(1H-,3X,'V62',1X,7(D11.4,1X))
      WRITE(6,548) (R62(I,I1,I2,I3),I3=J2,9)
  548 FORMAT(1H-,3X,'R62',1X,7(D11.4,1X))
```

```
      WRITE(6,537) (V63(I,I1,I2,I3),I3=J2,9)
  537 FORMAT(1H-,3X,'V63',1X,7(D11.4,1X))
      WRITE(6,549) (R63(I,I1,I2,I3),I3=J2,9)
  549 FORMAT(1H-,3X,'R63',1X,7(D11.4,1X))
      WRITE(6,538) (V6C(I,I1,I2,I3),I3=J2,9)
  538 FORMAT(1H-,3X,'V6C',1X,7(D11.4,1X))
      WRITE(6,551) (R6C(I,I1,I2,I3),I3=J2,9)
  551 FORMAT(1H-,3X,'R6C',1X,7(D11.4,1X))
      WRITE(6,539) (Q61(I,I1,I2,I3),I3=J2,9)
  539 FORMAT(1H-,3X,'Q61',1X,7(D11.4,1X))
      WRITE(6,546) (Q62(I,I1,I2,I3),I3=J2,9)
  546 FORMAT(1H-,3X,'Q62',1X,7(D11.4,1X))
      WRITE(6,541) (Q63(I,I1,I2,I3),I3=J2,9)
  541 FORMAT(1H-,3X,'Q63',1X,7(D11.4,1X))
      WRITE(6,542) (Q6T(I,I1,I2,I3),I3=J2,9)
  542 FORMAT(1H-,3X,'Q6T',1X,7(D11.4,1X))
      WRITE(6,543) (XMB6(I,I1,I2,I3),I3=J2,9)
  543 FORMAT(1H-,3X,'XMB6',1X,7(D11.4,1X))
      WRITE(6,544) (XMB60(I,I1,I2,I3),I3=J2,9)
  544 FORMAT(1H-,3X,'XMB60',1X,7(D11.4,1X))
      WRITE(6,365) (BETA6(I,I1,I2,I3),I3=J2,9)
  365 FORMAT(1H-,3X,'BETA6',1X,7(D11.4,1X))
      WRITE(6,545) (SIGB6(I,I1,I2,I3),I3=J2,9)
  545 FORMAT(1H-,3X,'SIGB6',1X,7(D11.4,1X))
   38 CONTINUE
      DO 411 I=1,K
      SIGTU1(I)=-1.*HS(I)+SIGB1(I,5)
      SIGTL1(I)=-1.*HS(I)-SIGB1(I,5)
      SIGTU2(I)=-1.*HS(I)+SIGB2(I,3)
      SIGTL2(I)=-1.*HS(I)-SIGB2(I,3)
      SIGTU3(I)=-1.*HS(I)+SIGB3(I,2)
      SIGTL3(I)=-1.*HS(I)-SIGB3(I,2)
      SIGTU4(I)=-1.*HS(I)+SIGB4(I,4,8)
      SIGTL4(I)=-1.*HS(I)-SIGB4(I,4,8)
      SIGTU5(I)=-1.*HS(I)+SIGB5(I,3,7)
      SIGTL5(I)=-1.*HS(I)-SIGB5(I,3,7)
      SIGTU6(I)=-1.*HS(I)+SIGB6(I,3,6,9)
      SIGTL6(I)=-1.*HS(I)-SIGB6(I,3,6,9)
  411 CONTINUE
C
C     FAILURE CRITERIA FOR BOLTED ROOF
C
      K1=0
      K2=0
      K3=0
      K4=0
      K5=0
      K6=0
      DO 400 I=1,K
      IF(TENSH(I).GE.SIGEU1(I).AND.COMSH(I).GE.DABS(SIGEL1(I))) K1=K1+1
      IF(TENSH(I).GE.SIGEU2(I).AND.COMSH(I).GE.DABS(SIGEL2(I))) K2=K2+1
      IF(TENSH(I).GE.SIGEU3(I).AND.COMSH(I).GE.DABS(SIGEL3(I))) K3=K3+1
      IF(TENSH(I).GE.SIGEU4(I).AND.COMSH(I).GE.DABS(SIGEL4(I))) K4=K4+1
      IF(TENSH(I).GE.SIGEU5(I).AND.COMSH(I).GE.DABS(SIGEL5(I))) K5=K5+1
      IF(TENSH(I).GE.SIGEU6(I).AND.COMSH(I).GE.DABS(SIGEL6(I))) K6=K6+1
  400 CONTINUE
      WRITE(6,555)K1,K2,K3,K4,K5,K6
  555 FORMAT(1H0,3X,'K1',I2,2X,'K2',I2,2X,'K3',I2,2X,'K4',I2,2X,'K5',I2,
     12X,'K6',I2)
      IF(K1.EQ.K) GO TO 401
      WRITE(6,424)
  424 FORMAT(//1H0,3X,'BOLTED-ROOF IS UNSTABLE')
      WRITE(6,416) (I,TENSH(I),SIGTU1(I),COMSH(I),SIGTL1(I),I=1,K)
  416 FORMAT(1H0,//3X,'I',I3,2X,'TENSH',2X,D12.5,2X,'SIGTU1',2X,D12.5,2X
     1,'COMSH',2X,D12.5,2X,'SIGTL1',2X,D12.5)
      IF(K2.EQ.K) GO TO 402
      WRITE(6,424)
```

```
      WRITE(6,417) (I,TENSH(I),SIGTU2(I),COMSH(I),SIGTL2(I),I=1,K)
417   FORMAT(1HO,//3X,'I',I3,2X,'TENSH',2X,D12.5,2X,'SIGTU2',2X,D12.5,2X
     1,'COMSH',2X,D12.5,2X,'SIGTL2',2X,D12.5)
      IF(K3.EQ.K) GO TO 403
      WRITE(6,424)
      WRITE(6,418) (I,TENSH(I),SIGTU3(I),COMSH(I),SIGTL3(I),I=1,K)
418   FORMAT(1HO,//3X,'I',I3,2X,'TENSH',2X,D12.5,2X,'SIGTU3',2X,D12.5,2X
     1,'COMSH',2X,D12.5,2X,'SIGTL3',2X,D12.5)
      IF(K4.EQ.K) GO TO 404
      WRITE(6,424)
      WRITE(6,419) (I,TENSH(I),SIGTU4(I),COMSH(I),SIGTL4(I),I=1,K)
419   FORMAT(1HO,//3X,'I',I3,2X,'TENSH',2X,D12.5,2X,'SIGTU4',2X,D12.5,2X
     1,'COMSH',2X,D12.5,2X,'SIGTL4',2X,D12.5)
      IF(K5.EQ.K) GO TO 405
      WRITE(6,424)
      WRITE(6,480)(I,TENSH(I),SIGTU5(I),COMSH(I),SIGTL5(I),I=1,K)
480   FORMAT(1HO,//3X,'I',I3,2X,'TENSH',2X,D12.5,2X,'SIGTU5',2X,D12.5,2X
     1,'COMSH',2X,D12.5,2X,'SIGTL5',2X,D12.5)
      IF(K6-K) 406,481,406
401   NB=1
      SA=PA(K)*B/Q1C(K,2)
      IF(SA.LT.B) GO TO 402
      GO TO 410
402   NB=2
      SA=PA(K)*B/Q21(K,3)
      IF(SA.LT.B) GO TO 403
      GO TO 410
403   NB=3
      SA=PA(K)*B/Q31(K,4)
      IF(SA.LT.B) GO TO 404
      GO TO 410
404   NB=4
      SA=PA(K)*B/Q41(K,5,5)
      IF(SA.LT.B) GO TO 405
      GO TO 410
405   NB=5
      SA=PA(K)*B/Q51(K,6,6)
      IF(SA.LT.B) GO TO 481
      GO TO 410
481   NB=6
      SA=PA(K)*B/Q61(K,7,7,7)
      IF(SA.LT.B) GO TO 421
      GO TO 410
406   WRITE(6,424)
      WRITE(6,420) (I,TENSH(I),SIGTU6(I),COMSH(I),SIGTL6(I),I=1,K)
420   FORMAT(1HO,//3X,'I',I3,2X,'TENSH',2X,D12.5,2X,'SIGTU6',2X,D12.5,2X
     1,'COMSH',2X,D12.5,2X,'SIGTL6',2X,D12.5)
      GO TO 415
410   WRITE(6,408) NB
408   FORMAT(1H1//,4X,'NO.OF BOLTS ALONG THE SPAN',6X,I2)
      SB=XL/(FLOAT(NB)+1.)
      WRITE(6,409) SB
409   FORMAT(1HO,3X,'BOLT SPACING ALONG THE SPAN, IN.',2X,F8.2)
      WRITE(6,413) SA
413   FORMAT(1HO,3X,'BOLT SPACING ALONG THE ENTRY, IN.',1X,F8.2)
      WRITE(6,425) BL
425   FORMAT(1HO,3X,'BOLT LENGTH, IN.',17X,F9.2)
      WRITE(6,423) PA(K)
423   FORMAT(1HO,3X,'BOLT TENSION, LBS.',15X,F9.2)
      WRITE(6,735)
      GO TO 415
421   WRITE(6,422) PA(K),K,NB
422   FORMAT(1H1,2X,'BOLT TENSION',1X,F9.2,'LAYER NO.',1X,I2,'NO.OF BOLT
     1S',1X,I2,1X,'ROW SPACING < B IN.')
      GO TO 410
415   STOP
      END
```

```
C
C     SUBROUTINE COE123
C
      SUBROUTINE COE123(XL,U,XM,UM,ZETAX,ALMDAX,X,SX,XX,G1X,C1X,G2X,C2X,
     1C2T,XK3C,XK31,A1,A2,B1,B2,C3C,C31,C3T,UM1,UM2,ZETA,ALMDA,H1,ZETAX2
     2,ALMDA2,S41,S42,A41,B41,A42,B42,XK41,XK42,CE4,C41,C42,C4T,C4MP,S5C
     3,S51,S52,A51,B51,D51,A52,B52,D52,A53,D53,XK51,XK52,XK53,CE5,C5C,C5
     41,C52,C5T,C5MC1,C5MC2,SC,I,J,TT,EI,B,HS,CDC,C3MP,XMO,SIGO,QA,F,T)
      DOUBLE PRECISION EIS(10),M(10),HS(10),SIGMTU(10),C1CS(10,10),A1(10
     1),SIGMTL(10),P31(10,1),P32(10,10),R(10),Q(10),XI(10),E(10),TRYY,T(
     110),W(10),SIGM1(10),COMSH(10),QA(10),WA(10),H(10),TENSH(10),PA(10)
     2,V2L2(10),V2L(10),HSET(10),U(10),ZETA(10),ALMDA(10),D1(10,10),SC(1
     30),Q(10),X(10),F(10),PB(10),P(10),IGM32(10),PB4(10),SIGM42(10),XMO
     4(10),TAU1(10),SEIS(10),SUMQ,SUMEIS,XM(10),UM(10,10),ZETAX(10,10),A
     5LMDAX(10,10),SX(10,10),XX(10,10),G1X(10,10),C1X(10,10),G2X(10,10),
     6C2X(10,10),C2T(10,10),XK3C(10),XK31(10,10),A2(10,10),B1(10,10),B2(
     710,10),C3C(10,10),C31(10,10),C3T(10,10),UM1(10,10),UM2(10,10),ZETA
     8X1(10,10),ALMDA1(10,10),ALMDA2(10,10),ZETAX2(10,10),S41(10,10),S42
     9(10,10),A41(10,10),B41(10,10,10),A42(10,10,10),B42(10,10),XK41(10,
     A10),XK42(10,10),CE4(10,10,10),C41(10,10,10),C42(10,10,10),C4T(10,1
     A0,10),C4MP(10,10,10),S5C(10),S51(10,10),S52(10,10),A51(10),B51(10,
     A10),D51(10,10),A52(10,10),B52(10,10),D52(10,10,10),A53(10,10),B53(
     A10,10,10),D53(10,10),XK51(10),XK52(10,10),XK53(10,10),CE5(10,10,10
     A),C5C(10,10,10),C51(10,10,10),C52(10,10,10),C5T(10,10,10),C5MC1(10
     A,10,10),C5MC2(10,10,10),B,TT(10),EI(10),CDC(10,10),C3MP(10,10),SIG
     A0(10),XL
      XMO(I)=QA(I)*XL**2/12.*F(I)
      SIGO(I)=6.*XMO(I)/(B*T(I)**2)
      XM(J)=FLOAT(J)/20.
      U(I)=XL/2.*DSQRT(HS(I)*B*TT(I)/EI(I))
      IF(U(I).GT.3.00) U(I)=3.00
      UM(I,J)=U(I)*XM(J)
      ZETAX(I,J)=12.*(2.*DCOS(U(I)-2.*UM(I,J))/DCOS(U(I))-2.-4.*U(I)**2*
     1(XM(J)-XM(J)**2))/(5.*U(I)**4)
      ALMDAX(I,J)=2.*(DCOS(U(I)-2.*UM(I,J))-DCOS(U(I)))/(U(I)**2*DCOS(U(
     1I)))
      X(I)=3.*(DTAN(U(I))-U(I))/(U(I)**3)
      SX(I,J)=5.*ZETAX(I,J)-4.*U(I)*X(I)*ALMDAX(I,J)/DTAN(U(I))
      ZETA(I)=12.*(2./DCOS(U(I))-2.-U(I)**2)/(5.*U(I)**4)
      ALMDA(I)=2.*(1.-DCOS(U(I)))/(U(I)**2*DCOS(U(I)))
      SC(I)=5.*ZETA(I)-4.*U(I)*X(I)*ALMDA(I)/DTAN(U(I))
      XX(I,J)=3.*(DSIN(2.*UM(I,J))/DCOS(U(I))-2.*UM(I,J))/(U(I)**3)
      G1X(I,J)=4.*XX(I,J)-3.*U(I)*ALMDAX(I,J)*ALMDA(I)/DTAN(U(I))
      C1X(I,J)=0.5*SX(I,J)/G1X(I,J)
      G2X(I,J)=DSIN(2.*UM(I,J))*DCOS(2.*UM(I,J)-U(I))/(8.*U(I)**3*DCOS(U
     1(I)))-XM(J)/(4.*U(I)**2)-(DCOS(U(I)-2.*XM(J)*U(I))-DCOS(U(I)))**2/
     2(4.*U(I)**3*DSIN(2.*U(I)))
      C2X(I,J)=SX(I,J)/(384.*G2X(I,J))
      C2T(I,J)=2.*C2X(I,J)
      XK3C(I)=SC(I)/48.
      XK31(I,J)=SX(I,J)/48.
      A1(I)=((DTAN(U(I))-U(I))/2.-(1.-DCOS(U(I)))**2/DSIN(2.*U(I)))/U(I)
     1**3
      A2(I,J)=(DSIN(2.*UM(I,J))/(2.*DCOS(U(I)))-UM(I,J)-(1.-DCOS(U(I)))*
     1(DCOS(2.*UM(I,J)-U(I))-DCOS(U(I)))/DSIN(2.*U(I)))/U(I)**3
      B1(I,J)=(DSIN(2.*UM(I,J))/DCOS(U(I))-2.*UM(I,J)+2.*(DCOS(U(I))-DCO
     1S(2.*UM(I,J)-U(I)))*(1.-DCOS(U(I)))/DSIN(2.*U(I)))/U(I)**3
      B2(I,J)=(DSIN(2.*UM(I,J))*DCOS(2.*UM(I,J)-U(I))/DCOS(U(I))-2.*UM(I
     1,J)-2.*(DCOS(U(I))-DCOS(2.*UM(I,J)-U(I)))**2/DSIN(2.*U(I)))/U(I)**
     23
      CDC(I,J)=A1(I)*B2(I,J)-A2(I,J)*B1(I,J)
      IF(CDC(I,J).EQ.0.0) GO TO 36
      C3C(I,J)=(XK3C(I)*B2(I,J)-XK31(I,J)*B1(I,J))/CDC(I,J)
      C31(I,J)=(A1(I)*XK31(I,J)-A2(I,J)*XK3C(I))/CDC(I,J)
      C3T(I,J)=C3C(I,J)+2.*C31(I,J)
      C3MP(I,J)=C3C(I,J)-C31(I,J)
      IF(DABS(C3MP(I,J))-0.0001) 7,7,35
```

```
      7 WRITE(6,6) C31(I,J),C3C(I,J),I,J
      6 FORMAT(1H-,3X,'C31',2X,D12.5,3X,'C3C',2X,D12.5,2X,'I',I3,2X,'J'
     1,I3)
        GO TO 35
     36 WRITE(6,38) CDC(I,J),I,J
     38 FORMAT(1H-,3X,'CDC',D12.5,3X,'I',I3,3X,'J',I3)
     35 RETURN
        END
C
C       SUBROUTINE COE45
C
        SUBROUTINE COE45(I,J,XL,U,XM1,XM2,UM1,UM2,ZETAX1,ALMDA1,ZETAX2,ALM
       1DA2,X,ALMDA,ZETA,S41,S42,A41,B41,A42,B42,XK41,XK42,CE4,C41,C42,C4T
       2,C4MP,S5C,S51,S52,A51,B51,D51,A52,B52,D52,A53,B53,D53,XK51,XK52,XK
       353,CE5,C5C,C51,C52,C5T,C5MC1,C5MC2,TT,EI,I1,I2,B,HS,XMO,SIGO,QA,F,
       4T)
        DOUBLE PRECISION EIS(10),M(10),HS(10),SIGMTU(10),C1CS(10,10),A1(10
       1),SIGMTL(10),P31(10,1),P32(10,10),R(10),Q(10),XI(10),E(10),TRYY,T(
       110),W(10),SIGM1(10),COMSH(10),QA(10),WA(10),H(10),TENSH(10),PA(10)
       2,V2L2(10),V2L(10),HSET(10),U(10),ZETA(10),ALMDA(10),D1(10,10),SC(1
       30),Q(10),X(10),F(10),VC(10),S(10),IQM32(10),PB4(10),SIGM42(10),XMO
       4(10),TAU1(10),SEIS(10),SUMQ,SUMEIS,XL
        DOUBLE PRECISION TT(10),XM1(10),XM2(10),UM1(10,10),UM2(10,10),ZETA
       8X1(10,10),ALMDA1(10,10),ALMDA2(10,10),ZETAX2(10,10),S41(10,10),S42
       9(10,10),A41(10,10),B41(10,10,10),A42(10,10,10),B42(10,10),XK41(10,
       A10),XK42(10,10),CE4(10,10,10),C41(10,10,10),C42(10,10,10),C4T(10,1
       A0,10),C4MP(10,10,10),S5C(10),S51(10,10),S52(10,10),A51(10),B51(10,
       A10),D51(10,10),A52(10,10),B52(10,10),D52(10,10,10),A53(10,10),B53(
       A10,10,10),D53(10,10),XK51(10),XK52(10,10),XK53(10,10),CE5(10,10,10
       A),C5C(10,10,10),C51(10,10,10),C52(10,10,10),C5T(10,10,10),C5MC1(10
       A,10,10),C5MC2(10,10,10),EI(10),B,SIGO(10)
        XMO(I)=QA(I)*XL**2/12.*F(I)
        SIGO(I)=6.*XMO(I)/(B*T(I)**2)
        XM1(I1)=FLOAT(I1)/20.
        XM2(I2)=FLOAT(I2)/20.
        U(I)=XL/2.*DSQRT(HS(I)*B*TT(I)/EI(I))
        IF(U(I).GT.3.00) U(I)=3.00
        UM1(I,I1)=U(I)*XM1(I1)
        UM2(I,I2)=U(I)*XM2(I2)
        ZETAX1(I,I1)=12.*(2.*DCOS(U(I)-2.*UM1(I,I1))/DCOS(U(I))-2.-4.*U(I)
       1**2*(XM1(I1)-XM1(I1)**2))/(5.*U(I)**4)
        ALMDA1(I,I1)=2.*(DCOS(U(I)-2.*UM1(I,I1))-DCOS(U(I)))/(U(I)**2*DCOS
       1(U(I)))
        ALMDA(I)=2.*(1.-DCOS(U(I)))/(U(I)**2*DCOS(U(I)))
        X(I)=3.*(DTAN(U(I))-U(I))/(U(I)**3)
        ZETA(I)=12.*(2./DCOS(U(I))-2.-U(I)**2)/(5.*U(I)**4)
        ZETAX2(I,I2)=12.*(2.*DCOS(U(I)-2.*UM2(I,I2))/DCOS(U(I))-2.-4.*U(I)
       1**2*(XM2(I2)-XM2(I2)**2))/(5.*U(I)**4)
        ALMDA2(I,I2)=2.*(DCOS(U(I)-2.*UM2(I,I2))-DCOS(U(I)))/(U(I)**2*DCOS
       1(U(I)))
        S41(I,I1)=5.*ZETAX1(I,I1)-4.*U(I)*X(I)*ALMDA1(I,I1)/DTAN(U(I))
        S42(I,I2)=5.*ZETAX2(I,I2)-4.*U(I)*X(I)*ALMDA2(I,I2)/DTAN(U(I))
        A41(I,I1)=(DSIN(2.*UM1(I,I1))*DCOS(U(I)-2.*UM1(I,I1))/DCOS(U(I))-2
       1.*UM1(I,I1)-2.*(DCOS(U(I)-2.*UM1(I,I1))-DCOS(U(I)))**2/DSIN(2.*U(I
       1)))/U(I)**3
        B41(I,I1,I2)=(DSIN(2.*UM1(I,I1))*DCOS(U(I)-2.*UM2(I,I2))/DCOS(U(I)
       1)-2.*UM1(I,I1)-2.*(DCOS(U(I)-2.*UM1(I,I1))-DCOS(U(I)))*(DCOS(U(I)-
       22.*UM2(I,I2))-DCOS(U(I)))/DSIN(2.*U(I)))/U(I)**3
        A42(I,I1,I2)=(DSIN(2.*UM1(I,I1))*DCOS(U(I)-2.*UM2(I,I2))/DCOS(U(I)
       1)-2.*UM1(I,I1)-2.*(DCOS(U(I)-2.*UM1(I,I1))-DCOS(U(I)))*(DCOS(U(I)-
       22.*UM2(I,I2))-DCOS(U(I)))/DSIN(2.*U(I)))/U(I)**3
        B42(I,I2)=(DSIN(2.*UM2(I,I2))*DCOS(U(I)-2.*UM2(I,I2))/DCOS(U(I))-2
       1.*UM2(I,I2)-2.*(DCOS(U(I)-2.*UM2(I,I2))-DCOS(U(I)))**2/DSIN(2.*U(I
       2)))/U(I)**3
        XK41(I,I1)=S41(I,I1)/48.
        XK42(I,I2)=S42(I,I2)/48.
        CE4(I,I1,I2)=A41(I,I1)*B42(I,I2)-A42(I,I1,I2)*B41(I,I1,I2)
```

```
      IF(CE4(I,I1,I2).EQ.0.) GO TO 12
      C41(I,I1,I2)=(XK41(I,I1)*B42(I,I2)-XK42(I,I2)*B41(I,I1,I2))/CE4(I,
     1I1,I2)
      C42(I,I1,I2)=(A41(I,I1)*XK42(I,I2)-A42(I,I1,I2)*XK41(I,I1))/CE4(I,
     1I1,I2)
      C4T(I,I1,I2)=2.*(C41(I,I1,I2)+C42(I,I1,I2))
      C4MP(I,I1,I2)=C41(I,I1,I2)-C42(I,I1,I2)
      IF(DABS(C4MP(I,I1,I2))-0.0001) 77,77,22
   77 WRITE(6,320) C41(I,I1,I2),C42(I,I1,I2),I,I1,I2
  320 FORMAT(1H-,3X,'C41',3X,D12.5,3X,'C42',3X,D12.5,1X,'I',I3,1X,'I1
     1',1X,I3,1X,'I2',I3)
   22 S5C(I)=5.*ZETA(I)-4.*U(I)*X(I)*ALMDA(I)/DTAN(U(I))
      S51(I,I1)=5.*ZETAX1(I,I1)-4.*U(I)*X(I)*ALMDA1(I,I1)/DTAN(U(I))
      S52(I,I2)=5.*ZETAX2(I,I2)-4.*U(I)*X(I)*ALMDA2(I,I2)/DTAN(U(I))
      A51(I)=((DTAN(U(I))-U(I))/2.-(1.-DCOS(U(I)))**2/DSIN(2.*U(I)))/U(I
     1)**3
      B51(I,I1)=(DSIN(2.*UM1(I,I1))/DCOS(U(I))-2.*UM1(I,I1)+2.*(DCOS(U(I
     1))-DCOS(2.*UM1(I,I1)-U(I)))*(1.-DCOS(U(I)))/DSIN(2.*U(I)))/U(I)**3
      D51(I,I2)=(DSIN(2.*UM2(I,I2))/DCOS(U(I))-2.*UM2(I,I2)+2.*(DCOS(U(I
     1))-DCOS(2.*UM2(I,I2)-U(I)))*(1.-DCOS(U(I)))/DSIN(2.*U(I)))/U(I)**3
      A52(I,I1)=(DSIN(2.*UM1(I,I1))/(2.*DCOS(U(I)))-UM1(I,I1)-(1.-DCOS(U
     1(I)))*(DCOS(2.*UM1(I,I1)-U(I))-DCOS(U(I)))/DSIN(2.*U(I)))/U(I)**3
      B52(I,I1)=(DSIN(2.*UM1(I,I1))*DCOS(U(I)-2.*UM1(I,I1))/DCOS(U(I))-2
     1.*UM1(I,I1)-2.*(DCOS(U(I)-2.*UM1(I,I1))-DCOS(U(I)))**2/DSIN(2.*U(I
     2)))/U(I)**3
      D52(I,I1,I2)=(DSIN(2.*UM1(I,I1))*DCOS(U(I)-2.*UM2(I,I2))/DCOS(U(I)
     1)-2.*UM1(I,I1)-2.*(DCOS(U(I)-2.*UM1(I,I1))-DCOS(U(I)))*(DCOS(U(I)-
     22.*UM2(I,I2))-DCOS(U(I)))/DSIN(2.*U(I)))/U(I)**3
      A53(I,I2)=(DSIN(2.*UM2(I,I2))/(2.*DCOS(U(I)))-UM2(I,I2)-(1.-DCOS(U
     1(I)))*(DCOS(2.*UM2(I,I2)-U(I))-DCOS(U(I)))/DSIN(2.*U(I)))/U(I)**3
      B53(I,I1,I2)=(DSIN(2.*UM1(I,I1))*DCOS(U(I)-2.*UM2(I,I2))/DCOS(U(I)
     1)-2.*UM1(I,I1)-2.*(DCOS(U(I)-2.*UM1(I,I1))-DCOS(U(I)))*(DCOS(U(I)-
     22.*UM2(I,I2))-DCOS(U(I)))/DSIN(2.*U(I)))/U(I)**3
      D53(I,I2)=(DSIN(2.*UM2(I,I2))*DCOS(U(I)-2.*UM2(I,I2))/DCOS(U(I))-2
     1.*UM2(I,I2)-2.*(DCOS(U(I)-2.*UM2(I,I2))-DCOS(U(I)))**2/DSIN(2.*U(I
     2)))/U(I)**3
      XK51(I)=S5C(I)/48.
      XK52(I,I1)=S51(I,I1)/48.
      XK53(I,I2)=S52(I,I2)/48.
      CE5(I,I1,I2)=A51(I)*(B52(I,I1)*D53(I,I2)-B53(I,I1,I2)*D52(I,I1,I2)
     1)-A52(I,I1)*(B51(I,I1)*D53(I,I2)-B53(I,I1,I2)*D51(I,I2))+A53(I,I2)
     2*(B51(I,I1)*D52(I,I1,I2)-B52(I,I1)*D51(I,I2))
      IF(CE5(I,I1,I2).EQ.0.) GO TO 13
      C5C(I,I1,I2)=(XK51(I)*(B52(I,I1)*D53(I,I2)-B53(I,I1,I2)*D52(I,I1,I
     12))-XK52(I,I1)*(B51(I,I1)*D53(I,I2)-B53(I,I1,I2)*D51(I,I2))+XK53(I
     2,I2)*(B51(I,I1)*D52(I,I1,I2)-B52(I,I1)*D51(I,I2)))/CE5(I,I1,I2)
      C51(I,I1,I2)=(A51(I)*(XK52(I,I1)*D53(I,I2)-XK53(I,I2)*D52(I,I1,I2)
     1)-A52(I,I1)*(XK51(I)*D53(I,I2)-XK53(I,I2)*D51(I,I2))+A53(I,I2)*(XK
     251(I)*D52(I,I1,I2)-XK52(I,I1)*D51(I,I2)))/CE5(I,I1,I2)
      C52(I,I1,I2)=(A51(I)*(B52(I,I1)*XK53(I,I2)-B53(I,I1,I2)*XK52(I,I1)
     1)-A52(I,I1)*(B51(I,I1)*XK53(I,I2)-B53(I,I1,I2)*XK51(I))+A53(I,I2)*
     2(B51(I,I1)*XK52(I,I1)-B52(I,I1)*XK51(I)))/CE5(I,I1,I2)
      C5T(I,I1,I2)=C5C(I,I1,I2)+2.*(C51(I,I1,I2)+C52(I,I1,I2))
      C5MC1(I,I1,I2)=C5C(I,I1,I2)-C51(I,I1,I2)
      C5MC2(I,I1,I2)=C5C(I,I1,I2)-C52(I,I1,I2)
      IF(DABS(C5MC1(I,I1,I2)).LT.0.0001.AND.DABS(C5MC2(I,I1,I2)).LT.0.00
     101) GO TO 8
      GO TO 11
    8 WRITE(6,230) C5C(I,I1,I2),C51(I,I1,I2),C52(I,I1,I2),I,I1,I2
  230 FORMAT(1H-,3X,'C5C',3X,D12.5,3X,'C51',3X,D12.5,3X,'C52',3X,D12.
     15,3X,'I',I3,3X,'I1',I3,3X,'I2',I3)
      GO TO 11
   12 WRITE(6,41) CE4(I,I1,I2),I,I1,I2
   41 FORMAT(///1H-,3X,'CE4',3X,D12.5,3X,'I',I3,3X,'I1',I3,1X,'I2',I3)
      GO TO 22
   13 WRITE(6,42) CE5(I,I1,I2),I,I1,I2
   42 FORMAT(1H-,3X,'CE5',3X,D12.5,3X,'I',I3,3X,'I1',I3,1X,'I2',I3)
```

```
   11 RETURN
      END
C
C     SUBROUTINE COE67
C
      SUBROUTINE COE67(I,J,XL,U,XM1,XM2,UM1,UM2,ZETAX1,ALMDA1,ZETAX2,ALM
     1DA2,X,ALMDA,ZETA,S61,S62,A61,B61,A62,B62,XK61,XK62,CE6,C61,C62,C6T
     2,XM3,UM3,ZETAX3,ALMDA3,S63,D61,D62,A63,B63,D63,XK63,C63,I3,C6M12,C
     36M13,TT,EI,I1,I2,B,HS,XMO,SIGO,QA,F,T)
      DOUBLE PRECISION EIS(10),M(10),HS(10),SIGMTU(10),C1CS(10,10),A1(10
     1),SIGMTL(10),P31(10,1),P32(10,10),R(10),Q(10),XI(10),E(10),TRYY,T(
     110),W(10),SIGM1(10),COMSH(10),QA(10),WA(10),H(10),TENSH(10),PA(10)
     2,V2L2(10),V2L(10),HSET(10),U(10),ZETA(10),ALMDA(10),D1(10,10),SC(1
     30),Q(10),X(10),F(10),VC(10),S(10),IGM32(10),PB4(10),SIGM42(10),XMO
     4(10),TAU1(10),SEIS(10),SUMQ,SUMEIS,XL
      DOUBLE PRECISION TT(10),XM1(10),XM2(10),UM1(10,10),UM2(10,10),ZETA
     8X1(10,10),ALMDA1(10,10),ALMDA2(10,10),ZETAX2(10,10),S61(10,10),S62
     9(10,10),A61(10,10),B61(10,10,10),A62(10,10,10),B62(10,10),XK61(10,
     A10),XK62(10,10),XK63(10,10),XM3(10),UM3(10,10),ZETAX3(10,10),DD,AL
     AMDA3(10,10),S63(10,10),D61(10,10,10),D62(10,10,10),A63(10,10,10),B
     A63(10,10,10),D63(10,10),C61(10,10,10,10),C62(10,10,10,10),C63(10,1
     A0,10,10),C6T(10,10,10,10),C6M12(10,10,10,10),C6M13(10,10,10,10),B,
     AEI(10),SIGO(10),CE6(10,10,10,10)
      XMO(I)=QA(I)*XL**2/12.^F(I)
      SIGO(I)=6.*XMO(I)/(B*T(I)**2)
      XM1(I1)=FLOAT(I1)/20.
      XM2(I2)=FLOAT(I2)/20.
      XM3(I3)=FLOAT(I3)/20.
      U(I)=XL/2.*DSQRT(HS(I)*B*TT(I)/EI(I))
      IF(U(I).GT.3.00) U(I)=3.00
      UM1(I,I1)=U(I)*XM1(I1)
      UM2(I,I2)=U(I)*XM2(I2)
      UM3(I,I3)=U(I)*XM3(I3)
      ZETAX1(I,I1)=12.*(2.*DCOS(U(I)-2.*UM1(I,I1))/DCOS(U(I))-2.-4.*U(I)
     1**2*(XM1(I1)-XM1(I1)**2))/(5.*U(I)**4)
      ALMDA1(I,I1)=2.*(DCOS(U(I)-2.*UM1(I,I1))-DCOS(U(I)))/(U(I)**2*DCOS
     1(U(I)))
      ALMDA(I)=2.*(1.-DCOS(U(I)))/(U(I)**2*DCOS(U(I)))
      X(I)=3.*(DTAN(U(I))-U(I))/(U(I)**3)
      ZETA(I)=12.*(2./DCOS(U(I))-2.-U(I)**2)/(5.*U(I)**4)
      ZETAX2(I,I2)=12.*(2.*DCOS(U(I)-2.*UM2(I,I2))/DCOS(U(I))-2.-4.*U(I)
     1**2*(XM2(I2)-XM2(I2)**2))/(5.*U(I)**4)
      ALMDA2(I,I2)=2.*(DCOS(U(I)-2.*UM2(I,I2))-DCOS(U(I)))/(U(I)**2*DCOS
     1(U(I)))
      ZETAX3(I,I3)=12.*(2.*DCOS(U(I)-2.*UM3(I,I3))/DCOS(U(I))-2.-4.*U(I)
     1**2*(XM3(I3)-XM3(I3)**2))/(5.*U(I)**4)
      ALMDA3(I,I3)=2.*(DCOS(U(I)-2.*UM3(I,I3))-DCOS(U(I)))/(U(I)**2*DCOS
     1(U(I)))
      S61(I,I1)=5.*ZETAX1(I,I1)-4.*U(I)*X(I)*ALMDA1(I,I1)/DTAN(U(I))
      S62(I,I2)=5.*ZETAX2(I,I2)-4.*U(I)*X(I)*ALMDA2(I,I2)/DTAN(U(I))
      S63(I,I3)=5.*ZETAX3(I,I3)-4.*U(I)*X(I)*ALMDA3(I,I3)/DTAN(U(I))
      A61(I,I1)=(DSIN(2.*UM1(I,I1))*DCOS(U(I)-2.*UM1(I,I1))/DCOS(U(I))-2
     1.*UM1(I,I1)-2.*(DCOS(U(I)-2.*UM1(I,I1))-DCOS(U(I)))**2/DSIN(2.*U(I
     1)))/U(I)**3
      B61(I,I1,I2)=(DSIN(2.*UM1(I,I1))*DCOS(U(I)-2.*UM2(I,I2))/DCOS(U(I)
     1)-2.*UM1(I,I1)-2.*(DCOS(U(I)-2.*UM1(I,I1))-DCOS(U(I)))*(DCOS(U(I)-
     22.*UM2(I,I2))-DCOS(U(I)))/DSIN(2.*U(I)))/U(I)**3
      D61(I,I1,I3)=(DSIN(2.*UM1(I,I1))*DCOS(U(I)-2.*UM3(I,I3))/DCOS(U(I)
     1)-2.*UM1(I,I1)-2.*(DCOS(U(I)-2.*UM1(I,I1))-DCOS(U(I)))*(DCOS(U(I)-
     22.*UM3(I,I3))-DCOS(U(I)))/DSIN(2.*U(I)))/U(I)**3
      A62(I,I1,I2)=(DSIN(2.*UM1(I,I1))*DCOS(U(I)-2.*UM2(I,I2))/DCOS(U(I)
     1)-2.*UM1(I,I1)-2.*(DCOS(U(I)-2.*UM1(I,I1))-DCOS(U(I)))*(DCOS(U(I)-
     22.*UM2(I,I2))-DCOS(U(I)))/DSIN(2.*U(I)))/U(I)**3
      B62(I,I2)=(DSIN(2.*UM2(I,I2))*DCOS(U(I)-2.*UM2(I,I2))/DCOS(U(I))-2
     1.*UM2(I,I2)-2.*(DCOS(U(I)-2.*UM2(I,I2))-DCOS(U(I)))**2/DSIN(2.*U(I
     2)))/U(I)**3
      D62(I,I2,I3)=(DSIN(2.*UM2(I,I2))*DCOS(U(I)-2.*UM3(I,I3))/DCOS(U(I)
```

```
     1)-2.*UM2(I,I2)-2.*(DCOS(U(I)-2.*UM3(I,I3))-DCOS(U(I)))*(DCOS(U(I)-
     22.*UM2(I,I2))-DCOS(U(I)))/DSIN(2.*U(I)))/U(I)**3
      A63(I,I1,I3)=(DSIN(2.*UM1(I,I1))*DCOS(U(I)-2.*UM3(I,I3))/DCOS(U(I)
     1)-2.*UM1(I,I1)-2.*(DCOS(U(I)-2.*UM1(I,I1))-DCOS(U(I)))*(DCOS(U(I)-
     22.*UM3(I,I3))-DCOS(U(I)))/DSIN(2.*U(I)))/U(I)**3
      B63(I,I2,I3)=(DSIN(2.*UM2(I,I2))*DCOS(U(I)-2.*UM3(I,I3))/DCOS(U(I)
     1)-2.*UM2(I,I2)-2.*(DCOS(U(I)-2.*UM3(I,I3))-DCOS(U(I)))*(DCOS(U(I)-
     22.*UM2(I,I2))-DCOS(U(I)))/DSIN(2.*U(I)))/U(I)**3
      D63(I,I3)=(DSIN(2.*UM3(I,I3))*DCOS(U(I)-2.*UM3(I,I3))/DCOS(U(I))-2
     1.*UM3(I,I3)-2.*(DCOS(U(I)-2.*UM3(I,I3))-DCOS(U(I)))**2/DSIN(2.*U(I
     2)))/U(I)**3
      XK61(I,I1)=S61(I,I1)/48.
      XK62(I,I2)=S62(I,I2)/48.
      XK63(I,I3)=S63(I,I3)/48.
      CE6(I,I1,I2,I3)=A61(I,I1)*(B62(I,I2)*D63(I,I3)-B63(I,I2,I3)*D62(I,
     1I2,I3))-A62(I,I1,I2)*(B61(I,I1,I2)*D63(I,I3)-B63(I,I2,I3)*D61(I,I1
     2,I3))+A63(I,I1,I3)*(B61(I,I1,I2)*D62(I,I2,I3)-B62(I,I2)*D61(I,I1,I
     33))
      IF(CE6(I,I1,I2,I3).EQ.0.) GO TO 13
      C61(I,I1,I2,I3)=(XK61(I,I1)*(B62(I,I2)*D63(I,I3)-B63(I,I2,I3)*D62(
     1I,I2,I3))-XK62(I,I2)*(B61(I,I1,I2)*D63(I,I3)-B63(I,I2,I3)*D61(I,I1
     2,I3))+XK63(I,I3)*(B61(I,I1,I2)*D62(I,I2,I3)-B62(I,I2)*D61(I,I1,I3)
     3))/CE6(I,I1,I2,I3)
      C62(I,I1,I2,I3)=(A61(I,I1)*(XK62(I,I2)*D63(I,I3)-XK63(I,I3)*D62(I,
     1I2,I3))-A62(I,I1,I2)*(XK61(I,I1)*D63(I,I3)-XK63(I,I3)*D61(I,I1,I3)
     2)+A63(I,I1,I3)*(XK61(I,I1)*D62(I,I2,I3)-XK62(I,I2)*D61(I,I1,I3)))/
     3CE6(I,I1,I2,I3)
      C63(I,I1,I2,I3)=(A61(I,I1)*(B62(I,I2)*XK63(I,I3)-B63(I,I2,I3)*XK62
     1(I,I2))-A62(I,I1,I2)*(B61(I,I1,I2)*XK63(I,I3)-B63(I,I2,I3)*XK61(I,
     2I1))+A63(I,I1,I3)*(B61(I,I1,I2)*XK62(I,I2)-B62(I,I2)*XK61(I,I1)))/
     3CE6(I,I1,I2,I3)
      C6T(I,I1,I2,I3)=2.*(C61(I,I1,I2,I3)+C62(I,I1,I2,I3)+C63(I,I1,I2,I3
     1))
      C6M12(I,I1,I2,I3)=C61(I,I1,I2,I3)-C62(I,I1,I2,I3)
      C6M13(I,I1,I2,I3)=C61(I,I1,I2,I3)-C63(I,I1,I2,I3)
      IF(DABS(C6M12(I,I1,I2,I3)).LT.0.0001.AND.DABS(C6M13(I,I1,I2,I3)).L
     1T.0.0001) GO TO 8
      GO TO 11
    8 WRITE(6,230) C61(I,I1,I2,I3),C62(I,I1,I2,I3),C63(I,I1,I2,I3),I,I1,
     1I2,I3
  230 FORMAT(1H-,3X,'C61',3X,D12.5,3X,'C62',3X,D12.5,3X,'C63',3X,D12.
     15,3X,'I',I3,3X,'I1',I3,3X,'I2',I3,3X,'I3',I3)
      GO TO 11
   13 WRITE(6,42) CE6(I,I1,I2,I3),I,I1,I2,I3
   42 FORMAT(1H-,3X,'CE6',3X,D12.5,3X,'I',I3,3X,'I1',I3,1X,'I2',I3,1X
     1,'I3',I3)
   11 RETURN
      END
C
C     SUBROUTINE FRIC1
C
      SUBROUTINE FRIC1(SUMTT1,TT1,N1,SUMTF1,BE1,ET1,B,AE1,YD1,AY1,SUMA1,
     ASUMAY1,SUME1,YC1,SMIZC1,YF1,XIA1,IZC1,IC1,SUMIA1,I,J,X1,V0,V1,QS1,
     AQSM1,VS1,TB1,US,U1.XMB,SIGBL,SIGBU,V2L1,SMETT1,CB1,F1,S1,XF1,ZETA1
     A,ALDA1,HS,QT,XL,XB,BL)
      DOUBLE PRECISION SUMTT1(10),TT1(10),SUMTF1,BE1(10),ET1(10),AE1(10)
     A,YD1(10),AY1(10),SUMA1,SUMAY1,SUME1,YC1,SMIZC1,YF1(10),XIA1(10),IZ
     AC1(10),SUMIA1,X1(10),V0,V1(10),QS1(10),QSM1(10),VS1(10),TB1(10),US
     A,U1,XMB,SIGBL,SIGBU,V2L1,ALDA1,CB1(10),SMETT1,F1,S1,XF1,ZETA1,HS(1
     A0),QT(10),B,XL,XB(10,10),BL
      SUMTT1(1)=TT1(1)
      YD1(1)=TT1(1)/2.
      DO 701 I=2,N1
      SUMTT1(I)=SUMTT1(I-1)+TT1(I)
      YD1(I)=SUMTT1(I-1)+TT1(I)/2.
  701 CONTINUE
      SUMTF1=SUMTT1(N1)
```

```
      BL=SUMTF1
      DO 714 I=1,N1
      BE1(I)=ET1(I)/ET1(1)*B
      AE1(I)=BE1(I)*TT1(I)
      AY1(I)=AE1(I)*YD1(I)
  714 CONTINUE
      SUMA1=0.0
      SUMAY1=0.0
      SMETT1=0.0
      DO 702 I=1,N1
      SUMA1=SUMA1+AE1(I)
      SUMAY1=SUMAY1+AY1(I)
      SMETT1=SMETT1+ET1(I)*TT1(I)
  702 CONTINUE
      SUME1=SMETT1/SUMTF1
      YC1=SUMAY1/SUMA1
      WRITE(6,600) YC1
  600 FORMAT(1H0,2X,'YC1',1X,D11.4)
      SMIZC1=0.0
      DO 703 I=1,N1
      YF1(I)=YC1-YD1(I)
      XIA1(I)=AE1(I)*YF1(I)
      IZC1(I)=AE1(I)*TT1(I)**2/12.+AE1(I)*YF1(I)**2
      SMIZC1=SMIZC1+IZC1(I)
  703 CONTINUE
      DO 704 I=1,N1
      IF(SUMTT1(I).GT.YC1) GO TO 705
  704 CONTINUE
  705 IF(I.EQ.1) IC1=I
      IF(I.NE.1) IC1=I-1
      WRITE(6,706) IC1
  706 FORMAT(1H0,3X,'IC1',I3)
      SUMIA1=0.0
      DO 707 I=1,IC1
      SUMIA1=SUMIA1+XIA1(I)
  707 CONTINUE
      DO 700 J=1,10
      CB1(J)=FLOAT(J)
      X1(J)=DSQRT(1./CB1(J))*(XL/2.)
      V0=QT(1)*XL/2.
      V1(J)=X1(J)/(XL/2.)*V0
      QS1(J)=V1(J)*SUMIA1/SMIZC1
      QSM1(J)=QS1(J)/2.
      VS1(J)=QSM1(J)*X1(J)
      TB1(J)=VS1(J)/US
  700 CONTINUE
      U1=XL*DSQRT(3.*HS(1)/(SUME1*SUMTF1**2))
      F1=3.*(DTAN(U1)-U1)/(U1**3)*U1/DTAN(U1)
      XMB=QT(1)*XL**2/12.*F1
      SIGBL=XMB*YC1/SMIZC1
      SIGBU=-1.*SIGBL*ET1(N1)/ET1(1)
      XF1=3.*(DTAN(U1)-U1)/(U1**3)
      ZETA1=12.*(2./DCOS(U1)-2.-U1**2)/(5.*U1**4)
      ALDA1=2.*(1.-DCOS(U1))/(U1**2*DCOS(U1))
      S1=5.*ZETA1-4.*U1*XF1*ALDA1/DTAN(U1)
      V2L1=QT(1)*XL**4/(384.*SUME1*SMIZC1)*S1
      WRITE(6,720) SIGBL,SIGBU,V2L1
  720 FORMAT(1H0,2X,'SIGBL',1X,D11.4,1X,'SIGBU',1X,D11.4,1X,'V2L1',1X,D1
     11.4)
      RETURN
      END
C
C     SUBROUTINE FRICM
C
      SUBROUTINE FRICM(SUMTT,TT,K,SUMTF,BE,EC,B,AE,YD,AY,SUMA,SUMAY,SUME
     A,YC,SUMIZC,YF,XIA,IZC,IC,SUMIA,X1,V0,V1,QS1,QSM1,VS1,TB1,US,U1,XMB
     A,SIGBL,SIGBU,V2L1,I,J,CB1,SUMETT,F1,S1,XF1,ZETA1,ALDA1,HS,QT
```

```
     A, XL, XB, SUMQT, BL)
      DOUBLE PRECISION SUMTT(10), TT(10), SUMTF, BE(10), EC(10), AE(10), YD(10
     A), AY(10), SUMA, SUMAY, SUME, YC, SUMIZC, YF(10), XIA(10), IZC(10), SUMIA, X1
     A(10), VO, V1(10), QS1(10), QSM1(10), VS1(10), TB1(10), US, U1, XMB, SIGBL, SI
     AGBU, V2L1, SUMETT, CB1(10), F1, S1, XF1, ZETA1, ALDA1, HS(10), QT(10)
     A, B, XL, XB(10, 10), SUMQT, BL
      SUMTT(1)=TT(1)
      YD(1)=TT(1)/2.
      DO 701 I=2, K
      SUMTT(I)=SUMTT(I-1)+TT(I)
      YD(I)=SUMTT(I-1)+TT(I)/2.
      WRITE(6, 500) SUMTT(I)
500   FORMAT(1H0, 3X, 'SUMTT', D12. 4)
701   CONTINUE
      SUMTF=SUMTT(K)
      BL=SUMTF
      DO 714 I=1, K
      BE(I)=EC(I)/EC(1)*B
      AE(I)=BE(I)*TT(I)
      AY(I)=AE(I)*YD(I)
714   CONTINUE
      SUMA=0. 0
      SUMAY=0. 0
      SUMETT=0. 0
      DO 702 I=1, K
      SUMA=SUMA+AE(I)
      SUMAY=SUMAY+AY(I)
      SUMETT=SUMETT+EC(I)*TT(I)
702   CONTINUE
      SUME=SUMETT/SUMTF
      YC=SUMAY/SUMA
      WRITE(6, 501) YC
501   FORMAT(1H0, 3X, 'YC', D12. 4)
      SUMIZC=0. 0
      DO 703 I=1, K
      YF(I)=YC-YD(I)
      XIA(I)=AE(I)*YF(I)
      IZC(I)=AE(I)*TT(I)**2/12. +AE(I)*YF(I)**2
      SUMIZC=SUMIZC+IZC(I)
703   CONTINUE
      DO 704 I=1, K
      IF(SUMTT(I). GT. YC) GO TO 705
704   CONTINUE
705   IF(I. EQ. 1) IC=I
      IF(I. NE. 1) IC=I-1
      WRITE(6, 706) IC
706   FORMAT(1H0, 3X, 'IC', I3)
      SUMIA=0. 0
      DO 707 I=1, IC
      SUMIA=SUMIA+XIA(I)
707   CONTINUE
      SUMQT=0. 0
      DO 709 I=1, K
      SUMQT=SUMQT+QT(I)
709   CONTINUE
      VO=SUMQT*XL/2.
      DO 700 J=1, 10
      CB1(J)=FLOAT(J)
      X1(J)=DSQRT(1. /CB1(J))*(XL/2. )
      V1(J)=X1(J)/(XL/2. )*VO
      QS1(J)=V1(J)*SUMIA/SUMIZC
      QSM1(J)=QS1(J)/2.
      VS1(J)=QSM1(J)*X1(J)
      TB1(J)=VS1(J)/US
700   CONTINUE
      U1=XL*DSQRT(3. *HS(1)/(SUME*SUMTF**2))
      F1=3. *(DTAN(U1)-U1)/(U1**3)*U1/DTAN(U1)
```

```
      XF1=3.*(DTAN(U1)-U1)/(U1**3)
      ZETA1=12.*(2./DCOS(U1)-2.-U1**2)/(5.*U1**4)
      ALDA1=2.*(1.-DCOS(U1))/(U1**2*DCOS(U1))
      S1=5.*ZETA1-4.*U1*XF1*ALDA1/DTAN(U1)
      XMB=SUMQT*XL**2/12.*F1
      SIGBL=XMB*YC/SUMIZC
      SIGBU=-1.*SIGBL*EC(K)/EC(1)
      V2L1=SUMQT*XL**4/(384.*SUME*SUMIZC)*S1
      WRITE(6,720) SIGBL,SIGBU,V2L1
  720 FORMAT(1H0,2X,'SIGBL',1X,D11.4,1X,'SIGBU',1X,D11.4,1X,'V2L1',1X,D1
     11.4)
      RETURN
      END
C
C     SUBROUTINE FRSPAC
C
      SUBROUTINE FRSPAC(J,XB,I,XL,CB1,CB2)
      DOUBLE PRECISION XB(10,10),XL,CB1(10),CB2(10)
      DO 710 I=1,10
      DO 710 J=1,I
      CB1(J)=FLOAT(J)
      CB2(I)=FLOAT(I)
      XB(I,J)=DSQRT((2.*CB1(J)-1.)/(2.*CB2(I)))*(XL/2.)
      WRITE(6,712)I,XB(I,J)
  712 FORMAT(1H0,3X,'I',I3,2X,'XB',1X,D11.4)
  710 CONTINUE
      RETURN
      END
```

VITA

The author was born on October 19, 1950 in Taiwan. He graduated from Kao Hsiung High School in June 1968. He received the Bachelor of Engineering degree in Mining Engineering in June 1972 from Cheng Kung University, Taiwan. He served in the Army from October 1972 through August 1974. He joined the Cheng Kung University in September 1974 for graduate study. He received the Master of Science degree in Mining Engineering in June 1976. After graduation, he worked as a Research Engineer in Mining Research and Service Organization (Taiwan) from July 1976 through December 1979. Since January 1980, he has been working toward a Doctor of Philosophy degree in Mining Engineering at West Virginia University.

APPROVAL OF EXAMINING COMMITTEE

Lyle K. Moulton, Civil Engineering

N. T. Sivaneri, Mechanical & Aerospace Engineering

A. W. Khair, Mining Engineering

Y. J. Wang, Mining Engineering

4/3/84
Date

Syd S. Peng, Mining Engineering, Chairman